

Scaling and connectivity assessment of critical source areas of diffuse pollution in urban catchments under a changing regime of high-intensity storms

vorgelegt von

M.Sc.

Nasrin Haacke

ORCID: 0000-0001-9065-729X

an der Fakultät VI - Planen Bauen Umwelt
der Technischen Universität Berlin
zur Erlangung des akademischen Grades

Doktorin der Ingenieurwissenschaften
- Dr.-Ing. -

genehmigte Dissertation

Promotionsausschuss:

Vorsitzende: Prof. Dr. Galina Churkina
Gutachterin: Prof. Dr. Eva Nora Paton
Gutachter: Prof. Dr. Reinhard Hinkelmann
Gutachter: Prof. Dr. Markus Disse

Tag der wissenschaftlichen Aussprache: 14. Oktober 2022

Berlin 2022

A drop of water, if it could write out its own history, would explain the universe to us.

Lucy Larcom

Acknowledgements

I am very grateful for having had the possibility of conducting this doctoral thesis at the Chair of Ecohydrology and Landscape Evaluation at Technische Universität Berlin within the DFG funded Research Training Group “Urban Water Interfaces” (UWI).

First and foremost, I want to express my sincere gratitude to my main supervisor Prof. Eva Paton for her enthusiasm, patience, generosity of time, and continuous support, both scientifically and mentally, throughout this thesis. At the same time, I would like to thank Prof. Reinhard (Phillip) Hinkelmann and Dr. Thomas Nehls for fruitful discussions, their open doors at any time and their great input into all aspects concerning this thesis.

I also want to thank all current and former chair members for creating a great working environment. Special thanks to Dr. Björn Kluge for his constructive exchange and excellent support during urban field work, and to Sidra Bibi, who shared an office with me most of the time and provided me with tea and inspiring talks when needed. I would also like to thank Joscha Vogel, Pedro Alencar, Karin Hoffmann, Moreen Willaredt and Laura Tams for the mutual support and the countless chats - you made this journey more enjoyable.

Many thanks to Prof. Hayley Fowler and Dr. Stephen Blenkinsop for the warm welcome into the Water Group during my research stay at Newcastle University (United Kingdom) as well as for the scientifically support and constructive discussions. I had a good time in Newcastle upon Tyne, which includes meeting two remarkable scientists, Sven Berendsen and Dr. Mathew Brown, who supported, inspired, motivated and cheered me up whenever I needed it and became close friends. Special thanks to Dr. Mathew Brown also for proofreading my thesis.

My warmest thanks go to my close friends Steffi Hoffmann, Denise Hanisch, Mimi Pokall, Jasmin Spanjer, Sam Schenk and Max Frick, who always lent a sympathetic ear to me, supported me, and at times put things into perspective when it was necessary. Finally, I would like to thank my beloved parents Fatme and Hassan Haacke, my grandma Christel Haacke and my sisters Shirin, Yasmin and Sabrin, who never stopped supporting, encouraging and believing in me throughout my life. I could not have completed this dissertation without you.

Berlin, May, 2022

Publications of cumulative doctoral thesis

First author publications (in chronological order):

1. **Haacke, N.** & Paton, E.N.: Analysis of diurnal, seasonal and annual distribution of urban sub-hourly to hourly rainfall extremes in Germany. *Hydrology Research*, 52 (2), 478-491, 2021; doi: 10.2166/nh.2021.181. Postprint.
2. **Haacke, N.** & Paton, E.N.: Impact-based classification of extreme rainfall events using a simplified overland flow model. Manuscript submitted for publication to *Urban Water Journal* on May 25, 2022, resubmitted with advised corrections on October 26, 2022.

Second author publication:

1. Paton, E.N. & **Haacke, N.**: Merging patterns and processes of diffuse pollution in urban watersheds: A connectivity assessment. *WIREs Water*, 8 (4), 2021; doi: 10.1002/wat2.1525. Postprint. This article is licensed under a Creative Commons license (CC BY NC 4.0; <https://creativecommons.org/licenses/by-nc/4.0/>).

An overview of all supplementary scientific work is given in Chapter 7.

This thesis was carried out as project W2 of the Research Training Group "Urban Water Interfaces (UWI)" (GRK 2032/2), which is funded by the German Research Foundation (DFG).

Abstract

Urban diffuse pollution is a serious global environmental issue. It comprises fluxes of dissolved and particulate pollutants associated with various land-use types and activities that enter the urban water catchment through precipitation or runoff processes from different urban surfaces. The cumulative effect of diffuse pollution can significantly negatively impact human well-being and ecosystem health by deteriorating the water quality of urban surface water bodies. Climate change and urbanisation exacerbate this effect due to changing precipitation patterns, an increase in extreme rainfall events and impervious areas, resulting in increased flushing and remobilisation of pollutants. To tackle this problem, diffuse pollution needs effective management. Existing approaches, however, are neither cost-efficient nor economical. In the last decade, new impact controlling developments have been introduced to control and reduce runoff rates by creating infiltration and retention areas and identifying critical source areas and pollution pathways. However, successful pollution mitigation and source control strategies in urban areas can only be implemented with accurate knowledge of hydrological, structural and pollutant connectivity and the factors impacting them. This is the focus of this thesis.

In the first study, crucial patterns of pollution source areas are categorized, and current knowledge of their spatiotemporal variations is collated. Urban alterations of transport processes that enhance, delay, or inhibit diffuse pollution transport from source areas through the urban watershed are detailed. Subsequently, diffuse pollution patterns and processes are conceptually merged by the simultaneous assessment of urban structural and functional connectivity relevant to pollutant transfer. The study concludes that only a holistic systems approach may help tackle current and future pollution rates under different environmental conditions.

Studies 2 to 4 focus on factors influencing urban connectivity. One major factor is extreme rainfall, leading to widely-hydrologically connected areas or in extreme cases to urban flash floods. While there is much known about daily rainfall extremes, short-duration (hourly to sub-hourly) extreme rainfall events have not been sufficiently investigated regarding their temporal and spatial occurrence patterns across Germany. The second study follows up on this and identifies regional diurnal patterns in extreme rainfall events across Germany, a unified seasonal consensus that they occur during the summer months, and no trend in their frequency within the analysed time period (2000 – 2019). Additionally, large-scale circulation patterns were not detected as a potential driving force of such events.

The third study introduces a novel methodology to classify extreme rainfall events based on their potential to generate overland flow on a typical urban asphalt surface. Besides the maximum rainfall intensity, this approach considers the full dynamics of rainstorm events, including characteristics such as their length, precipitation amount, mean intensity and flow

depths. Rainfall events generating substantial overland flow are assigned to several impact classes indicating increasing flow depths and thus more substantial impact. The results show that it is appropriate to use flow depth per time as an indicator of generated overland flow impacts, thus improving the characterization of rainfall events.

The last study focuses on urban surface representation as another factor influencing urban connectivity. It includes the identification of individual depressions on three differently paved real urban study sites and quantifies their depression storage capacity using a terrestrial laser-scanning method. Results show that depressions vary significantly in space, size, and volume, so averaged depression storage depths should not be used to characterise respective pavement designs, as typically done in hydrological modelling. However, this study needs to include more sites to gain more comprehensive results.

Zusammenfassung

Die städtische Verschmutzung durch diffuse Schadstoffe ist weltweit ein ernstes Umweltproblem. Sie umfasst den Eintrag gelöster und partikelförmiger Schadstoffe, die mit verschiedenen Flächennutzungsarten und Aktivitäten in Verbindung gebracht werden und durch Niederschläge oder Abflussprozesse von verschiedenen städtischen Flächen in das städtische Wassereinzugsgebiet gelangen. Die kumulative Wirkung der diffusen Verschmutzung kann das menschliche Wohlergehen und die Gesundheit der Ökosysteme durch die Verschlechterung der Wasserqualität städtischer Oberflächengewässer erheblich beeinträchtigen. Der Klimawandel und die Urbanisierung verschärfen diesen Effekt durch veränderte Niederschlagsmuster, die Zunahme extremer Niederschlagsereignisse und versiegelter Flächen, was zu einer verstärkten Abschwemmung und Remobilisierung von Schadstoffen führt. Um dieses Problem in den Griff zu bekommen, muss die diffuse Verschmutzung wirksam bekämpft werden. Die bisherigen Ansätze sind jedoch weder kosteneffizient noch wirtschaftlich. In den letzten zehn Jahren wurden neue Entwicklungen zur Eindämmung der Auswirkungen eingeführt, um die Abflussmengen zu kontrollieren und zu verringern, indem Versickerungs- und Rückhalteflächen geschaffen und kritische Quellenbereiche und Verschmutzungspfade identifiziert wurden. Strategien zur Verringerung der Umweltverschmutzung und zur Kontrolle der Schadstoffquellen in städtischen Gebieten können jedoch nur dann erfolgreich umgesetzt werden, wenn genaue Kenntnisse über die hydrologische, strukturelle und schadstoffbezogene Konnektivität und die sie beeinflussenden Faktoren vorliegen. Dies ist der Schwerpunkt der vorliegenden Arbeit.

In der ersten Studie werden relevante Muster von Verschmutzungsquellen kategorisiert und der aktuelle Wissensstand über ihre räumlichen und zeitlichen Variationen zusammengetragen. Städtische Veränderungen der Transportprozesse, die den Transport diffuser Verschmutzung aus den Quellgebieten durch das städtische Einzugsgebiet verstärken, verzögern oder hemmen, werden detailliert beschrieben. Anschließend werden diffuse Verschmutzungsmuster und -prozesse durch die gleichzeitige Bewertung der für den Schadstofftransport relevanten strukturellen und funktionalen städtischen Konnektivität konzeptionell zusammengeführt. Die Studie kommt zu dem Schluss, dass nur ein ganzheitlicher Systemansatz dazu beitragen kann, aktuelle und zukünftige Verschmutzungsraten unter verschiedenen Umweltbedingungen zu bewältigen.

Die Studien 2 bis 4 befassen sich mit Faktoren, die die Konnektivität in urbanen Räumen beeinflussen. Ein wesentlicher Faktor sind extreme Niederschläge, die zu hydrologisch großflächig verbundenen Gebieten oder im Extremfall zu städtischen Sturzfluten führen können. Während über tägliche Niederschlagsextreme viel bekannt ist, sind kurzzeitige (stündliche bis sub-stündliche) extreme Niederschlagsereignisse hinsichtlich ihres zeitlichen und räumlichen Auftretens in Deutschland nicht ausreichend untersucht worden. Die zweite

Studie knüpft daran an und identifiziert regionale tageszeitliche Muster extremer Niederschlagsereignisse in Deutschland, einen einheitlichen saisonalen Konsens, dass sie in den Sommermonaten auftreten, und keinen Trend in ihrer Häufigkeit innerhalb des untersuchten Zeitraums (2000 - 2019). Auch großräumige Zirkulationsmuster als mögliche treibende Kraft für solche Ereignisse konnten nicht festgestellt werden.

In der dritten Studie wird eine neuartige Methode zur Klassifizierung extremer Niederschlagsereignisse auf der Grundlage ihres Potenzials zur Erzeugung von Oberflächenabfluss auf einer typischen städtischen Asphaltfläche vorgestellt. Neben der maximalen Niederschlagsintensität berücksichtigt dieser Ansatz die gesamte Dynamik von Regenereignissen, einschließlich Merkmalen wie Länge, Niederschlagsmenge, mittlere Intensität und Abflusstiefe. Niederschlagsereignisse, die einen beträchtlichen Oberflächenabfluss erzeugen, werden verschiedenen Belastungsklassen zugeordnet, die auf zunehmende Fließtiefen und damit auf größere Auswirkungen hinweisen. Die Ergebnisse zeigen, dass es angemessen ist, die Fließtiefe pro Zeit als Indikator für die Auswirkungen des Oberflächenabflusses zu verwenden und so die Charakterisierung von Regenereignissen zu verbessern.

Die letzte Studie konzentriert sich auf die Darstellung der städtischen Oberfläche als weiteren Faktor, der die urbane Konnektivität beeinflusst. Sie umfasst die Identifizierung einzelner Senken auf drei unterschiedlich gepflasterten, realen städtischen Untersuchungsflächen und quantifiziert deren Speicherkapazität mit Hilfe eines terrestrischen Laserscanning-Verfahrens. Die Ergebnisse zeigen, dass die Vertiefungen in Bezug auf Fläche, Größe und Volumen erheblich variieren, so dass gemittelte Speichertiefen von Vertiefungen nicht zur Charakterisierung der jeweiligen Straßenbeläge herangezogen werden sollten, wie es in der hydrologischen Modellierung üblich ist. Es wird empfohlen, diese Studie um weitere Standorte und Untersuchungsflächen zu erweitern, um fundierte Ergebnisse zu erhalten.

Table of Contents

Acknowledgements	v
Publications of cumulative doctoral thesis	vi
Abstract	vii
Zusammenfassung	ix
Table of Contents	xi
List of Figures	xv
List of Tables	xix
1 Introduction	1
1.1 Motivation	1
1.2 Diffuse pollution and connectivity in urban areas	3
1.3 Extreme rainfall	5
1.3.1 Data availability	9
1.3.2 Spatial and temporal variability of extreme rainfall	10
1.3.3 Implications of extreme rainfall	13
1.4 Aim and research objectives	15
1.5 Outline of this thesis including articles	17

2	Merging patterns and processes of diffuse pollution in urban watersheds: A connectivity assessment	19
2.1	Introduction	20
2.2	Spatial and temporal patterns of diffuse pollution on urban surfaces	22
2.2.1	Spatial patterns of diffuse pollution	22
2.2.2	Temporal dynamics of diffuse pollution	29
2.3	Distribution processes of diffuse pollution within urban catchments	30
2.3.1	Variable hydrologic partitioning in cities	31
2.3.2	Critical source area concept for urban diffuse pollution	32
2.3.3	Buffers, barriers, and boosters in urban watersheds	33
2.4	Merging patterns and processes of urban diffuse pollution	34
2.4.1	Structural and functional connectivity of diffuse pollution in cities	35
2.4.2	Implications for the management of diffuse pollution in cities	37
2.4.3	Future research directions	38
2.5	Conclusion	39
3	Analysis of diurnal, seasonal, and annual distribution of urban sub- hourly to hourly rainfall extremes in Germany	41
3.1	Abstract	41
3.2	Introduction	42
3.3	Data and method	43
3.3.1	Study area	43
3.3.2	Data availability	44
3.3.3	Threshold selection	44
3.3.4	Atmospheric CTs and CPs	46
3.3.5	Analysis tools	46
3.4	Results	46

3.4.1	Diurnal distribution of heavy storm events	46
3.4.2	Seasonal distribution of heavy storm events	50
3.4.3	Annual distribution of heavy storm events	50
3.5	Discussion	52
3.5.1	Timing of extreme events	52
3.5.2	Atmospheric CTs and extreme events	54
3.5.3	Future research and way forward	55
3.6	Conclusion	56
4	Impact-based classification of extreme rainfall events using a simplified overland flow model	57
4.1	Abstract	57
4.2	Introduction	58
4.3	Impact-based rainfall classification method	59
4.3.1	Event delineation	60
4.3.2	Overland flow model	61
4.3.3	Impact-based classification of rainfall events	63
4.3.4	Data requirement and test stations	63
4.4	Evaluation of impact-based rainfall classification method	64
4.4.1	Evaluation of event delineation	64
4.4.2	Evaluation of overland flow model	65
4.4.3	Evaluation of impact-based classification	66
4.5	Application of the impact-based classification method: A time-series analysis .	69
4.6	Discussion	71
4.7	Conclusion	72

5	Pilot study: Depression storage capacities of different real urban surfaces quantified by a terrestrial laser scanning-based method	75
5.1	Introduction	75
5.1.1	State of research	75
5.1.2	Aims of the study	76
5.2	Materials and Methods	76
5.2.1	Study sites	76
5.2.2	Morphological survey through terrestrial laser scanning	77
5.2.3	Data processing	77
5.3	Results and Discussion	78
5.3.1	Spatial distribution of depressions	78
5.3.2	Storage capacities of real urban surfaces	79
5.3.3	Conclusion and Outlook	82
6	Synthesis	85
6.1	Main findings and conclusions	85
6.2	Challenges and future research	89
6.2.1	Applicability of the connectivity concept in urban areas	90
6.2.2	Future research in extreme rainfall classification and analysis	91
7	Supplementary contributions	95
	Bibliography	97

List of Figures

1.1	Animal faeces (a), car oil spills (b), cigarette butts (c), and organic litter in combination with tyre abrasion products forming foam (d) as examples of diffuse urban pollution.	4
1.2	Hydrologically well connected different urban surfaces during a heavy rainfall event (a), runoff retained in tree pit with lime blossoms (b) and in depressions in urban surfaces (c, d).	5
1.3	A flooded train station after extreme rainfall (a) and a flooded street due to blocked drains (b), both in Berlin.	7
1.4	Flood processes that are impacted by changes in sub-daily extreme precipitation. The most dominant processes with the highest certainties are in bold, while those with positive (+) and negative (-) contributions are also identified (Wasko et al., 2021).	8
1.5	Availability and length of existing sub-daily precipitation data sets across the globe (Lewis et al., 2019). Dots indicate rain gauge locations and are coloured by record length, that is, the time between the initial and the last recorded values, respectively. Black boxes represent current continental-scale convection-permitting model domains at a horizontal grid spacing of <5km (Fowler et al., 2021).	10
1.6	(a) Three women walking through flooded streets in Berlin after days of heavy rainfall (Christianthiel.net, 2017) and (b) drone view of streets and houses heavily damaged by historic floods in Rochefort, Belgium in July 2021 (Great Pics – Ben Heine, 2021).	15
1.7	Overview of all chapters and their content interfaces.	18

2.1	(a) Centralized versus (b) decentralized approaches for urban drainage (red line: drainage network, red arrows: storm-water outlet points into rivers, blue arrows: street runoff, infiltration, and evapotranspiration).	22
2.2	End-of-pipe sampling of diffuse pollution at storm-water outlets in urban catchment.	23
2.3	Spatial source area patterns that dominate or influence urban diffuse pollution: (a–d) pollution patterns that accumulate, (e–f) static pollution patterns, (g) management routines affecting pollution patterns, and (h–j) hydrologically relevant patterns—(h) degree and type of sealing, (i) antecedent moisture pattern, and (j) slope. Pink shading shows the extent and magnitude of the different pollution patterns (except it depicts the degree of sealing in h) and the slope magnitude in (i). Gray shading in (j) shows the magnitude of soil moisture.	24
2.4	Concurrency dynamics of pollutant accumulation and hydrological and pollutant connectivity as a function of rainfall-runoff response and management routines (reprinted with permission from Bracken et al. (2015)).	30
2.5	Two scenarios illustrating the different spatial extents of urban variable contributing areas for a (a) small and (b) large rainfall event (shades of blue) and associated potential to transport pollutants.	32
2.6	Buffers, barriers, and boosters of urban diffuse pollution: (a) swale directly after rain event, (b) blocked gully, and (c) stormwater outlet and rain gutter. .	34
3.1	Frequency distribution of extreme 10-min (upper row) and 60-min (lower row) rainfall events at all stations sorted from south to north. Circular plots show the percentage of CTs and CPs that co-occurred during the storms. All acronyms are explained in Table 3.1.	45
3.2	Diurnal distribution of short-duration heavy storm events across Germany of (a) 10-min duration (≥ 10 mm) and (b) 60-min duration (≥ 20 mm). Red mark represents the median, and the number of events is given in blue. Hourly frequency distribution, including information about prevailing CTs and CPs, is shown for 10-min events in (c) and 60-min events in (d). All acronyms are explained in Table 3.1.	48

3.3	Diurnal frequency distribution of short-duration heavy storm events across Germany. The pie chart represents 24-h clock, whereby left pie charts represent 10-min events (≥ 10 mm), and right pie charts represent 60-min events (≥ 20 mm). Colours represent classifications: blue = accumulation of events over 12 h, yellow = bimodal distribution, and red = homogeneous distribution (modified after Paton and Haacke (2021)).	49
3.4	Seasonal distribution of short-duration heavy storm events across Germany of (a) 10-min duration (≥ 10 mm) and (b) 60-min duration (≥ 20 mm). Red mark represents the median. Weekly frequency distribution, including information about prevailing CTs and CTs, is shown for 10-min events in (c) and 60-min events in (d). All acronyms are explained in Table 3.1.	51
3.5	Annual distribution of short-duration heavy storm events across Germany of (a) 10-min duration (≥ 10 mm) and (b) 60-min duration (≥ 20 mm). Red mark represents the median. Annual frequency distribution, including information about prevailing CTs and CPs, is shown for 10-min events in (c) and 60-min events in (d). All acronyms are explained in Table 3.1.	52
4.1	(a) Schematic showing the identification of individual rainfall events. (b) Delineated rainfall events in 2010 for the station Würzburg. Point sizes represent precipitation amounts.	60
4.2	Schematic representation of the model street.	61
4.3	Example flow depth dynamics of three rainfall types: (a) drizzle, (b) convective, and (c) continuous rainfall.	63
4.4	(a) Flow depths dynamics of multiple delineated rainfall events; (b) classification of rainfall events corresponding to flow depth categories in a three-dimensional scatterplot (output for Würzburg). Colour coding: grey: events generating no overland flow, green: class 1, yellow: class 2, orange: class 3, red: class 4 (see Tab. 4.2 for threshold values).	64
4.5	Output of the autocorrelation analysis (AutoA method) for Würzburg station for the whole period (1990 – 2020) and all four seasons. The x-axis is in 10 min time steps. Abbreviations: ACF: autocorrelation function. Lines show the mean of ACF for 1990 – 2020 (black), summer (June – August; red), autumn (September – November; orange), winter (December – February; blue), and spring (March – May; green). The dashed horizontal line is the critical correlation for a significance level of 10%.	66

4.6	Development of flow depths with increasing model domain. Each line represents a single rainfall event. Events were chosen with regard to peak intensity, which ranged between 1 and 14 mm/10 min.	67
4.7	Comparison of detected extreme events between (a) the proposed impact-based classification method (red: events of class 4, orange: events of class 3, grey: all other events), and (b) a conventional classification method using rainfall intensity thresholds (red: events selected by using thresholds according to Tab. 4.3, grey: all other events).	68
4.8	Seasonal rainfall frequency distribution of class 4 (first row), class 3 (second row), class 2 (third row), and class 1 (fourth row) events in Würzburg, Hamburg, and Potsdam.	70
4.9	Seasonal (first row) and annual (second row) number of classified storm events for a period of 31 years for Würzburg and Hamburg (1990 – 2020) and for 28 years for Potsdam (1993 – 2020). Colours show events of classes with: no overland flow (grey), class 1 (green), class 2 (yellow), class 3 (orange), and class 4 (red, see Tab. 4.2 for thresholds).	70
5.1	Overview map of study sites (yellow boxes) in the centre of Berlin (yellow star), Germany. Pavement designs are shown in boxes on the right: (1) small concrete pavers, (2) old brick pavers, (3) new brick pavers.	77
5.2	Elevation and depression distribution map of study site 1 with (a) unfilled and (b) filled depressions.	79
5.3	Elevation and depression distribution map of study site 2 with (a) unfilled and (b) filled depressions.	80
5.4	Elevation and depression distribution map of study site 3 with (a) unfilled and (b) filled depressions.	80
5.5	Water depth distribution of all study sites: (a) study site 1, (b) study site 2, and (c) study site 3.	81
5.6	(a) Storage capacity ($\log[m^3]$) of individual depressions for each study site and (b) Cumulative storage capacity (%) plotted against the total area (%). Points in both graphs show individual depressions.	82

List of Tables

3.1	Large-scale atmospheric CTs and CPs according to Werner and Gerstengarbe (2010). (This table shows patterns identified in this study area only.)	47
4.1	Typical parameterisation of a street surface.	63
4.2	Classification of the delineated rainfall events for Würzburg station from 1990 – 2020.	68
4.3	Extreme rainfall events and their threshold values according to DWD (n.d. a, b).	68
5.1	Data of dimension, depression storage capacity, sink area of depressions, and the number of identified depressions for the different real paving system designs analysed using terrestrial laser scanning.	79

Chapter 1

Introduction

1.1 Motivation

Between 1950 and 2018, the world's urban population grew more than fourfold, from ~ 0.8 billion to ~ 4.2 billion (United Nations et al., 2019). Consequent increases in population density and the increasing demands of urban environments have strongly modified the urban water cycle, severely impacting urban water quality and availability. Furthermore, urbanisation fundamentally alters hydrological and surface processes, causing widespread ecological degradation (Russell et al., 2019).

The urban landscape has a noticeable impact on meteorological, hydrological and pollutant dynamics. Meteorological dynamics are known to be affected by a changing climate, but also urban characteristics. The concentration of heat-absorbing materials, heat-generating processes, and the lack of cooling vegetation contribute to increased temperatures in urban areas (urban heat island (UHI) effect) and impact rainfall proliferation (Oke, 1982; Pagenkopf, 2011). Indeed, the UHI effect has been shown to increase convective summer storms in areas downwind of cities (Ashley et al., 2012; Bentley et al., 2010). Furthermore, the presence of natural and anthropogenic aerosols, which contribute to thermal insulation and act as condensation nuclei for cloud-microphysical processes, can similarly impact or heighten such dynamics. These atmospheric changes profoundly impact the magnitude, variability, and frequency of rainfall events, not just within a city or urban environment but also at regional scales (Burian and Shepherd, 2005). Therefore, there is a pressing need to understand the impact these changes have on rainfall events, the spatiotemporal scales at which they occur, and the consequence of such events (e.g., on stormwater infrastructure, flood risk, and water quality).

A changing regime of high-intensity storms directly affects the hydrological and pollutant dynamics in urban areas, which constitute a complex patchwork of impervious and pervious

surfaces (e.g., sidewalks, roads, roofs, and artificial and natural green spaces). They are sources for a suite of contaminants, so-called diffuse pollutants (e.g., heavy metals, nutrients, litter, rubber residue, microbial contaminants, synthetic chemicals, and pharmaceuticals), harmful to humans and aquatic ecosystems. Historically, conventional (centralised) urban stormwater management practices were considered the most practical solution to urban drainage water and diffuse pollution by removing water as fast as possible. In the past three decades, however, a paradigm shift has taken place, from getting rid of runoff towards retaining it by employing so-called Water Sensitive Urban Designs (WSUD), also known as Low Impact Developments (LID), or Nature Based Solutions (NBS) (Tuomela et al., 2019). They are Sustainable Urban Drainage Systems (SUDSs) that are awarded multiple benefits, e.g. stormwater pollution management, flood mitigation, waterway health protection, microclimate improvement and enhancing the amenity of urban landscapes (Deletic et al., 2019). However, to achieve these benefits, a better understanding of pollution patterns, pollution transport processes, and relevant impact factors, like intense rainfall and urban surface representation, is first required.

Widespread impervious surfaces in urban areas significantly influence hydrological dynamics by altering surface-runoff and runoff-generating processes (Rim, 2011). Generally, impervious surfaces have demonstrated increased runoff volumes, reduced runoff lag times, increased flood return periods and elevated peak discharges during storm events (Aryal et al., 2007). However, runoff, infiltration, and pollutant transport are affected differently by the nature of surface materials (Ragab et al., 2003; Mansell and Rollet, 2009) and rainfall characteristics (Rim et al., 2010), leading to complex hydraulic runoff and pollutant dynamics that are not fully understood. This lack of understanding can be attributed, among other things, to the simplified representation of non-ideal urban surfaces in hydrological models, for example the inaccurate representation of relevant surface characteristics such as depression storage.

Pollutant transport is strongly dependent on the hydrological and structural connectivity of urban surfaces. Structurally connected urban surfaces facilitate the transport and redistribution of pollutants, even during moderate rainfall events. In contrast, transport is hindered as the urban landscape becomes more heterogeneous, requiring higher rainfall intensities. In other words, the grade of hydrological and pollutant connectivity is strongly dependent on the level of structural connectivity (Turnbull et al., 2018). Furthermore, the issue of scale is critical. Localised alterations to gradients and surfaces can affect how water and pollutants are detained and routed across areas. Whilst the local response of surfaces may dampen out at larger scales, local pluvial flooding may occur in some instances where flat, impervious surfaces with low runoff ratios (such as bitumen), depressions, clogged gullies and slopes are present. While large depressions may contribute to pluvial flooding, depressions of all sizes can act as retention elements (buffer), preventing runoff and storing water until its capacity is reached. These elements are often seen as critical source areas of

diffuse pollution, as pollutants get retained. However, the interplay between structural, hydrological, and pollutant connectivity in urban areas remains, to date, poorly understood and a critical area of further research.

This thesis aims to contribute to urban pollution mitigation management by explicitly addressing to current research gaps regarding the spatial and temporal patterns of contaminant fluxes, the occurrence and impact of high-intensity rainfall events, and the impact of realistically represented non-ideal, impervious urban surfaces on runoff.

1.2 Diffuse pollution and connectivity in urban areas

Good quality freshwater is essential for human health, for promoting healthy and biodiverse aquatic ecosystems, and for agriculture and food production, three major components of the European Green Deal (European Commission, 2021). Despite significant progress in reducing conventional water pollutants and improving freshwater quality, pollution loads from urban point and non-point sources, the main two categories of pollution identified by environmental protection agencies, remain a critical challenge (National Geographic Society, 2019).

While point-source pollution is defined as any contaminant that enters the environment from an easily identified and confined place (Dressing, 2018), non-point source pollution, or diffuse pollutants, cannot easily be attributed to a single source, enter the environment over an extensive area and sporadic timeframe, and are related, in part, to certain uncontrollable meteorological events (Loague and Corwin, 2005). Hence, they are more complicated to monitor and mitigate against, particularly in urban areas, which are spatially and temporally highly heterogeneous and dynamic. Here, diffuse pollution originates from multiple sources stemming from the complex city layout. Extensive reviews by Duncan (1995) and Göbel et al. (2007) describe the wide range of diffuse pollutants, they include heavy metals, oil and organic salts from roads, sidewalks, car parks and roof surfaces, organic and anthropogenic litter from urban green (gardens, yards, street trees) and the deposition of atmospheric contaminants (Fig. 1.1). Another crucial source of diffuse pollution is the sewer network, which can discharge wastewater, a mixture of surface runoff and raw sewage containing microbial pathogens and micropollutants, through combined sewer overflows during periods of extreme rainfall.

Once present within a catchment, diffuse urban pollutants can be mobilised during rainfall events (Eriksson et al., 2007). As rainfall flows over impermeable and, to a lesser extent, permeable surfaces, it can mobilise and transport pollutants from various sources (including those previously identified). Critical source areas can occur where diffuse pollution sources coincide with high mobilisation potential and hydrologically sensitive areas, with the highest propensity for surface runoff generation, pollutant transport, and delivery via

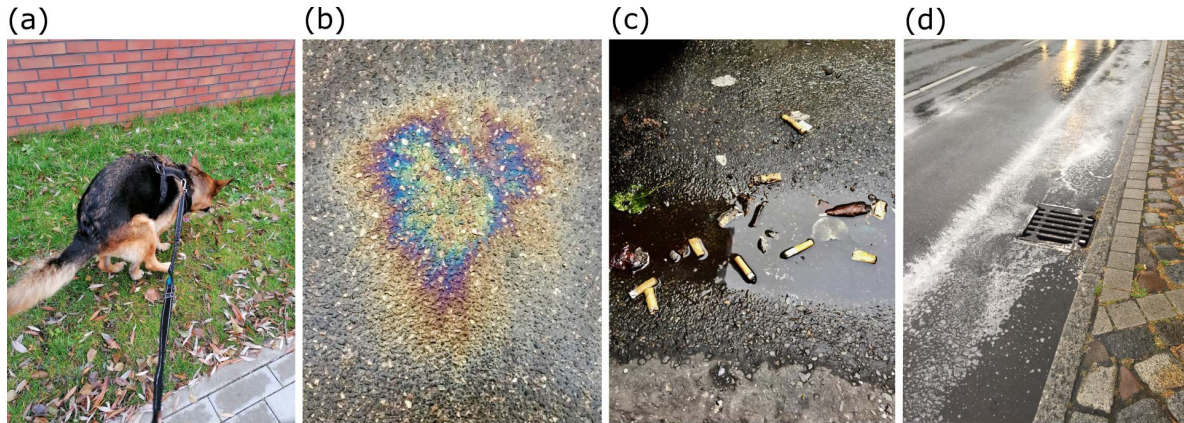


Figure 1.1: Animal faeces (a), car oil spills (b), cigarette butts (c), and organic litter in combination with tyre abrasion products forming foam (d) as examples of diffuse urban pollution.

hydrologically connected pathways (Thomas et al., 2016). Key factors influencing the load of pollutants mobilised during a particular event include current and historical land use activities (e.g. industrial, commercial, highways, residential), the nature of a catchments surface (e.g. permeable, impermeable, surface texture and depth), the intensity and frequency of rainstorms (Duncan, 1995; Corada-Fernández et al., 2017) and the weather conditions between storms, as well as the inherent biological and chemical characteristics of the pollutants themselves (Lundy and Wade, 2013). Hence, the amount of diffuse urban pollution mobilised can be highly variable, even within a single catchment area (Lundy et al., 2012).

The concept of connectivity has been used in many disciplines to explain functioning of complex systems and has proven to be a particularly valuable concept in both research and management (Turnbull et al., 2018). Generally, connectivity can be defined as the degree to which a system facilitates the movement of matter and energy through itself (Connecteur WG 1, 2018). The study of connectivity is frequently divided into structural and functional connectivity (Turnbull et al., 2008; Bracken and Croke, 2007). Here, structural connectivity describes the extent to which units are physically linked or connected (Bracken et al., 2013), and functional connectivity describes dynamic processes operating within structurally connected units and thus allows the transport of water (hydrological connectivity) and matter (pollutant connectivity) between sources and outlets (Wainwright et al., 2011). In rural catchments, the concept of connectivity has successfully been applied for understanding processes involved in pollutant transfer across multiple scales.

In urban catchments, dynamic processes occur mainly on and between pervious and impervious urban surfaces and between these surfaces and the urban drainage system. These elements become increasingly hydrologically connected during high-intensity events (Fig. 1.2). However, runoff and pollution transport can respond differently to different storm

events (Wainwright et al., 2011). Impervious areas can produce runoff and deliver pollutants already in minor rainfall events, whereas pervious areas only contribute runoff and pollutants intermittently, depending on event magnitude and the presence and strength of different elements in urban watersheds. These elements (e.g., swales, blocked gullies, rain gutters) can slow, prevent, or accelerate the transport of water and pollution. The presence of cracks and other forms of surface modification, like depressions, generated due to subsurface roots growth or careless construction work, additionally impact runoff and pollutant pathways. However, hitherto, the impacts of these non-ideal structures have not been analysed.

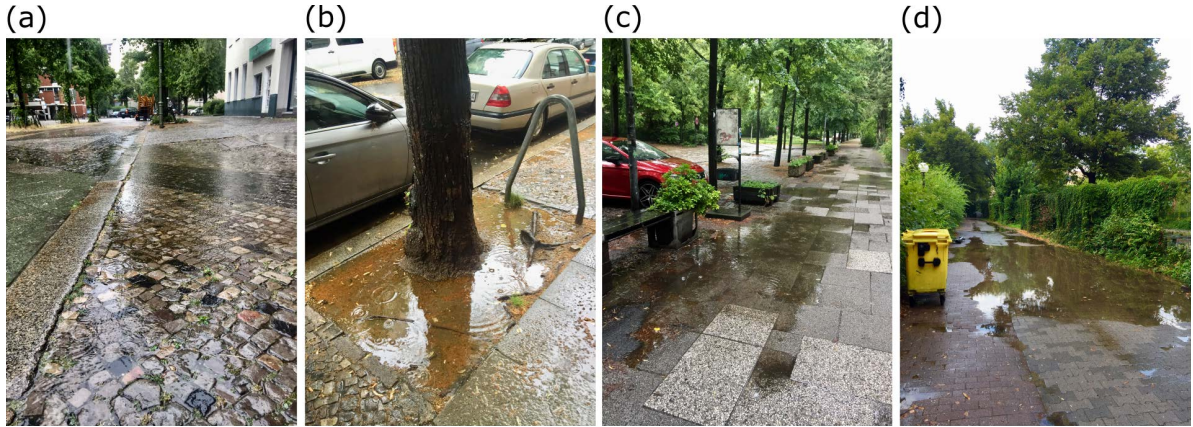


Figure 1.2: Hydrologically well connected different urban surfaces during a heavy rainfall event (a), runoff retained in tree pit with lime blossoms (b) and in depressions in urban surfaces (c, d).

Generally it can be said, that pollutant connectivity is strongly influenced by structural and hydrological connectivity (Bracken and Croke, 2007). Within urban catchments, however, feedback and interactions are highly complex and our current understanding of urban connectivity is still limited. More investigation and quantification is needed regarding the impact of the above mentioned key factors on water and pollutant transfer. In this thesis, two of them, surface texture and rainfall events, are examined more thoroughly.

1.3 Extreme rainfall

Extreme rainfall is one of the most costly and dangerous natural hazards worldwide and is characterised by precipitation events of large intensity in relation to their duration (Müller and Pfister, 2011). Definitions of extreme rainfall depend on the field of application and are typically dictated by field- and study-specific objectives. Therefore, there is no precise definition of extreme rainfall (Seneviratne et al., 2012; Stephenson, 2008).

Popular definitions of rainfall extremes include 11 indices recommended by the Expert Team on Climate Change Detection and Indices (ETCCDI; Zhang et al., 2011; Peterson, 2005) and are either based on threshold exceedance or the probability of occurrence of given

quantities. These include the number, percentage, or fraction of hours or days with maximum precipitation sums above a fixed threshold or above the 90th, 95th, or 99th percentile, generally defined for given time frames (days, month, season, annual) (Peterson, 2005). Alexander et al. (2019) provide more information on how and why these indices are used, including their misuse. One advantage of using predefined extreme indices is that it allows for comparisons across regions and modelling and observational studies. Indeed, collaborative international efforts to monitor extremes using extreme indices are ongoing (Peterson and Manton, 2008). However, extreme indices used in the scientific literature typically reflect ‘moderate extremes’, for example, events occurring 5 - 10% of the time (Seneviratne et al., 2012).

More extreme ‘extremes’ are often investigated using Extreme Value Theory (EVT). EVT is an approach used to estimate extreme values (e.g., Coles, 2001) by deriving a probability distribution of events from the tail of a probability distribution, that is, its far upper or lower ranges. Such events occur less frequently than once per year or per period of interest, i.e., generally less than 1 to 5% of the considered overall observation period. EVT is used to derive a complete probability distribution for such extreme events, which can also help identify the probability of an event occurring outside of the observed data range. Two different approaches can be used to estimate the parameters of such probability distributions. In the block maximum approach, parameters are estimated for maximum values of consecutive blocks of a time series (e.g., years). While for the peaks over threshold approach, the estimation is based on events that exceed a high threshold. In Germany, for example, there is a warning of extreme rainfall at ≥ 40 mm per hour or ≥ 60 mm within six hours (Deutscher Wetterdienst (DWD), n.d.[b]). The return period, or recurrence interval, is another metric used to analyse the frequency of extreme rainstorms. It is defined as the average time length between two events of the same or greater magnitude and can be derived from quantiles of a parametric probability distribution fitted to the extreme values of the recorded data.

Independently of the chosen method of analysis, all definitions of rainfall extremes are limited in their relationship to impacts (Seneviratne et al., 2012). This is due to the following reasons: 1) an event from the extreme tails of a probability distribution is not necessarily extreme in its impact; 2) impact-related thresholds can vary in space and time; that is, single absolute thresholds will not reflect extremes across space and time (e.g., season, decade); 3) events that are not extreme in a statistical sense can lead to extreme conditions or impacts by co-occurring with other events or adverse catchment conditions.

Extreme conditions associated with extreme rainfall are flooding (see Section 1.3.3) and landslides, which can threaten human life, damage buildings and infrastructure, disrupt transport and communications and cause damage to crops and livestock. However, the temporal scales of extreme rainfall relevant to specific impacts vary enormously between areas (Westra et al., 2014). For flood events, rainfall intensities that occur over several hours or days are relevant. For flash floods, sub-daily rainstorm events of very short duration

(10-min to a few hours) with very high intensities are significant and particularly hazardous in small mountainous and urban catchments as they occur with little warning (De Toffol et al., 2009). Cities are particularly vulnerable to such floods (Arnbjerg-Nielsen et al., 2013) because urban drainage infrastructure systems are typically outdated, have insufficient capacity to cope with contemporary runoff volumes and have an increase in impervious areas (Fig. 1.3). Furthermore, the most severe water quality impacts from diffuse pollution in urban catchments occur during extreme rainfall (particularly after a dry spell), when rainfall induces enhanced runoff of pollutants into the waterways.



Figure 1.3: A flooded train station after extreme rainfall (a) and a flooded street due to blocked drains (b), both in Berlin.

Studies have shown that rainfall extremes (independent of the definition) are now occurring more frequently and with increased intensity in many parts of the world due to a warming climate (Westra et al., 2013; Fischer and Knutti, 2016; Guerreiro et al., 2018; see Section 1.3.2). Variations in climate are induced by internal variability and external forces, both natural, such as changes in solar irradiance and volcanism, and anthropogenic, such as greenhouse gas and aerosol emissions, principally due to the burning of fossil fuels, and land use and land cover changes (Seneviratne et al., 2012). Relevant large-scale impacts of external forcing include net temperature increases, enhanced atmospheric moisture content, and increased land-sea contrast temperatures, affecting atmospheric circulation (Allan et al., 2020). Central to understanding increases in extreme rainfall due to climate warming is the Clausius–Clapeyron (CC) relation, which states atmospheric saturation specific humidity increases at a rate of $\sim 7\%$ per degree of warming (K^{-1}) near the Earth’s surface. As rainfall extremes are limited by the amount of atmospheric moisture content available, rainfall frequency and intensity changes are expected to scale with the CC relation (Trenberth et al., 2003).

However, changes in extreme rainfall are not uniform in space and result from multiple interacting factors at both large and regional (local) scales; they thus vary by region (Tabari, 2020). The Intergovernmental Panel on Climate Change (IPCC) Fifth Assessment Report (AR5) concluded that “it is likely that since 1950 the number of heavy rainfall events over

land has increased in more regions than it has decreased” (Pachauri et al., 2015). This is based on multiple studies showing that extreme rainfall over land has intensified on average, with about two-thirds of rainfall stations showing increases in daily precipitation (Groisman et al., 2005; Alexander et al., 2006; Westra et al., 2013).

While there are advances in understanding changes to daily extremes, drivers and patterns of sub-daily (up to a few hours and sub-hourly) extremes and how they might change in the future are still not fully understood. There is general agreement that atmospheric temperatures can lead to more extreme and short-duration rainfall and that sub-daily extreme rainfall is intensifying more rapidly than rainfall measured at daily time scales (Lenderink and van Meijgaard, 2008; Haerter et al., 2010; Berg et al., 2013). Sub-daily extremes are often initiated by convective storms when warmer air at the Earth’s surface rises quickly on a hot day in colder surroundings. As it ascends, it cools and forms enormous cumulonimbus clouds (Fig. 1.4).

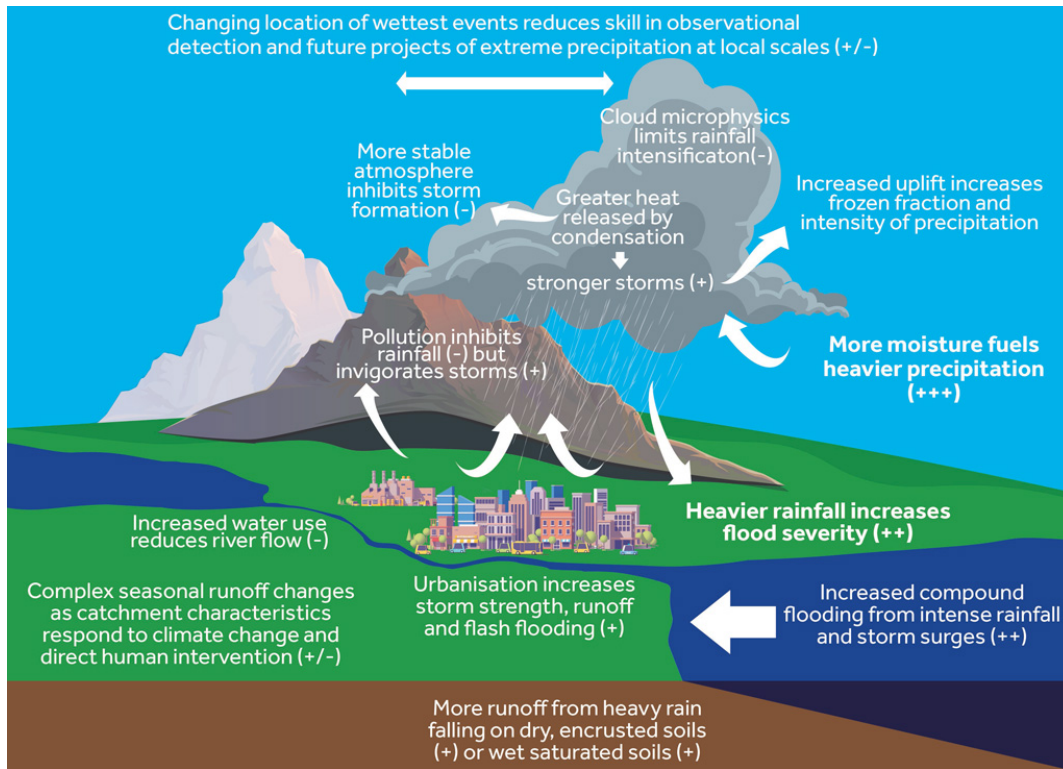


Figure 1.4: Flood processes that are impacted by changes in sub-daily extreme precipitation. The most dominant processes with the highest certainties are in bold, while those with positive (+) and negative (-) contributions are also identified (Wasko et al., 2021).

Potential drivers influencing convective storms are orography (Siler and Roe, 2014; Siler and Durran, 2016; Li, 2018), weather types (Moron et al., 2019), propagation of moisture convection (Ploshay and Lau, 2010), coastal effects (Kikuchi and Wang, 2008), land-use changes including deforestation (Lawrence and Vandecar, 2015), and urbanisation (Lorenz et al., 2019) through increases in anthropogenic aerosols (Schmid and Niyogi, 2017; Zhao

et al., 2019) or the UHI effect (Wu et al., 2019; Li et al., 2020). Indeed, the latter has emerged as a nascent research area. Niyogi et al. (2006) and Ganeshan et al. (2013) found a dominant influence of the UHI on the diurnal precipitation cycle, shifting rainfall events in cities to afternoon and night. Other factors like urban size and structure (Kingfield et al., 2018), different climate zones, or entangling factors also cause heavier rainfall regimes. Studies, for example, evaluated urban modification of storms within coastal cities (Comarazamy et al., 2010; Shepherd et al., 2010; Hosannah and Gonzalez, 2014), cities located near artificial reservoirs (e.g., Haberlie et al., 2016), or in deserts (Diem and Brown, 2003), and cities with complex terrains (Freitag et al., 2018).

Detecting changes in extreme rainfall from convective storms is complicated as sub-daily datasets are not widely available and often only cover short periods (see Section 1.3.1). However, understanding sub-daily extreme rainfall from both a scientific and impact-centred perspective is crucial for flood risk management and effective pollution mitigation management in urban catchments.

1.3.1 Data availability

An essential criteria constraining data availability when analysing extreme rainfall is the respective time scales on which they occur since this determines the required temporal resolution for their assessment. For most parts of the world, precipitation data with extensive temporal resolution (e.g. monthly, seasonal and annual values) is available from the late 19th to early 20th century, facilitating the analysis of unusually wet periods of a month or longer. To examine changes in extreme precipitation over short time scales, high-resolution temporal data, such as daily or sub-daily observations, is required. Typically, however, such data does not exist, or if it does, it does so for a minimal, contemporary period, at best from the 1950s, but in many regions from the 1970s (Trenberth et al., 2007; Seneviratne et al., 2012). In Germany, for example, ~6,000 rain gauges record daily data, of which ~3,800 (63%) have records dating back 40 years or more. In contrast, only ~1,400 rain gauges record sub-daily data, with records dating back 16 years (Climate Data Center, 2021). Consequently, a large-scale initiative to collect and collate sub-daily precipitation data across multiple continents, the Global Sub-Daily Rainfall (GDSR) dataset (Lewis et al., 2019), was recently undertaken (Fig. 1.5). Even when sufficient data is available, several problems can still limit analysis and interpretation. Firstly, many countries do not freely distribute their highest temporal resolution data. Secondly, there can be issues with measurement quality. And thirdly, the homogeneity of precipitation data varies spatially within a country, resulting in patchy coverage.

Another common source of daily and sub-daily precipitation data is spatially interpolated rain gauge measurements (Rauthe et al., 2013; Paulat et al., 2008). However, the resolvable

spatial resolution is highly dependent on the density of rain gauges, which, for conventional networks, is insufficient to resolve the strong precipitation gradients associated with sub-daily rainfall, especially in mountainous regions (Panziera et al., 2018). In recent years, radar-derived precipitation measurements have also been utilised due to the continuous improvements in the algorithms used for quantitative precipitation estimates and the availability of time series radar data with sufficient homogeneity. However, radar-based time series are short in duration, often only spanning a decade (Panziera et al., 2018), and are therefore not suitable for tracking long-term changes in precipitation.

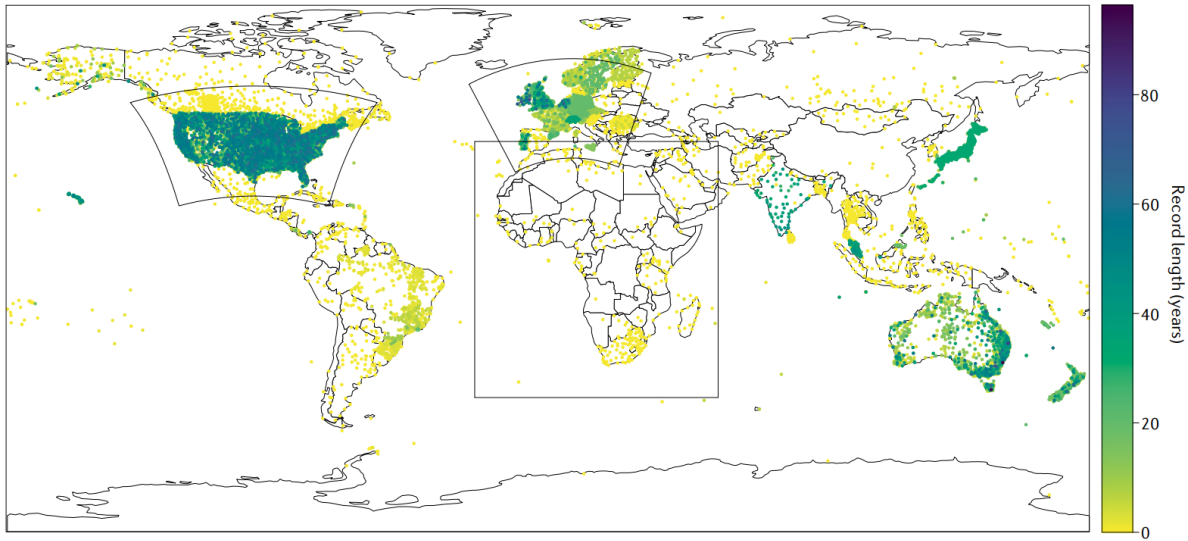


Figure 1.5: Availability and length of existing sub-daily precipitation data sets across the globe (Lewis et al., 2019). Dots indicate rain gauge locations and are coloured by record length, that is, the time between the initial and the last recorded values, respectively. Black boxes represent current continental-scale convection-permitting model domains at a horizontal grid spacing of <5km (Fowler et al., 2021).

1.3.2 Spatial and temporal variability of extreme rainfall

A changing climate leads to variability in the frequency, intensity, spatial extent, duration, and timing of weather and climate extremes and can result, among other things, in unprecedented extreme rainfall. The IPCC's Fifth Assessment Report (Pachauri et al., 2015) highlights an intensification of extreme rainfall events in North America and Europe and projects further increases in extremes as global temperatures rise (Collins et al., 2013). Furthermore, observational studies indicate that at higher temperatures, the peak intensity of rainfall events will increase; yet changes in their size are location-dependent, decreasing in Australia (Wasko et al., 2016) and Germany (Haerter et al., 2010) but increasing in the Netherlands (Lochbihler et al., 2017) for example. However, the detection of trends is dependent on the chosen definition of extreme events, which creates challenges when interpreting results, especially when comparing across studies. Furthermore, the study of

extreme rainfall events is complex, owing to the spatiotemporal heterogeneity of rainfall intensities and, as previously discussed, the lack of sufficient data resolution and observation density. The World Meteorological Organization (World Meteorological Organization, 2018) recommends the non-parametric Mann-Kendall test and Sen’s slope estimator test for statistical trend detection. A Mann-Kendall test determines a consistently increasing or decreasing trend, whereas a Sen’s slope test assesses the magnitude of change. The primary outcomes of independent studies focussing on the spatial and temporal variability of extreme rainfall across the globe are summarised below.

Across the continental U.S., both hourly and daily rainfall extremes have significantly increased over the last six decades (Barbero et al., 2017), though trends are more apparent in daily extremes than in hourly extremes. Strong seasonality is also evident, with widespread increases in the magnitude and frequency of hourly and, to a lesser extent, daily extremes during winter. An increase during summer was also projected for both hourly and daily extremes across the U.S. (Harding and Snyder, 2015); however, this has only been observed for eastern and central regions (Pryor et al., 2009; Kunkel et al., 2013; Mallakpour and Villarini, 2015).

In Australia, a continental increase and intensification of daily and hourly rainfall was detected at a multi-decadal time scale (Guerreiro et al., 2018). However, only increases observed at the daily scale were within the range associated with natural variability. In a study by Dare and Davidson (2015), the largest inter-seasonal variation in the frequency of daily heavy rainfall events was detected in tropical and subtropical zones, with the highest frequency in summer. In the midlatitude zone, primarily along Australia’s southeast coast, the smallest inter-seasonal variation and highest frequency occur in winter and spring.

For daily precipitation records in China, an increase in heavy rainfall (Ma et al., 2015) has been detected across the country. Though large, distinctive regional and seasonal patterns (Zhai et al., 2005) are evident due to the country’s complex topography and extensive zonal and meridional range (Xu et al., 2015; Miao et al., 2016; Sun et al., 2017). Increases in rainfall intensities dominate eastern China; in contrast, southwestern China exhibits a significant drying tendency (Xiao et al., 2017). Furthermore, a decrease in summer precipitation has been observed in both north and south China (Xu et al., 2015). These results contradict the upward trend in summer maximum hourly rainfall (Xiao et al., 2017).

In Europe, the number of days with extreme rainfall has increased on average by 45% when comparing the periods 1951-1980 and 1981-2013 (Fischer and Knutti, 2016). Using gridded daily rainfall data across Europe, a positive and negative scaling rate of extreme rainfall with temperature has been reported in winter and summer, respectively (Zeder and Fischer, 2020). These observations correspond with results from Central Europe, where trend analysis of daily rainfall data from 1950 to 2000 signifies a general increase in extreme events during winter,

spring and autumn and a decrease in rainfall during summer (Hundechea and Bárdossy, 2005; Zolina et al., 2008). Conversely, sub-daily rainfall extremes in central and southern Europe are most common in summer (European Environment Agency, 2019). Like daily rainfall extremes, sub-daily extremes have also increased across Europe, even in regions with decreased mean rainfall, but there is large variability across regions and seasons (Westra et al., 2014).

More specifically, in the United Kingdom (UK), historical trends in daily and multi-day extreme rainfall events have been extensively studied. More intense winter rainfall has been observed since the 1960s (Osborn and Hulme, 2002; Maraun et al., 2008), especially in northern and western parts of the UK (Jenkins et al., 2009), with some evidence of an even longer-term trend starting from the 1930s (Osborn and Hulme, 2002; Simpson and Jones, 2014). In contrast, extreme summer daily rainfall events have shown little change or have even declined in intensity throughout most of the UK (Fowler and Kilsby, 2003). This pattern was confirmed by Jones et al. (2013), who found an increased frequency of extreme daily rainfall events in the UK during spring, autumn, and winter, but a decrease in summer. Blenkinsop et al. (2017) summarised the climatology of UK hourly extremes, noting that the highest frequency and intensity of hourly extreme rainfall events occur in summer, with most events during the late afternoon (excluding winter), a pattern also observed for convective precipitation (Darwish et al., 2018). In addition, Hand et al. (2004) reported that extreme rainfall events are unlikely to occur in February, March, and April, with convective events most likely in June, July, and August.

In Germany, a general increase in daily extreme rainfall has been detected, although this is spatially variable, and opposing trends are evident (Poschlod and Ludwig, 2021; Deumlich and Gericke, 2020). Eggert et al. (2015) used radar data to analyse the temporal and spatial scaling of extreme convective and stratiform rainfall. They found that convective extremes were considerably more frequent in South Germany than in North Germany, with apparent seasonal differences, the highest occurrence in summer. Conversely, stratiform extremes showed much less regional and seasonal variability. Lengfeld et al. (2019) also found variability in the spatial extent of Germany’s hourly and daily rainfall events. They observed a positive correlation between daily extremes and mountainous regions, which dominate South Germany. However, the distribution of hourly extremes was more random and not linked to orography. Although, short-term convective systems were more prevalent in the eastern part of the Northern Lowlands, around the city of Berlin. This observation is consistent with extensive studies by Pagenkopf (2011) and Lorenz et al. (2019), who evaluated the spatiotemporal variability of rainfall within Berlin and identified that urbanisation impacted rainfall intensity and duration. However, the temporal variability of intense, short-duration (hourly and sub-hourly) rainfall events and the spatial scales at which they occur, i.e. within a city or country, remain uncertain and require further research.

1.3.3 Implications of extreme rainfall

An increase in the frequency of extreme rainfall is often associated with a corresponding increase in flooding. Yet, global-scale flood assessments have predicted increases and decreases in future floods as a consequence of global warming (Allan et al., 2020; Arnell and Gosling, 2016; Hirabayashi et al., 2013), albeit using varying hydrological and climate models, scenarios, bias-correction methods, and flood indicators. Consequently, a common perspective on future flooding is problematic (Kundzewicz et al., 2017). Indeed, the response of flooding and streamflow (e.g., peak flow rate) to changing rainfall characteristics (e.g., rainfall volume) under global warming is complex and non-linear (Allan et al., 2020; Stephens et al., 2015). This non-linearity is strongly influenced by other factors, including storage components, such as land surface and subsurface memory (groundwater, soil moisture, snow cover, snowmelt, rain-on-snow, rain-on-ice), transfer components, such as the interaction between spatial and temporal rainfall patterns and the configuration of river networks, surface properties and characteristics (terrain, vegetation, degree of imperviousness and channelization), and artificial interventions, such as reservoirs (Stephens et al., 2015; Westra et al., 2014). As most of these factors are also subject to climate change, the complexity and diversity of flood-generation processes, including direct human influence on catchment characteristics, are growing. Thus, it is impossible to directly extrapolate the intensification of rainstorm events to changes in flood hazards.

Generally, a flood is defined as “the overflowing of the normal confines of a stream or other body of water, or the accumulation of water over areas not normally submerged. Floods include fluvial (riverine, river) floods, flash floods, pluvial (urban) floods, coastal floods, and glacial lake outburst floods” (Seneviratne et al., 2012). Fluvial floods commonly emerge in large catchment areas after persistent rainfall or snowmelt, which leads to high surface and groundwater runoff and relatively slow-rising water levels. Flash floods are rapid flood events caused by intense, timely and concentrated precipitation, potentially augmented by orographic features (Gaume et al., 2009; Borga and Morin, 2014). According to Gaume et al. (2009), flash floods are triggered by diverse hydrological and meteorological processes and are associated with higher fatalities than riverine and pluvial equivalents. Flash floods usually occur in mountainous regions, where they can trigger debris flows and/or hyperconcentrated flows (Laudan et al., 2017). In contrast to riverine floods, flash floods originate from catchments where geographical features, such as steep slopes and defined channels, result in rougher flow dynamics such as velocity, sediment transport and discharge (Borga and Morin, 2014). Here, potential damage to buildings occurs through erosion and physical impacts, which are not distinct damage patterns of fluvial flooding (Kreibich and Thielen, 2009). Pluvial floods are more frequent in urban areas and are typically caused by overwhelmed sewer systems and surface runoff after high-intensity rainfall events (Maksimović et al., 2009, Fig. 1.6a). They are thus a leading cause of water quality

deterioration in surface water bodies. Increased nutrients from sewer overflows and wastewater treatment plant effluent can cause eutrophication in receiving water bodies (Rui et al., 2018), leading to significant algal and cyanobacterial blooms in lakes and reservoirs (Jackson et al., 2007; Komatsu et al., 2007). Extreme rainfall is also linked with increases in pesticide and sediment release of pharmaceuticals and pathogens in surface waters (Bloomfield et al., 2006; Lissemore et al., 2006; Zhu et al., 2005; Oppel et al., 2004). However, the effect of inundation on urban surface water quality is usually temporary and highly dependent on the type and concentration of pollutants in stormwater runoff (Rui et al., 2018). Suspended Solids (SS), Biochemical Oxygen Demand (BOD), Chemical Oxygen Demand (COD) and Dissolved Organic Carbon (DOC) usually tend to increase during the flood phase and then return to pre-flood levels (Rui et al., 2018). Furthermore, pluvial flooding can lead to groundwater contamination and disease outbreak. For example, in the United States, over the last 50 years, half of the waterborne disease outbreaks occurred after an extreme rainfall event (Charron et al., 2004; Hunter, 2003; Curriero et al., 2001).

In Europe, flood damage has grown considerably, and many destructive floods have been recorded in recent decades (Kundzewicz et al., 2017). More intense and concentrated rainfall in central Europe is predicted to increase severe flash floods, impacting regions previously not prone to flooding in mountainous but also upland regions (Laudan et al., 2017). Most catastrophic floods recorded across Europe have been linked to persistent atmospheric circulation patterns (Lenggenhager et al., 2019; Zanardo et al., 2019), leading to increased atmospheric moisture with the potential to amplify the severity of rainfall extremes (Murawski et al., 2016; Laudan et al., 2017). However, flood projections are not always in agreement at local and regional scales. A European study by Alfieri et al. (2015) concluded that, on average, flood peaks with return periods greater than 100 years are projected to double in frequency within three decades. This largely corroborates findings by Rojas et al. (2011, 2012) and Roudier et al. (2016) but contradicts projections of changes in flood hazards by Hirabayashi et al. (2013), who indicated flood frequency would decrease in Northern, Central and Southern Europe.

The most recent severe flood in Europe occurred between 12 and 25 July 2021, affecting 12 countries (Austria, Belgium, Czech Republic, Croatia, France, Germany, Italy, Luxembourg, Netherlands, Romania, Switzerland, the United Kingdom; Fig. 1.6b). Two hundred and forty-two people lost their lives, and ~€10 billion worth of property damage was caused. In Germany, particularly the states of North Rhine-Westphalia and Rhineland-Palatinate, a coincidence of adverse conditions, including intense rainfall caused by cyclone Bernd (12 to 15 July 2021), saturated soil and catchments with steep-sided slopes, led to the proliferation of streams and subsequently flash floods (Thieken et al., 2021; Junghänel et al., 2021). Similar adverse and unfavourable conditions led to severe flooding in May 2016 in the catchment area of the Orlacher Bach in Braunsbach, a municipality in southern Germany (Laudan et al., 2017).



Figure 1.6: (a) Three women walking through flooded streets in Berlin after days of heavy rainfall (Christianthiel.net, 2017) and (b) drone view of streets and houses heavily damaged by historic floods in Rochefort, Belgium in July 2021 (Great Pics – Ben Heine, 2021).

1.4 Aim and research objectives

The overarching aim of this thesis is a better understanding of the spatial and temporal patterns of pollution fluxes in urban catchments as well as the identification of critical source areas of diffuse pollution to help mitigate against the degradation of urban water bodies, their ecosystems and public health. To reach this aim, the concept of connectivity was transferred to urban settings for the first time. Then, heavy rainfall events were analysed regarding their spatiotemporal occurrence for the area of Germany and their impacts on an urban surface as they are considered the most influencing events regarding pollution mobilisation and distribution. Finally, non-ideal (realistic) urban surfaces were analysed in more detail to better understand the impact of surface modifications on rainfall-runoff responses.

The specific objectives of this thesis are:

Objective 1: Collation of current knowledge regarding patterns and processes of diffuse pollution in urban watersheds, and assessment of urban functional and structural connectivity.

Sustainable management of urban waters has not yet been achieved due to a lack of knowledge on diffuse pollution source areas and their pathways to urban waterways and water bodies (e.g., streams, rivers, and groundwater). The aim of this objective is to contribute to these knowledge gaps by collating literature on the spatial patterns of diffuse pollution, temporal dynamics of diffuse pollution, and distribution processes of diffuse pollution within urban catchments. Furthermore, it will be examined how patterns and processes of urban diffuse pollution can be theoretically merged within a hydrological and pollutant connectivity framework to practically enhance future management of urban waters. In a final step, knowledge gaps and future

research directions will be listed to help guide future research and urban drainage strategies to achieve sustainable water management, and at the same time, avoid repeating past urban drainage mistakes.

Objective 2: Analysis of the temporal occurrence of short and heavy rainstorms and categorisation of the prevailing large-scale atmospheric circulation patterns for 22 meteorological stations across Germany.

Knowledge about the timing of short and extreme rainstorms for all time lines (day, season, year) is important for several reasons: it provides emergency services and highway patrols with more detailed information to plan emergency responses, it facilitates the optimisation of street cleaning schedules and routines to reduce drain clogging (e.g., organic litter production, waste products) and thus localised urban flooding, and it assists research by quantifying the dynamics of flash floods and diffuse pollution in situ. However, little is known about the timing of sub-hourly to hourly rainstorm events. This objective aims at filling this knowledge gap by assessing the diurnal, seasonal and annual distribution of sub-hourly and hourly rainstorm events over the last 20 years for multiple urban centres across Germany. Additionally, large-scale atmospheric circulation patterns occurring during these events will be investigated as a first trend indicator for future risk assessment.

Objective 3: Development of a new rainfall classification method based on individual rainfall event impacts of generated overland flow on a simplified urban model surface.

A widely used approach is to classify rainfall events by intensity and use this as an indirect indicator of their impact. This objective assumes that the impact of rainfall events is not sufficiently described by their intensity, leading to the misclassification of rainfall events. This hypothesis is consistent with the misinterpretation of rainfall events by considering intensities only (Dunkerley, 2008, 2017, 2020), as well as with the sensitive relationship between event characteristics and overland flow generation in highly sealed areas (Moftakhari et al., 2018). A new and impact-based classification approach will be developed to test this hypothesis. It will include rainfall event delineation from high-resolution time-series data, the computation of overland flow depth for each individual rainfall event using a simplistic urban model surface and a new rainfall event classification as a function of overland flow. The ability of this classification approach to describe seasonal and annual occurrences of classified rainfall events and variations in rainstorm impact will be evaluated using high-resolution time-series data from three different urban stations in Germany.

Objective 4: Quantification of the depression storage capacity of different real urban surfaces using a terrestrial laser-based method.

Urban runoff is often overestimated due to the poor characterisation of the heterogeneous

nature of urban surfaces in urban runoff models. This is because little attention has been given to understanding rainfall-runoff partitioning on urban surfaces and the role of urban topography on a sub-meter scale, particularly meso-topographical structures like sinks generated by, e.g., root growth or subsoil consolidation. This objective aims to spatially identify and quantify the storage capacity of depressions on three different urban study sites in Berlin and to evaluate the contribution of individual depressions to the total storage capacity. Results will help better understand pollution transport processes and the formation of critical source areas. A terrestrial laser scanner (TLS) will be used to collect high-resolution (millimetre range) morphological surface data, which will be processed in a Geographic Information System (GIS). This method and approach were tested and validated for 11 ideal pavements on a plot scale by Nehls et al. (2015).

1.5 Outline of this thesis including articles

This thesis is structured into seven chapters consisting of the introduction (**Chapter 1**), three peer-reviewed journal articles, of which two are published and one submitted for publication, one pilot study, and a synthesis (Fig. 1.7).

Chapter 2 (Objective 1): Paton, E.N. & Haacke, N.: Merging patterns and processes of diffuse pollution in urban watersheds: A connectivity assessment, *WIREs Water*, 8 (4), 2021; doi:10.1002/wat2.1525. Postprint.

Chapter 3 (Objective 2): Haacke, N. & Paton, E.N.: Analysis of diurnal, seasonal and annual distribution of urban sub-hourly to hourly rainfall extremes in Germany, *Hydrology Research*, 52 (2), 478-491, 2021; doi:10.2166/nh.2021.181. Postprint.

Chapter 4 (Objective 3): Haacke, N. & Paton, E.N.: Impact-based classification of extreme rainfall events using a simplified overland flow model, submitted to *Urban Water Journal* on May 25, 2022.

Chapter 5 (Objective 4): Pilot study: Quantification of the depression storage capacity of different real urban surfaces using a terrestrial laser-based method.

Chapter 6 synthesises the outcomes of this thesis and gives an outlook for future research.

Chapter 7 gives an overview of supplementary scientific work.

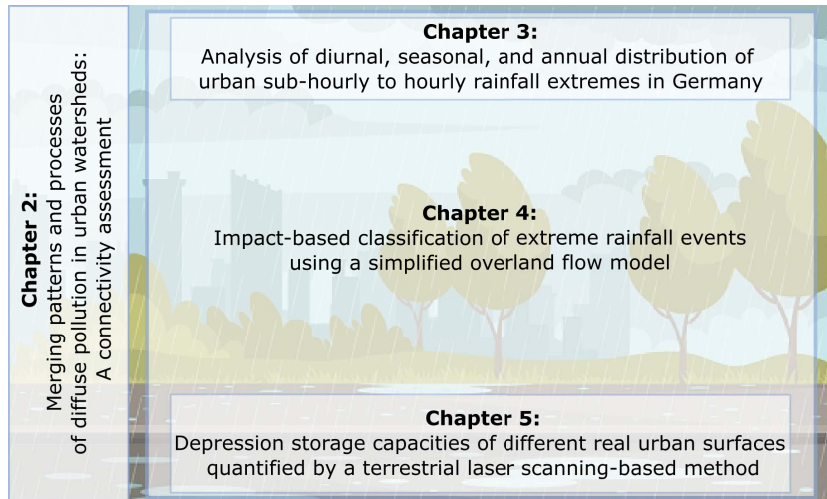


Figure 1.7: Overview of all chapters and their content interfaces.

Chapter 2

Merging patterns and processes of diffuse pollution in urban watersheds: A connectivity assessment

This study was published in WIREs Water as:

Paton, E.N. & Haacke, N.: Merging patterns and processes of diffuse pollution in urban watersheds: A connectivity assessment. *WIREs Water*, 2021; doi: 10.1002/wat2.1525

This is the postprint version of the article.

Abstract

Urban diffuse pollution affects water resources as much as its rural counterpart does; however, it is considerably less studied. The full complexity of the urban landscape needs to be addressed to apprehend the diversity of surface layouts and covers, multiple pollution sources, and the diverse changes caused by different types of drainage systems. In this article, crucial patterns of pollution source areas are categorized, and current knowledge on their temporal and spatial variations are collated. Urban alterations of transport processes that enhance, delay, or inhibit diffuse pollution transport from source areas through the urban watershed are detailed. Current knowledge regarding diffuse pollution patterns and processes is conceptually merged by the simultaneous assessment of urban structural and functional connectivity relevant for pollutant transfer. Applying a more holistic approach is considered a prerequisite for identifying critical source areas of diffuse pollution within complex urban catchments, to minimize the transfer of particular harmful pollutants and to enhance future management of urban waters.

2.1 Introduction

Diffuse pollution of urban water resources remains a serious global environmental problem, despite considerable efforts undertaken in the past. Urban diffuse pollution comprises fluxes of dissolved or particulate pollutants that enter urban water resources through precipitation, infiltration, or runoff processes from streets, yards, roofs, commercial areas, and heavily modified urban soils. Such pollutants have detrimental impacts on the quality of both surface water and groundwater. *Diffuse* pollution must be distinguished from urban *point-source* pollution, where contaminants enter the environment from easily identified sites, such as the outlet of an industrial or sewage treatment plant (Fletcher et al., 2013). In contrast, diffuse pollution, sometimes also called non-point pollution, originates from widespread activities with no definitive discrete source.

In the past, a ubiquitous drainage and sewage system in industrialized cities was believed to be the most practical solution to the pollution problem stemming from urban stormwater and sewage (Chocat et al., 2007). However, the deteriorating quality of urban waters has continuously raised concerns (Makepeace et al., 1995). At the same time, regulations such as the EU water framework directive demand good ecological status for urban waters. Common pollutants in urban waters include trace organics, heavy metals, nutrients, contaminated sediments, petroleum by-products, pesticides, and pathogens (see, e.g., reviews by Miller and Hutchins (2017) for urban rivers and Jurado et al. (2012) or Howard and Gerber (2018) for groundwater). Some of the toxicants cause lethal and sub-lethal effects on aquatic organisms; O₂ deficit and eutrophication occur frequently due to elevated organic matter (Wenger et al., 2009). Hence, a sustainable management of urban waters has not yet been achieved.

A current research frontier is the analysis of how pollutants are retained within the complex landscapes of cities and released laterally toward rivers and vertically toward groundwater during high-intensity storm events. The identification of source areas and the resulting mobilization of pollutants during storm events from urban surfaces continue to be significant challenges in the research on urban water pollution (Fletcher et al., 2013; Pitt et al., 2004a; Pitt et al., 2004b; Wang et al., 2017). Addressing this problem is not simple because the urban contribution to diffuse pollution varies widely as a complex function of surface cover and sealing, connection degree and type of drainage systems, soil types and their urban transformations, climate, topography, and management approaches, such as the frequency of street and snow cleaning routines (Duncan, 1995; Göbel et al., 2007). The poorly defined and poorly identified spatial layout of pollutant sources in urban landscapes makes the identification and control of diffuse pollution particularly difficult.

Urban diffuse pollution is directly linked to the excessive alterations of the hydrological regime due to urbanization, that is, high levels of impermeable surface areas, altered river systems, and up to 100% of the city area connected to sewage and drainage networks (however,

a significant smaller percentage is achieved in most cities of the global south as quantified by Corcoran et al. (2010)). Impacts of the implementation of drainage systems are higher runoff and pollutant peaks, less recharge to the groundwater (i.e., much more lateral than vertical water distributions), and decreased lowflow conditions (Cristiano et al., 2017; Fletcher et al., 2013). Currently, there is a trend of moving away from traditional, hard engineering, and centralized urban drainage solutions toward a more natural drainage approach to reduce the peakedness of drainage and sewer overflow. This step-change involves an increasing extent of decentralized and natural measures for rainwater management (Golden and Hoghooghi, 2018) known under several names, such as sustainable urban drainage (SUD) measures, nature-based solutions, or green infrastructure (see Fletcher et al. (2015) for a full review of terminologies). This trend results in a paradigm shift from wanting to remove urban water rapidly toward wanting to keep it in the city for as long as possible.

For both centralized and decentralized drainage approaches, we have incomplete knowledge regarding the precise source of the pollutants, if and when they accumulate, and their pathways toward urban rivers or groundwater (Lundy and Wade, 2013). The transition from a traditional to a decentralized urban drainage is ultimately a change in the connectivity of vertical and horizontal water fluxes. This transition relates to a change from artificially increased lateral and heavily reduced vertical water fluxes in the centralized drainage approach to considerably more vertical fluxes down (groundwater) and up (evapotranspiration) in decentralized approaches (Golden and Hoghooghi, 2018). Figure 2.1 depicts the differences in the main flow directions between the two systems: (a) the centralized systems with mostly horizontal flow patterns (blue lines indicate the street runoff, red lines represent the drainage and sewage network, and the red arrows locate flows toward the treatment plant or toward storm-water outlet points (also called combined sewer overflows from which excess waste and drainage water is discharged directly into the rivers during heavy rainfall); (b) the decentralized systems with a significant increase in vertical flow patterns toward groundwater or the atmosphere (blue arrows), retention and storage of water in different storage units, and no storm-water outlet points into the river.

We argue that the handling of diffuse pollution should address the prevalent and changing nature of the connectivity of water and pollutant flows in either drainage system. The concept of hydrological connectivity has proven to be very useful for understanding diffuse pollution in rural catchments (such as studies on nutrient export causing eutrophication, e.g., Heathwaite et al. (2005), Dupas et al. (2015), González-Sanchis et al. (2015), and Stachelek and Soranno (2019)), but has not yet been applied to urban settings. We use the connectivity definition by Turnbull et al. (2018), who define hydrological and pollutant connectivity as the degree to which a system facilitates the transfer of water and pollutants through itself, through coupling relationships between its components. In this review, we take a holistic perspective on urban diffuse water pollution dynamics to address the full complexity of associated urban connectivity, patterns and processes including urban

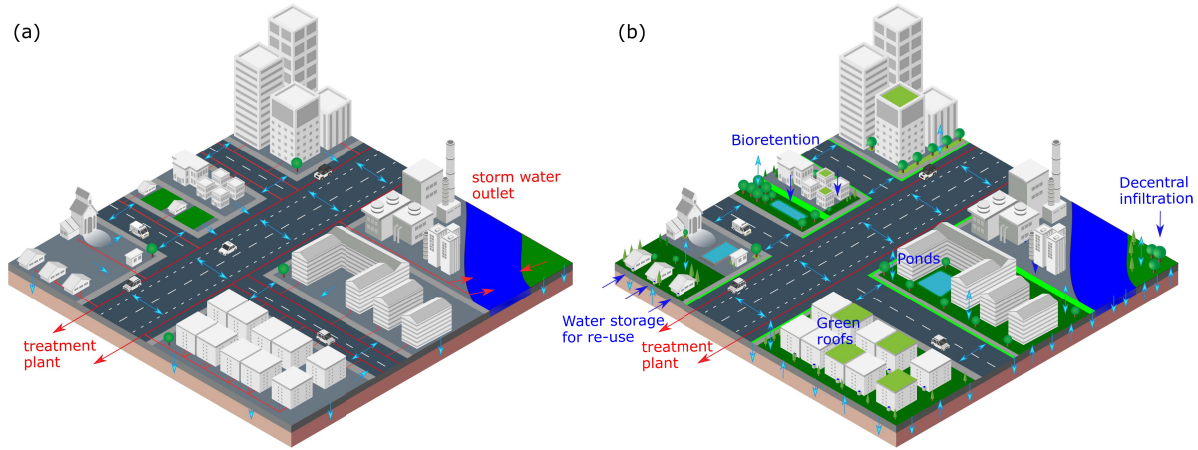


Figure 2.1: (a) Centralized versus (b) decentralized approaches for urban drainage (red line: drainage network, red arrows: storm-water outlet points into rivers, blue arrows: street runoff, infiltration, and evapotranspiration).

surface heterogeneity, meteorological, hydrological, and soil variability, drainage systems, and decentralized drainage measures. Process-descriptions of (dis)connectivity of water and pollutant movement throughout urban catchments will facilitate the identification of critical source areas of the cityscape, where significant amounts of pollution that end up in urban waters are generated (Brierley et al., 2006). Consequently, pollution control of the critical source areas is likely to be more cost-effective than attempts to control pollution across the cityscape (Steuer et al., 1997).

We presume that only a better understanding of the interlinked dynamics of source areas and pathways will enable better management of urban water resources. In this study, we assemble the current knowledge to achieve this goal. (a) We classify crucial *patterns* of pollution source areas and variables that dominate or influence urban diffuse pollution. (b) We then discuss the urban alterations of transport *processes* that enhance, delay, or inhibit diffuse pollution transport from source areas through the urban watershed. (c) Finally, we examine how we can theoretically merge patterns and processes of urban diffuse pollution within a hydrological and pollutant connectivity framework and practically enhance future management of urban waters.

2.2 Spatial and temporal patterns of diffuse pollution on urban surfaces

2.2.1 Spatial patterns of diffuse pollution

The quantification of diffuse pollution patterns involves two methodologies: an adapted end-of-pipe field approach and the source area sampling.

Adapting an end-of-pipe field approach, diffuse pollution originating from sealed surfaces is frequently quantified in stormwater at sampling points inside the drainage systems, at sewer overflow points, or directly in urban rivers. Recent studies by Eriksson et al. (2007) and Pal et al. (2014) and Corada-Fernández et al. (2017), for example, quantified emerging organic contaminants such as surfactants, algal toxins, or priority substances in urban rivers or aquifers. However, these studies do not relate contamination directly to potential source areas. Thus, in these examples, diffuse pollution is sampled applying a method that is more applicable for point source pollution using storm-water outlets as collectors of pollution originating from various sources. Figure 2.2 illustrates this "simplified" end-of-pipe perspective by showing the efforts of quantifying pollution loads from storm-water outlets or inside water-bodies (highlighted circle) but ignoring the hidden complexity "upstream" of these outlet points (depicted as a gray shaded cityscape).

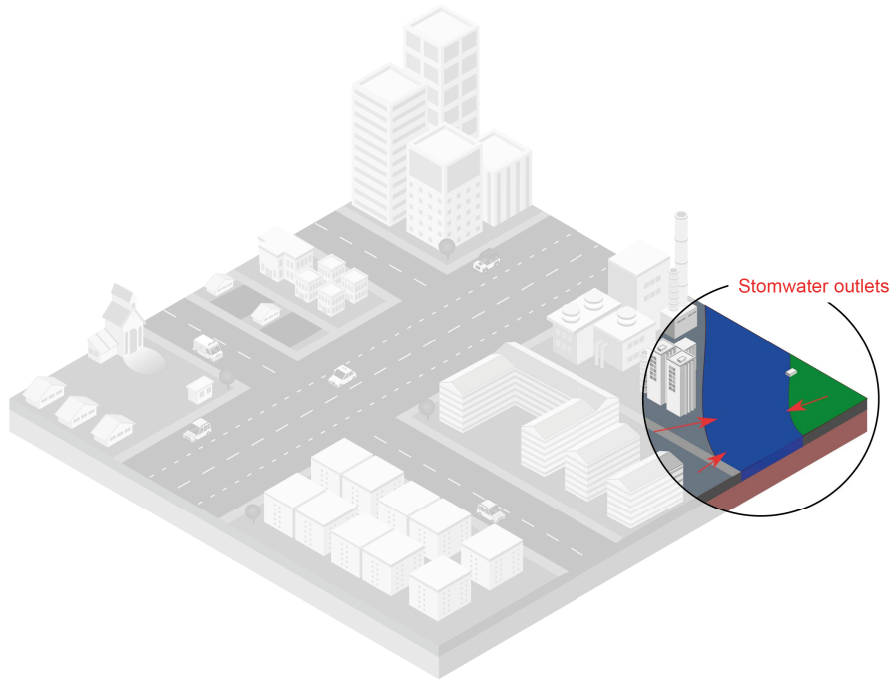


Figure 2.2: End-of-pipe sampling of diffuse pollution at storm-water outlets in urban catchment.

The source area sampling examines the degree of pollution directly on urban surfaces by quantifying either the potentially available pollution load or pollutant concentration in sheet flow running on these surfaces (Fig. 2.3). The reviews by Duncan (1995), Pitt et al. (2004a), and Pitt et al. (2004b) and Göbel et al. (2007) compiled literature on a wide range of different surface types and parameters that showed the highest contribution to diffuse pollution. Sampled source area pollution included heavy metals and organic salts on roads, sidewalks, car parks and different roof surfaces, organic litter from urban green (parks, yards, and street trees) and contaminants due to atmospheric deposition. These studies demonstrate the vast extent of current knowledge on contaminant concentrations and their potential sources.

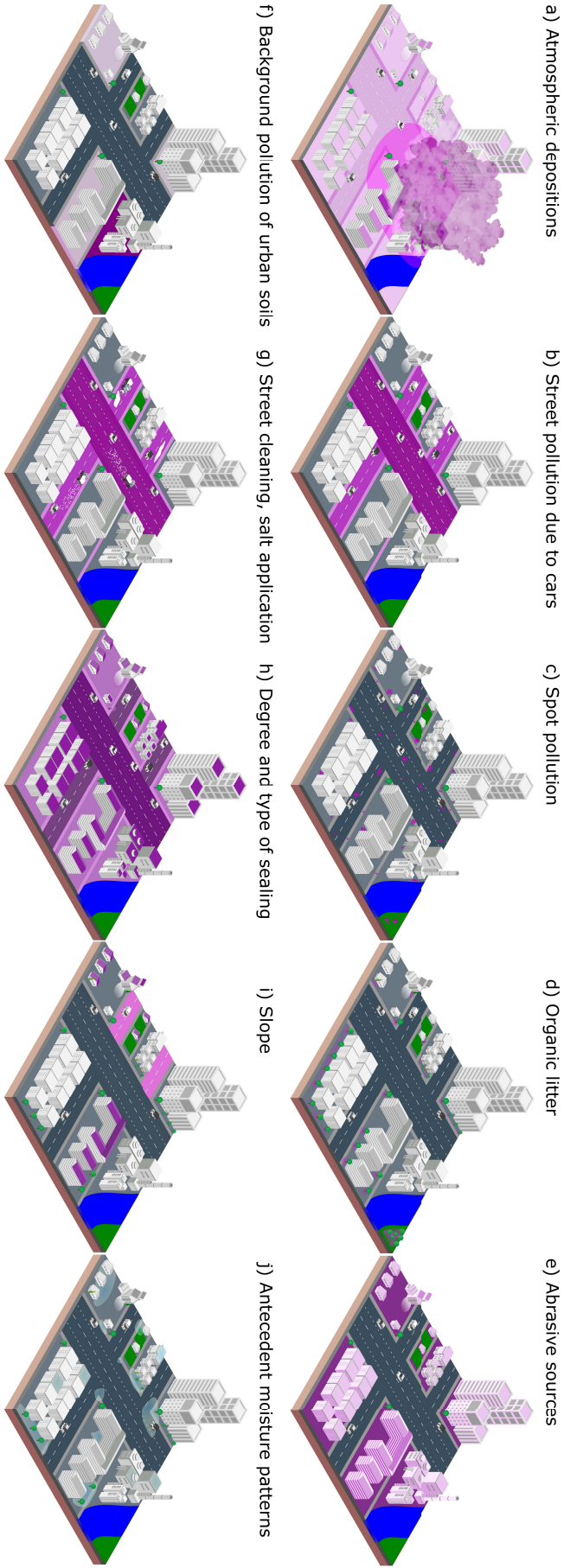


Figure 2.3: Spatial source area patterns that dominate or influence urban diffuse pollution: (a–d) pollution patterns that accumulate, (e–f) static pollution patterns, (g) management routines affecting pollution patterns, and (h–j) hydrologically relevant patterns—(h) degree and type of sealing, (i) antecedent moisture pattern, and (j) slope. Pink shading shows the extent and magnitude of the different pollution patterns (except it depicts the degree of sealing in h) and the slope magnitude in (i). Gray shading in (j) shows the magnitude of soil moisture.

However, a coherent categorization of all different source types, their intrinsic spatial patterns, and temporal dynamics have not yet been performed consistently. We propose to group urban patterns that dominate or influence diffuse pollution into four categories: (a) pollution patterns that accumulate or build up on the surface, (b) static pollution patterns (considered relatively stationary from years to decades), (c) management patterns that influence pollution structure, and (d) hydrological response factors that influence the generation of overland flow or infiltration toward groundwater (Fig. 2.3). Current knowledge on pollution types, their spatial compositions, and temporal dynamics of the four categories are discussed in the following paragraphs by identifying existing detailed review studies or gaps in the literature.

Pollution patterns that accumulate

- (a) *Dry and wet atmospheric deposition* result in the vertical transfer of a wide range of pollutants in dissolved and particulate form from the atmosphere to all urban surfaces (streets, buildings, and plant surfaces). These pollutants include nitrogen, sulfur, and phosphorus deposition (see, e.g., Vet et al. (2014) for a recent global assessment), heavy metals such as Pb, Zn, Cu, Cd, and Cr (Göbel et al., 2007), Hg (recent studies, e.g., Lynam et al. (2016)), and polycyclic aromatic hydrocarbons (PAHs, e.g., Kim and Young (2009)). Sources are typically related to major anthropogenic air pollution due to power stations, industries, traffic fumes, and heating.

Deposition patterns show strong spatial variations within cities with generally more pollution in central and industrial areas and thus depend considerably on city size, structure, climate, and traffic volume (Göbel et al., 2007). Temporal variations include seasonal variations due to different annual rainfall distributions and different intensities of air pollution from power stations and heating systems in the winter season (Pitt et al., 2004b). Long-term patterns are detected for sulfur, whose emissions declined significantly in line with reduction policies over the last two decades (Vet et al., 2014). Other long-term variations have resulted from a significant increase in pollution loads in rapidly growing cities over the last several decades, specifically for Hg, as assessed by Wu et al. (2018) for Beijing.

- (b) *Street pollution due to cars* originate from automobile emissions and inadequate automotive maintenance (Campbell et al., 2004; Wada et al., 2015). Pollutants include airborne heavy metal particulates, such as Pb attributed to emissions from motor vehicle exhausts and heavy metals, PAHs, and microplastics originating from mechanical operation wear, such as road surface abrasion, tire abrasion, and brake pad abrasion (Barjenbruch, 2018; Crabtree et al., 2008; Göbel et al., 2007; Pitt et al., 2004b; Poudyal et al., 2016). Drip losses lead to local contamination with mineral oil hydrocarbons (Göbel et al., 2007). Tire wear has been identified as a significant source of Zn (Pitt et al., 2004a). The degree of contamination depends primarily on the

amount and fraction of the total traffic (Pitt et al., 2004b; Wada et al., 2015), rainfall patterns including dry spell length defining the length of accumulation time (Schiff et al., 2016), and cleaning routines.

Studies on the temporal variations of street pollution have not yet been conducted.

- (c) *Spot pollution* comprises single-point pollution on a relatively small spatial extent. It may be as diverse as rubbish (e.g., paper cups and packaging, chewing gum), cigarettes (Roder Green et al., 2014), animal droppings on streets and pavements, accidental spills from cars (Duncan, 1995; Poudyal et al., 2016; Revitt et al., 2014), petrol stations or building sides (paints, tar, concrete, dust, etc.; Björklund (2010)).

Studies on the spatial and temporal variations of spot pollution have not yet been conducted.

- (d) *Organic litter* comprises leaves, blooms, pollen, fruits, honeydew, and branches from urban green, mostly from street trees and green facades, and can be found on streets, pavements, and car parks. Compared with artificial litter, the mass of organic litter is significantly higher (Duncan, 1995). Organic litter may be contaminated by dry deposition, retention, and accumulation of particulate air pollutants (heavy metal, sulfur, etc.) on leaves and pollen (see Section 2.2.1a).

Organic litter production is highly seasonal and peaks when trees bloom and shed their leaves (in moderate climates generally in April/May and autumn, respectively). A comprehensive analysis of these seasonal distributions or a spatial assessment is not yet available.

Static pollution patterns

- (e) *Abrasive sources* from building surface materials (vertical and horizontal) such as concrete, asphalt/tar shingles, galvanized metals, bitumen-based roofing felt, roofing fabric, plastic/vinyl/fiberglass roofing panels, wood products, paints and (incorporated) additives have the potential to release significant amounts of pollutants into urban runoff (Clark et al., 2008; Clark et al., 2002; Göbel et al., 2007). The release of pollutants from building surfaces depends strongly on the material, its age, slope, exposure of the surface, and climatic variables such as temperature, pH of precipitation, rainfall energy, and drop size (splash erosion; Burkhardt et al. (2011), Duncan (1995), Göbel et al. (2007), and Müller et al. (2019)). While weathering is the dominant process for metal release of construction materials, additives are mostly leached. Most research on pollutants from building surface materials focuses on metals (e.g., Bürgel et al. (2016), Clark et al. (2008), and Pitt et al. (2004b)). This research showed that for both pilot-scale field tests and laboratory experiments, traditional galvanized metal roofing contributed to significant concentrations of Cu, Zn, and Pb due to corrosion. Several studies have investigated the leaching amounts of additives, such as fungicides (e.g., Carbendazim), herbicides (e.g., Mecoprop, Isoproturon), and

pesticides (Diuron, Terbutryn), which are mostly used in roof and facade paints to prevent undesirable growth (moss, lichen, and algae), and root penetration (Burkhardt et al., 2011; Wicke et al., 2012). Little is known about other organic micropollutants, such as industrial additives (e.g., nonylphenols and phthalates) that are commonly used in plastic products such as PVC materials (Müller et al., 2019) and are listed as priority substances in Annex 1 of the European Union directive on priority substances (Directive 2013/39/EU, 2013).

The dynamics of pollution from abrasive sources appears to be particularly challenging because no estimates exist on their spatial extent and variations for urban built environments and new building additives with different chemical compositions emerge on a yearly basis (Müller et al., 2019). The study of their seasonal variations is a new research field and some first laboratory experiments indicate higher pollution loads in the summer months, linked to higher radiation rates, which promotes increased leaching of additives (Bollmann et al., 2016).

- (f) *Background pollution of urban soils* refers to the extensive presence of pollutants that originate from the historical urban usage and contamination of the ground, which may be washed or leaked out. The pollution in urban soils is manifold and originates from modifications during building construction and demolition, former sewage farms, old waste or debris landfills (including rubber from war damages), and former industrial and brownfield sites. The types of pollution are very diverse and include nutrient leaching (mostly by former sewage farms, Hass et al. (2012)), PAHs, heavy metals, and sulfates (from debris landfills and industrial sites, Mekiffer (2008), Mekiffer and Wessolek (2011), and Nehls et al. (2013)), mineral oil hydrocarbons, biocides, dioxins, furans, and PCBs (from former urban industrial and brownfield sites, Bürgel et al. (2016) and Wessolek et al. (2016)).

Spatial information on pollution patterns, such as heavy metal concentrations as well on physical properties and buffer capacities of urban soil is available for cities that foster urban soil data management systems such as the environmental atlas of Berlin (Umweltatlas Berlin, 2021) or the New York City Soil Survey (NYCSS, 2021). Temporal information is normally not readily available.

Management routines affecting pollution patterns

- (g) *Street cleaning* clears pavements, streets, gullies, and parking spaces, from litter (organic and others), mostly by manual sweeping or by cleaner trucks equipped with vacuum and sprayers to loosen particles (Calvillo et al., 2015; Chang et al., 2004). With modern machines, sediment, and pollutant particles down to the size of PM10 are cleaned from street surfaces (Chang et al., 2004). A special form of cleaning is the application of pesticides for weed control on mosaic pavements (Wessolek et al., 2011). Weed control of pavements is considered necessary in many cities as pavements covered with moss can easily get slippery which may affect pedestrian safety. In particular, the herbicide

glyphosate was applied in many cities around the world; however, its adverse impacts on the environment put this practice into question and led to a reduction in its usage in some regions (e.g., in Denmark, Kristoffersen et al. (2004)). Cleaning intervals vary widely as a function of traffic magnitude (major streets more frequent than smaller streets), season (more frequent cleaning of leaf fall in autumn), region (daily cleaning in some southern European cities), daily to monthly cleaning, e.g., in Boston (City of Boston, 2018), London (Bromley, 2019), and Berlin (Berliner Stadtreinigung, 2018).

- (h) *Road salt application for de-icing* on road and pavement surfaces for winter traffic safety is a common practice in many areas in the temperate zone since the 1930s. With sodium chloride (NaCl) or calcium chloride (CaCl₂) applied during the winter months (Blomqvist, 1998; Göbel et al., 2007; Ramakrishna and Viraraghavan, 2005).

The spatial distribution and frequency of application vary widely as a function of climatic variables and the traffic safety category of the streets (major streets more frequent). Most cities have detailed management plans detailing under which streets need salt applications (e.g., Berliner Stadtreinigung (2018)). Due to detrimental environmental impacts on street trees and urban waters (e.g., review by Amundsen et al. (2010)), de-icing has recently been prohibited on pavements and most minor streets or is only allowed to be used under extreme conditions in several German and Austrian cities. In comparison, de-icers remain a common method in countries with particularly long and cold winters, such as Russia, Canada, and Scandinavia.

Hydrologically relevant patterns affecting diffuse pollution mobilization

The following three spatial patterns are not pollution patterns per se, but hydrologically relevant surface properties that control if overland flow is generated for the mobilization and transfer of diffuse pollution.

- (i) *The degree and type of surface sealing* determine infiltration rates and is one of the most influential factors for runoff generation and pollution mobilization (Shuster et al., 2007; Miles and Band, 2015; Lim, 2016), more details on process implications in Section 2.3.1). The degree of sealing varies between 10 and 25% for less densely built-up areas to 55–85% for inner-city areas (DWA-M 609-1). Sealed surfaces can consist of a single continuous cover (e.g., asphalt, metal, or concrete) or assemblies of individual pavers with joints in between (e.g., cobblestone, sett stones, stone or concrete plates, or grass pavers; Timm et al. (2018) for a review) with larger infiltration and lower runoff rates for the latter group. The terms degree of sealing and fraction of impervious area cannot be equally set as the latter term suggests nearly no infiltration, whereas the former is characterized by a wide range of different infiltration rates. The type of sealing has a significant influence on runoff generation. New sealing materials such as super porous asphalt and other mixed paver types specifically designed as stormwater remediation methods exhibit considerably larger infiltration rates than conventional asphalt (Timm

et al., 2018). Sound spatial information exists for the urban degree of sealing with large resolution data up to 1 m are widely available (see Weng (2020) for a full review on current techniques), whereas spatial information on the type of sealing appears to be much less readily available.

- (j) *Antecedent moisture patterns* have been neglected in urban hydrology until recently. The prevailing thought was that urban catchments consist of mostly impervious surfaces where antecedent moisture patterns do not influence rainfall-runoff responses (e.g., Smith et al. (2013)). However, the modeling study by Hettiarachchi et al. (2019) for an urban catchment in Minnesota (USA) showed that antecedent moisture patterns can have a significant impact on runoff generation, especially where parts of the urban catchment employ decentralized approaches of rainwater management such as enhanced local infiltration with swales. Moisture patterns are highly surface- and time-dependent and an important driver for runoff generation (see more in Section 2.3.1).
- (k) *Slope and surface roughness* determines runoff generation and pollution transport, with steep streets and high-pitched roofs being the main contributors. High-resolution data on slopes are readily available through several remote-sensing products (e.g., DigitalGlobe, 2006; Klemas, 2015) and are frequently used to locate steep streets and traffic areas prone to flooding. Roof-top analysis tools exist to evaluate the spatial distribution of flat and steep roof slopes (Grunwald et al., 2017) thus making them a valuable information source for a detailed slope assessment of the urban landscape.

2.2.2 Temporal dynamics of diffuse pollution

The previous sub-sections provided some first indications on the seasonal to decadal dynamics of various pollutants. However, it became apparent that for many pollution sources, the temporal variations are not known. The categorization of the pollutant sources reflects their different temporal dynamics during the year: static pollutants (abrasive sources and background pollution of soils) are thought to not vary significantly across the year. Pollutants originating from management routines (road salt or pesticides for weed control) vary according to a prescribed management schedule following city safety regulations. Pollutants that accumulate (e.g., litter, street pollution, wet and dry deposition) show more complex variations during the year. They are significantly influenced by the length of intermittent dry periods, the magnitude and timing of rainstorm events, and the timing of management routines such as the cleaning of street surfaces.

The importance of timing for accumulated pollution is illustrated in Figure 2.4. During dry periods, there is a linear increase in pollutant amount, resulting in a build-up over days to weeks followed by a rapid decrease after a large rainstorm event (first black bar) or street

cleaning actions (gray bar). However, if a second rainstorm event of a similar magnitude occurs only a short time later (second black bar), pollutant accumulation is insignificant and unlikely to cause any diffuse pollution.

This concurrency dynamics of pollutant accumulation and transport mechanisms (in the form of hydrological and pollutant connectivity) are addressed in the next two sections.

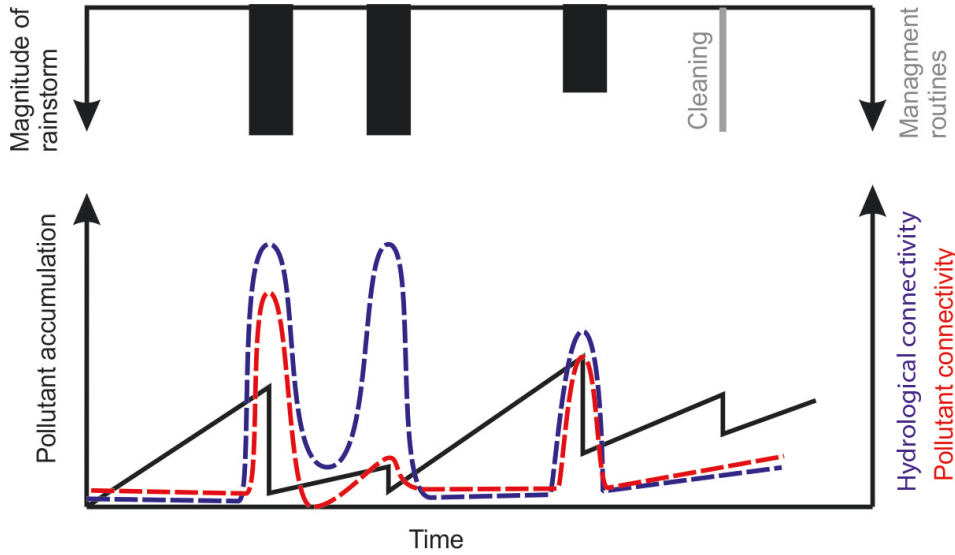


Figure 2.4: Concurrency dynamics of pollutant accumulation and hydrological and pollutant connectivity as a function of rainfall-runoff response and management routines (reprinted with permission from Bracken et al. (2015)).

2.3 Distribution processes of diffuse pollution within urban catchments

We established that diffuse pollution originates from various sources in the city stemming from a complex city layout. Similarly, complex is the series of pathways through which pollutants can be discharged via the drainage systems into the urban river or via runoff into the upper soil layer or groundwater resources in the direct vicinity of source areas. Transport processes are significantly altered in an urban catchment compared to their rural counterparts. The characteristic modifications in their slope distributions, infiltration rates, localized pollution patterns, and completely different setup of flow pathways (or their obstructions) require novel approaches for studying and understanding the interplay of runoff generation and transport mechanisms.

2.3.1 Variable hydrologic partitioning in cities

Transport of pollutants occurs either in dissolved form (such as road salt), suspended or semi-suspended (larger components such as litter) or in the particulate form attached to suspended sediments as a function of the infiltration rate, runoff amount and velocity. The urban area does not uniformly generate runoff toward the drainage network or vertical fluxes toward groundwater following rainfall events. As in rural catchments, the size of the contributing area is event-dependent with a non constant ratio in rainfall-runoff transformation (Duncan, 1995; Lim, 2016).

Smaller rainfall events result in immediate runoff from heavily sloped and sealed surfaces such as roofs and steep streets; some infiltration into the upper soil layer of unpaved surfaces may occur (Fig. 2.5a, and a smaller peak for hydrological connectivity in Fig. 2.4). However, most urban surfaces do not become hydrologically active during smaller rainfall events (Shuster et al., 2007). In contrast, larger rainfall events with durations exceeding 15–30 min and rainfall heights above a certain threshold result in much larger hydrologically connected areas, including both sealed and unsealed surfaces, such as urban green spaces such as parks, yards, street tree pits, or vacant lots. Extreme rainfall events with magnitudes above a certain threshold (according to Westra et al. (2014) and Guerreiro et al. (2017), higher than ~ 20 mm/hr, but heavily depending on surface conditions and antecedent moisture conditions) are likely to result in urban flash floods. Such an occurrence relates to all urban surfaces contributing to runoff generation, groundwater recharge, or excessive ponding on sealed surfaces (Fig. 2.5b and larger peak for hydrological connectivity in Fig. 2.4). For the last two scenarios, limited amount of empirical data are available to correlate rainfall intensity and duration with the surface condition and runoff generation on the district scale; we identify this fact as a major research gap. A notable exception is the study by Kelleher et al. (2020), who estimated the extent to which vacant lots in cities modulate hydrologic partitioning under varying rainfall intensities.

In drainage studies, the effective impervious area (EIA) or directly connected impervious area (DCIA) is frequently employed to describe the impervious area fraction of an urban watershed that is hydraulically (as a function of rainfall-response) or physically connected to the storm sewer system, respectively (Ebrahimian et al., 2016; Hwang et al., 2017). A problem with the impervious attribute is that for its quantification, the different types of surface sealing are often not considered (see Section 2.2.1i for a wide range of sealing types). Miles and Band (2015) and Lim (2016) adopted the variable source area (VSA) concept to urban catchments to include the influence of pervious surface areas as a contributing area of urban runoff generation. However, all indicators have several drawbacks, which limit their use when dealing with diffuse pollution transfer. They only evaluate lateral water fluxes but not the connectedness to the groundwater, and only describe the hydrological connectivity but do not provide information if the connected surfaces are actually polluted and hence contribute

to diffuse pollution at all.

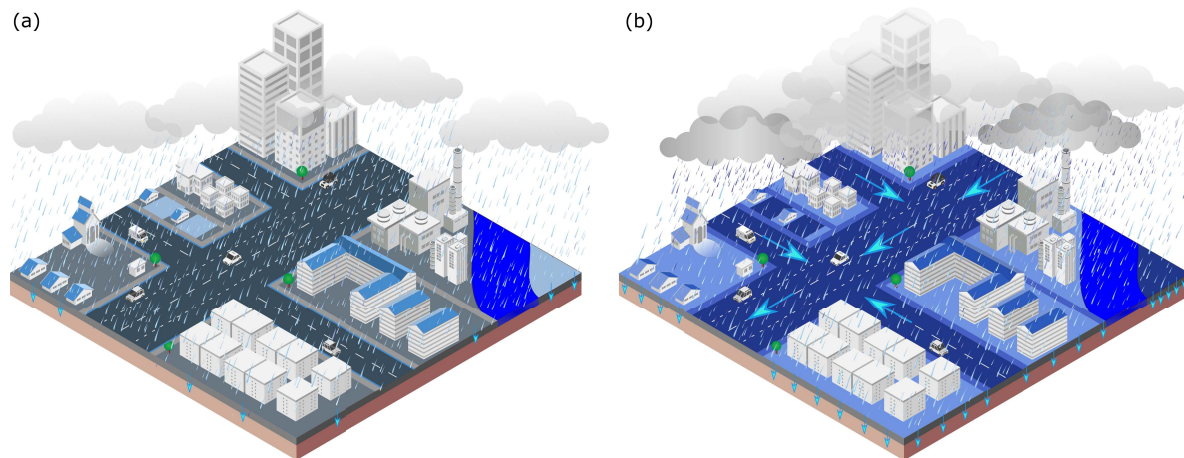


Figure 2.5: Two scenarios illustrating the different spatial extents of urban variable contributing areas for a (a) small and (b) large rainfall event (shades of blue) and associated potential to transport pollutants.

2.3.2 Critical source area concept for urban diffuse pollution

Identification (and subsequent management) of areas that contribute most of the pollutants to urban water resources are of critical importance. These so-called "critical source areas" after Shore et al. (2014) are usually small in size, particularly heavily polluted (Wang et al., 2017) and located in such a way that pollutant supply and transport coincide in time and space (Heathwaite et al., 2005). Those fractions of the urban surfaces that contribute disproportionately large amounts to or transport pollutants within the drainage network or groundwater are referred to as "effective catchment areas". They are thought to be considerably smaller than quantified by the indicators EIA, DCIA, and VSA.

The concept of critical source areas appears to be more suitable for a system's evaluation of multiple-source diffuse pollution in urban catchments than the impervious area indicators. The concept of the critical source area was previously used for erosion and diffuse pollution assessment in rural catchments to isolate sediment and nutrient transfer from runoff generation (Fryirs et al., 2007b; Fryirs et al., 2007a; Heathwaite et al., 2005). In agricultural catchments, it has allowed a much better way of targeting and managing pollution hazards. Confining mitigation to critical source areas, which tend to be the source of disproportionately large amounts of pollution, was significantly more effective (and costs less) than employing universal controls (Strauss et al., 2007).

Despite its conceptual advantages, the critical source area concept has been applied only in a few studies on urban diffuse pollution. Wang et al. (2017) and Tuomela et al. (2019) applied the concept to identify nutrient, sediment, and pollutant sources in residential areas. Steuer et al. (1997) measured contaminant concentrations from different relatively homogenous urban

source surfaces including rooftops, parking lots, and residential lawns of 1–72 ha in an attempt to relate the measured pollutant concentrations at the outlets to the specific surface types. In the study by Björklund (2010), a substance flow analysis was employed in a section of an urban motorway to identify source areas of contaminants (phthalates, with detrimental effects on hormone balance of animals), and scale up the potential amount of phthalate emission from annual stormwater discharge.

A transfer of the critical source area concept to the multiple pollutant patterns across urban surfaces is still pending. A comprehensive analysis of the overlap of pollution supply and transport potential will result in a multi-dimensional matrix of relevant source areas. First, the critical source areas and corresponding effective catchment areas are likely to be very different areas for urban rivers and groundwater. Second, one has to expect very different kinds of critical source areas for the diverse urban pollution patterns, as described in the previous section.

2.3.3 Buffers, barriers, and boosters in urban watersheds

The transfer of diffuse pollution is accelerated, delayed, clogged, or inhibited by different elements in an urban watershed, which may function accordingly as pollutant buffers, barriers, and boosters. The terms are borrowed from recent geomorphological and erosion research, where they provide a valuable framework for understanding the various processes involved in matter movement from source areas through a watershed to its outlet (Blanco-Canqui and Lal, 2010; Fryirs, 2013).

Buffers are elements in the urban watershed that prevent or delay diffuse pollution from entering the drainage system. Most of the vegetated areas in cities function as buffers through enhanced infiltration and retention of fine matter (Tedoldi et al., 2017). Special forms of buffers are most elements of decentralized urban drainage measures for stormwater control, including infiltration areas, swales, and urban wetlands (Miles and Band (2015) for a recent review). Indeed, one of the main functions of decentralized drainage measures is to disconnect impervious surfaces such as streets and rooftops from the central drainage system and at the same time enhance infiltration of rainfall (Ebrahimian et al., 2016). In a study by Driscoll et al. (2015), the capacity to capture or leak stormwater and pollutants (nitrogen, phosphorus, and chloride) was quantified for individual bioretention systems. Ahiablame et al. (2012) study contains an extensive database of heavy metal and nutrient loads retained by decentralized drain-age measures. Another form of retention is given by "accidental" types of buffers as compiled by Palta et al. (2017), which refer to urban wetlands that developed not deliberately on abandoned or low-lying urban areas and become retention areas of water and matter flow.

Barriers disrupt diffuse pollution flow moving along major flow routes in and outside the drainage network and include intentional barriers such as bioretention systems (Ahiablame

et al., 2012), stormwater retention ponds, and artificial ponds or unintentional barriers such as blockages in gutters and clogging of gully holes (Fig. 2.6). There are no systematic studies that quantify the timing and location of unintentional barriers for cities, and their effects on pollutant transfer are not clear but are likely to result in the dispersal of pollutants upstream of the barrier.

Boosters are surface elements that enhance the propagation of diffuse pollution and may have diverse boosting functions: (a) rain gutter and gully holes are boosters toward the drainage network, (b) stormwater outlets of combined sewer systems are boosters toward urban surface waters, whereas (c) decentralized drainage measures such as infiltration areas and swales may function as boosters for dissolved pollution flow toward the groundwater. Interestingly, decentralized drainage measures can function both as buffers and as boosters depending on flow directions. Although initially designed as a pollutant buffer toward the drainage network, they concurrently function as a booster that enhances the propagation of water and dissolved pollutants toward groundwater.



Figure 2.6: Buffers, barriers, and boosters of urban diffuse pollution: (a) swale directly after rain event, (b) blocked gully, and (c) stormwater outlet and rain gutter.

2.4 Merging patterns and processes of urban diffuse pollution

Diverse, frequently changing pollution patterns and components (Fig. 2.3), nonlinear rainfall-runoff, and transport relationships (Fig. 2.5) determine the magnitude of urban diffuse pollution. We argue here that an end-of-pipe perspective of evaluating pollutant transfer at the outlets of urban catchments (see Section 2.2) cannot comply with the complexity of a typical urban layout. We see here an analogy to recent efforts of diffuse pollution management in rural catchments. The redistribution of nutrients and sediments could not be understood by simply quantifying nutrient and sediment fluxes at the outlets of agricultural catchments (Bailey et al., 2013; Heathwaite et al., 2005). Whether pollution occurs toward urban rivers or groundwater depends on how well the pollutants are connected to the outlet of the catchment or the groundwater. The previously mentioned critical source area concept, but also the notion of buffers, barriers, and boosters are part of recent advancements in connectivity studies. This science has become a transformative concept in

understanding and describing what is considered to be complex systems (Turnbull et al., 2018).

2.4.1 Structural and functional connectivity of diffuse pollution in cities

Although widely used in environmental disciplines, the concept of connectivity (as defined in the first chapter) has, to our knowledge, not yet been systematically applied to study transfer processes of water and diffuse pollution in urban systems. However, ecological connectivity research on movements of animals or green bands in urban areas is considerably more advanced, as reviewed by LaPoint et al. (2015), but is not further considered in this article.

Approaches to the study of hydrological and pollutant connectivity are frequently divided into the aspects of structural connectivity and functional connectivity (Turnbull et al., 2008; Wainwright et al., 2011; Bracken and Croke, 2007). Both aspects of connectivity were discussed in the previous sections, but not under these names.

Structural connectivity refers to the extent to which urban surfaces are physically linked or connected (e.g., Bracken et al. (2013) and Wainwright et al. (2011)) and, according to Turnbull et al. (2018), thus derives from the urban system's spatial configuration or "anatomy". Examples of structural connectivity relate to the physical connectedness of sealed areas channeling water fluxes toward the urban drainage networks, decentralized drainage measures such as swale infrastructure next to streets, increasing infiltration rates into the upper soil layer, and contiguous pollution patterns such as on metal roofs or street surfaces. The effective catchment area, already described in Section 2.3.2, reflects the degree to which urban catchment pollution is structurally connected laterally and longitudinally (i.e., along major flow lines) toward the drainage network or vertically to the groundwater. Finally, buffer, barrier, and booster may modulate the structural connectivity by intentionally or unintentionally increasing, decreasing, or disrupting it.

Functional connectivity describes dynamic processes operating within structurally connected surfaces and induces the actual transport and fluxes of water and matter between source areas and outlets (Wainwright et al., 2011). According to Bracken and Croke (2007), functional connectivity can be understood to mean both the short-term variations in antecedent conditions and nonlinear rainfall-runoff catchment response (as discussed in Section 2.3.1 under the name of variable hydrologic partitioning) and the longer-term catchment development, such as the long-term changes of urban infrastructure and the drainage network (as presented in Fig. 2.1 the current move from central to decentral drainage measures). Even the gradual increase in surface sealing through omnipresent infill housing development, which we can see in many cities at the moment, can be assigned to functional connectivity, as it affects hydrological partitioning on a larger time scale.

An urban complex system possesses structural and functional connectivity. According to the systematic review by Turnbull et al. (2018), the structure always affects the function and often (but not always) function affects the structure. Figure 2.4 underlines this point by visualizing how pollutant connectivity depends on the accumulation state of pollutants on urban surfaces. A large rainfall event might lead to large pollutant connectivity if a particular pollutant had accumulated over some time (peak 1 in Fig. 2.4). However, the same rainfall event might result in much smaller pollutant connectivity otherwise (peak 2 in Fig. 2.4). It is important to point out here that the degree of hydrological connectivity and pollutant connectivity can be very dissimilar (as illustrated in Fig. 2.4), and high hydrological connectivity does not always coincide with high pollutant connectivity. Therefore, it is particularly important to simultaneously quantify and monitor the structural and functional components of an urban system. To understand pollution dynamics over time, it needs to be taken into account that surface runoff and infiltration processes change pollutant patterns, redistribute pollutants horizontally and vertically, and will set new conditions for the coming storm events.

Recent advances in connectivity science include the development of novel monitoring and modeling tools that explicitly consider structural and functional aspects of catchment system. Connectivity monitoring tools are currently being applied to evaluate for example structural changes in topography influencing runoff generation, and pollutant and sediment transfer. Topography changes are evaluated through morphological budgeting (Heckmann and Vericat, 2018), runoff and flow path network analysis for runoff connectivity assessment (Ferreira et al., 2016; Masselink et al., 2017), sediment fingerprinting to identify temporal and spatial variability of source areas and transport pathways (Masselink et al., 2017; Sherriff et al., 2018), and analysis of hysteresis loops to link hydrological and pollutant connectivity (Keesstra et al., 2019; Lloyd et al., 2016). Monitoring of source areas and pathways was carried out so far mostly for rural settings; urban settings have not received much attention yet (Russell et al., 2019).

Modeling of pollutant redistribution within urban sub-catchments or in the upper soil zone is currently not implemented in drainage models. Current drainage models, such as the SWMM model (Rossman, 2010), include pollutant build-up, wash-off processes, and reduction in pollutant build-up due to street cleaning operations (see Tu and Smith (2018), table 1 for a recent review of field and modeling studies on build-up processes of suspended sediment, total nitrogen, and phosphorus). However, neither an implicit nor an explicit representation of connectivity is included in urban catchment models yet. An improved urban model should for example include structural connectivity by incorporating interconnected pollution patterns typical for urban surfaces or specific model algorithms that can reproduce functional connectivity, as suggested by Nunes et al. (2018) for rural catchments.

2.4.2 Implications for the management of diffuse pollution in cities

The linchpin of diffuse pollution management is source control, that is, the reduction or avoidance of pollutant accumulation on urban surfaces wherever possible. As a universal source control of complex urban surfaces is not possible, a connectivity assessment of pollutants may help in the identification of critical urban source areas, for which management practices should be prioritized (see Section 2.3.2 and Wang et al. (2017)).

After providing a comprehensive list of the diverse forms of diffuse pollution in Section 2.2, we used the summary term diffuse pollution in the last two sections. What we do not assess in this study is which of the pollutants are particularly harmful or have toxic impacts on surface or groundwater resources concerning usage capacities, human health, and habitat impact. The development of a hierarchical ranking of priorities (as, e.g., suggested conceptually by Aschonitis et al. (2018)) for interventions both spatially explicit (i.e., critical source areas) and requiring pollutants, were beyond the scope of this article. The water framework directive list of priority substances may be used as guidance (Directive 2008/105/EC (2008), Annex I).

Beyond source control, we argue for a step-change toward the active management of structural and functional connectivity aspects in urban catchments. To enable this process, a process-based understanding of the connectivity of urban systems needs to be established, just as understanding the role of connectivity for diffuse pollution in a rural area, so that "conceptual rather than solely empirical understanding drives how water managers interpret" the urban and specifically the drainage system (Bracken et al., 2013). For this purpose, monitoring guidelines for diffuse pollution need to be updated so that not only first-flush concentration measurements at the outlet of sub-catchments (Poudyal et al. (2016), see Section 2.2) is used for pollution quantification. Monitoring techniques for the structural and functional aspects of connectivity need to be developed for the urban context, such as for the spatial-temporal identification of effective catchment areas of diverse pollutants, runoff and flow path assessments, and redistribution patterns of matter as a function of rainstorm events. Up to this point, connectivity monitoring techniques are only employed in rural catchments (see Section 2.4.1).

The spatial and temporal interplay of pollutant buffers, barriers, and boosters (Fryirs, 2013) and their distributions in urban catchments (see Section 2.3.3 for details) require a coordinated assessment. Knowledge regarding their functioning would help urban drainage managers in identifying when and where connectivity patterns need to be maintained or altered, thus enabling or avoiding intentional or unintentional pollutant fluxes to urban water resources, respectively. A multi-scale analysis of the functioning and breaching capacity of buffers and barriers should identify when urban surfaces are strongly disconnected, diffusely connected, or completely connected (Fryirs, 2013). This analysis may guide future re-design of urban drainage strategies, as is already underway with the recent

ubiquitous expansion of decentralized SUD measures (Zhao et al., 2018) in cities. Particular care must be taken here so that altering connectivity patterns at one location does not result in detrimental effects in the system (e.g., from buffer to booster: decoupling roof areas from the drainage network to diminish effects of combined sewage systems on surface water may result in increased groundwater pollution due to the installation of rain gardens).

Continuous urbanization across the globe (McGrane, 2016) and a predicted increase in pluvial flooding due to climate change in many regions (e.g., Kendon et al. (2014) and Miller and Hutchins (2017)) have set the conditions for more urban activities, pollution accumulation, and runoff events. Therefore, very likely creating an increase in diffuse pollution in the nearer future. A system's approach may help tackle current and future pollution rates under different sets of environmental conditions.

2.4.3 Future research directions

The previous sections identified several knowledge gaps: the limited knowledge on the temporal variations of pollutant source areas concerning their size and pollution intensity (Section 2.2), limited availability of empirical data, and limited process understanding of rainfall-runoff responses on mixed urban surfaces (Section 2.3), and ultimately limited prediction of the timing of pollutant connectivity for different boundary conditions. In order to overcome the apparent lack of data, future field studies should focus on data collection within individual street canyons, that is, entire sections of streets including road, pavement and tree pit surfaces, building facades, and roofs of the surrounding buildings. Street canyons of different compositions and layouts or sub-districts containing a mixture of built and vacant lots to study changing pollution and runoff patterns needs to be assessed for intrinsic pollution patterns. Sampling locations should include different city types (new/old/industrial) and sizes (small town-to-city scales), building types, central to suburban locations, high to low degrees of sealing, different traffic amounts, and high to low-income areas. Weekly sampling over several seasons, similar to the data collection in rural catchments, will then provide a reliable base for further process studies. The major drawback is the high demand for resources that would be required for such a study and the question to which extent the results would be scalable to other cities.

To scale pollution to larger areas and to predict pollution under changing boundary conditions, urban catchment models need to evolve. Their current inability to handle complex terrain and pathways calls for a paradigm shift away from classical drainage models toward urban process models comprising structural and functional connectivity parameterizations and process descriptions. For the validation of these new model tools, it is essential to have before-mentioned field data.

Finally, diffuse pollution is seen to be more of a problem in industrialized cities in the

developed world. It is less in focus in cities of the developing world, where maintenance of public hygiene and extreme pollution of urban waters mostly from point sources leads the agenda (Chocat et al., 2007; Corcoran et al., 2010). Findings on the effects and functioning of urban connectivity may help to guide future research and re-design of urban drainage strategies to achieve sustainable management and at the same time, avoiding repeating past urban drainage mistakes.

2.5 Conclusion

This study illustrated that very diverse spatial pollution patterns exist, which can become potential source areas of diffuse pollution in cities. Some pollutant patterns, for example, heavy metal originating from street surfaces or metal roofs, are better studied than others, such as street litter, abrasive sources, or priority substances. A comprehensive survey showed that little is known about the temporal variations of most pollution patterns (e.g., seasonal or annual variations) and the concurrency dynamics of pollutant build-up and pollutant connectivity as a function of rainfall timing. For active management of diffuse pollution, distribution processes must be studied, by considering the typical spatial layout of urban critical source areas and the interplay of pollutant buffers and boosters (e.g., in the form of decentralized drainage measures) and barriers (intentional as an integral part of, and unintentional due to the malfunctioning of the drainage system).

We conclude that a holistic approach for the simultaneous investigation of urban structural and functional connectivity relevant to pollutant transfer is essential for the identification of particular harmful diffuse pollution within complex urban catchments. Understanding pollutant connectivity is, in turn, a prerequisite to improve buffer and increase barrier functions against particular harmful pollutants and to enable compliance tests for pollution control for emerging pollutants such as microplastics, novel additives or priority substances from urban surfaces.

Acknowledgements

Two excellent reviews from anonymous reviewers helped to improve an earlier version of this article. This work was supported by the Deutsche Forschungsgemeinschaft as part of the Research Training Group Urban Water Interfaces. Open access funding enabled and organized by Projekt DEAL.

Chapter 3

Analysis of diurnal, seasonal, and annual distribution of urban sub-hourly to hourly rainfall extremes in Germany

This study was published in Hydrology Research (IWA Publishing) as:

Haacke, N. & Paton, E.N.: Analysis of diurnal, seasonal, and annual distribution of urban sub-hourly to hourly rainfall extremes in Germany. *Hydrology Research*, 2021;
doi: 10.2166/nh.2021.181

This is the postprint version of the article.

3.1 Abstract

The timing of short extreme rainstorm, which was usually thought to occur on midsummer afternoons, was investigated to improve future mitigation options for infrastructure and safety from localised flash flooding. Using a peak-over-threshold approach, the timing of 10- and 60-min extreme events was filtered from high-resolution rainfall series assessing diurnal, seasonal, and annual distributions and analysed for spatial variations and prevailing atmospheric circulation types (CTs). The diurnal distribution showed a clear deviation from that of the entire rainfall regime. A complex spatial pattern was identified with distinct timing signatures of storms in the northern (mostly afternoon) and southern regions (a bimodal distribution with a second peak in the early morning) of Germany and a more homogenous diurnal distribution of events across the central regions. Most storms occurred in summer, but 42% of 10-min events occurred outside the summer months (June–July–August). A distinct annual clustering of extremes was identified, which varied

distinctly between the 10- and 60-min extremes, indicating that the sub-hourly and hourly events were far from running continuously. The timing of extreme events on the investigated time scales was not dominated by the occurrence of specific CTs in most cases, suggesting that other factors control these extremes.

3.2 Introduction

The trend behaviour of daily rainfall extremes has been well studied with a consensus on a significant but regionally varying upward trend in their occurrence (Westra et al., 2014; Barbero et al., 2019). Fewer studies have analysed hourly or sub-hourly heavy rainstorms due to the general lack of adequate, high-resolution rainfall series over longer periods. Several time-series analyses (De Toffol et al., 2009; Müller and Pfister, 2011; Guerreiro et al., 2018; Kendon et al., 2018) have provided evidence on the amplification of rainfall extremes on hourly and sub-hourly timescales over the last two to three decades. Researchers also estimated sub-daily extreme rainfall intensity to change to a greater degree than daily ones towards the end of this century, as atmospheric temperature increases under climate change (Berg et al., 2013; Westra et al., 2014; Morrison et al., 2019). Surprisingly, little is known about the timing of the hourly to sub-hourly rainstorm events for any timeline (day, season, and year). Storms in Central Europe are thought to occur mostly in the late afternoon and to a lesser extent in the late (Meredith et al., 2019) or early morning (Ghada et al., 2019) and during the summer months (Jacobeit et al., 2017; Hofstätter and Stahl, 2018; Ghada et al., 2019); however, the extent of their occurrence at other times during the day or year has not been studied yet. A similar knowledge gap exists regarding their annual incidence: Are there years with event clusters and others with hardly any events?

The shorter, sub-hourly rainfall extremes are considered problematic for urban water management as their daily counterparts, but for different reasons. Daily extremes can result in a partial or complete failure of urban drainage systems and repeated sewage overflows and urban river flooding often, which affects the entire city area (Fletcher et al., 2013). Sub-hourly to hourly extremes cause damage at different spatial scales: blocking, clogging, or overflowing of gutters frequently results in immediate, very localised flooding (Glaser and Stangl, 2004; Arnbjerg-Nielsen, 2006) which directly impacts the safety of pedestrians, traffic, and infrastructure. The high kinematic energy of the short extremes results in increased splash erosion and leaching of pollutants from abrasive sources such as building facades (Blocken et al., 2013; Bollmann et al., 2016). Combined with high first-flush concentrations from polluted street surfaces (Poudyal et al., 2016), they produce a highly concentrated pollution load sewage overflow into urban rivers.

Knowledge of the timing of the trigger events is essential to make the resulting nuisances manageable today and in the future. Information on diurnal timing may provide fire brigades

and traffic wardens with a clearer picture of emergency response. Seasonal street cleaning routines can be optimised to minimise the clogging of gutters from various sources, such as organic litter production, which is known to be highly seasonal (Duncan, 1995) and peaks when trees bloom and shed their leaves (in moderate climates normally in April/May and autumn, respectively). Knowledge of the likely timing of extremes is also essential for the planning of any future scientific monitoring campaign that may aim to quantify the dynamics of urban flash floods and diffuse pollution *in situ* (Vitry et al., 2017).

The objective of this study is to address the current knowledge gap in the timing of short and heavy rainstorms. For a set of 22 urban centres, we selected the largest 10- and 60-min extreme events exceeding a predefined threshold. We then assessed their (1) diurnal distributions, (2) seasonal distributions, and (3) annual distributions over the past 20 years across Germany. Sub-hourly trend analysis was hampered until early 2000, when an increasing number of rainfall stations provided sub-hourly information (Brieber and Hoy, 2019). This study was limited to 22 stations with adequate data quality since 2000 from urban regions homogeneously distributed over Germany. The resulting analysis period of 20 years is considered too short for reliable trend analysis and appropriate risk assessment concerning changing climate dynamics, such as increased heat waves (Fenner et al., 2019), which might drive very localised convective rainstorm patterns. However, we additionally categorised large-scale atmospheric circulation patterns (CPs), which co-occurred with extreme events, as a first trend indicator for future risk assessment.

Although studies presented here are for urban regions across Germany, this study also presents sorting methods and corresponding R routines, which can be readily transferable to other regions in Europe or beyond, where the timing of sub-hourly extremes is, to the best of our knowledge, equally understudied.

3.3 Data and method

3.3.1 Study area

Germany is in the temperate climate zone in the transition zone between the maritime climate of Western Europe and the continental climate of Eastern Europe. Weather is dominated by the prevailing circulation types (CTs) in this transition zone and leads to the following climatic differentiations in Germany: (1) oceanic climate from the Atlantic in the west, (2) maritime climate in the north, (3) continental climate in the east and southeast, and (4) subtropical climate in the southwest.

3.3.2 Data availability

A total of 22 urban meteorological stations with precipitation records for 10- and 60-min aggregation times (representing 10- and 60-min events) were available from the German Weather Service (Climate Data Center, n.d.) for the period 2000–2019, which fulfilled data consistency standards (less than 10% of missing data) and a homogenous distribution across Germany. One hour of no precipitation was chosen as a separator for two events to ensure independence from events. Information about the prevailing CTs and CPs after Hess and Brezowsky (1969) was provided in daily resolution by the German Weather Service.

3.3.3 Threshold selection

The IPCC (2012) defines a climate extreme as the occurrence of a value of a climate variable above (or below) a threshold value near the upper (or lower) end of the range of observed values of the variable. For the selection of extremes (extreme precipitation in this study), three conceptual approaches exist: the peak-over-threshold approach, the percentile-based approach, and the block maxima approach. The peak-over-threshold approach considers all values exceeding a certain threshold, i.e. a fixed threshold with a specifically associated impact (Sulikowska and Wypych, 2020). Thresholds can vary depending on the geographical context, researcher or manager goals, or other factors (McPhillips et al., 2018). The difficulty of using this approach lies in the choice of threshold

Percentile-based thresholds can be derived from statistical cumulative density functions generated from the observed data or some conceptual distributions for precipitation extremes (such as generalised extreme value) and define a given part of the observations (e.g., upper 10, 5, and 1% if using the 90th, 95th, or 99th percentile) as 'extreme'. This approach is limited by the fact that the frequency of occurrence is assumed to be known and that identified extremes are not necessarily 'extreme' because of their impact (IPCC, 2012; Sulikowska and Wypych, 2020). The block maxima approach consists of dividing the observation period into non-overlapping periods of equal size (i.e. weeks, months, seasons, and years) and restricts attention to the maximum observation in each period (Gumbel, 1958). The new observations created thus follow an extreme value distribution. By using this approach, however, relevant high observations may be ignored, and some lower observations are retained.

In this study, the peak-over-threshold approach was favoured as it allows the identification of events by a certain value of interest, without ignoring relevant events or including irrelevant events. It also provides a regional comparison of actual rainstorm magnitudes entailing urban flash flood hazards across Germany for the same rainfall depth, intensity, and duration. A fixed threshold will also allow a subsequent nationwide coordinated approach for the testing and planning of mitigation measures.

Extreme events were extracted using a threshold of 10 mm for 10-min and 20 mm for 60-min extreme events. Both thresholds were derived from recent studies on subdaily extreme rainfall by Peterson (2005), Zhang and Zhai (2011), and Westra et al. (2014) and were shown to have a specific impact on urban flooding by Guerreiro et al. (2018). By using these thresholds, a total of three hundred and nine 10-min storms and one hundred and eighty-five 60-min storms were identified at the 22 stations within the last 20 years.

Different total numbers of events were identified for the stations varying between three 10-min (six 60-min) events for List auf Sylt and seventeen 10-min (twenty-eight 60-min) events for Munich. An apparent increase in storm number is evident from north to south for both durations (Fig. 3.1); no clear variation in storm number was found from west to east.

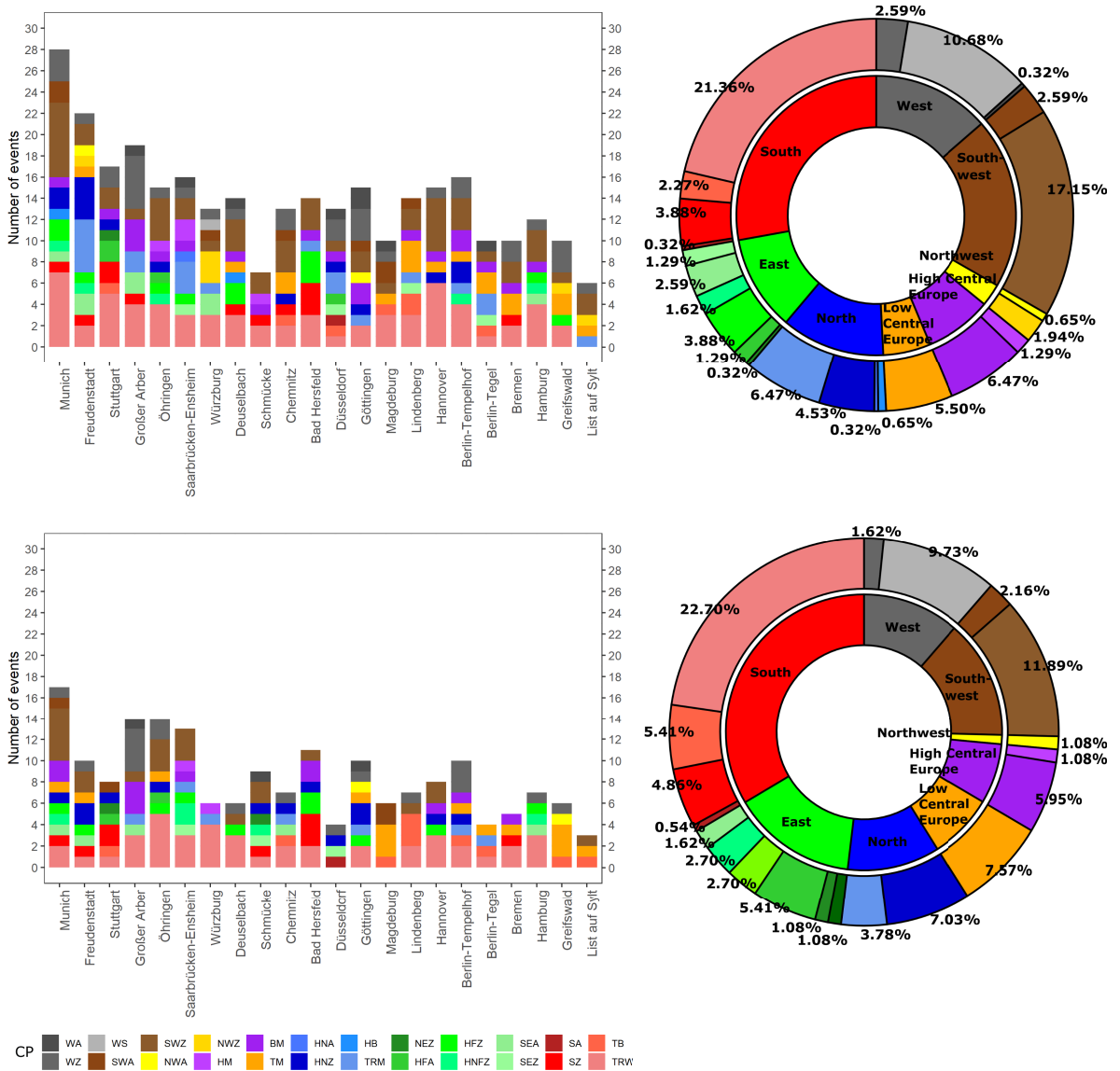


Figure 3.1: Frequency distribution of extreme 10-min (upper row) and 60-min (lower row) rainfall events at all stations sorted from south to north. Circular plots show the percentage of CTs and CPs that co-occurred during the storms. All acronyms are explained in Table 3.1.

3.3.4 Atmospheric CTs and CPs

Atmospheric CTs summarise the wind direction, humidity, pressure, and thermal properties of air masses, describing the fundamental processes that link large-scale atmospheric conditions with near-surface climate phenomena (Ghada et al., 2019). One of the defining features of CTs is the wind direction of the air mass advection as summarised in Table 3.1. The table also comprises the atmospheric CPs associated with each CT (see Werner and Gerstengarbe (2010) for an in-depth description of each CP). Each sampled storm event was assigned to the prevailing atmospheric CTs and CPs on that day (Fig. 3.1). All major CTs and a total of 23 (20) CPs were detected to co-occur during the 10- and 60- min extreme storms. Most storms occurred with air mass inflow from the southern directions (28 and 34%, with a trough over Western Europe (TRW days) being the most dominant pattern), followed by air masses approaching from south-western (20 and 14%) and western (14 and 11%) directions. There appears to be no difference regarding CTs co-occurring with extreme events between the northern part (potentially influenced by large water bodies) and the southern part of Germany (influenced by the Alps) (Fig. 3.1).

3.3.5 Analysis tools

Statistical analysis was performed using the statistical software R (R Development Core Team, 2018). An R routine for the automatic identification, calculation, and visualisation of diurnal, seasonal, and annual extremes for multiple time series was developed and is available for the research community under an R Cran GUI public licence.

3.4 Results

3.4.1 Diurnal distribution of heavy storm events

The majority (79%) of storm events occurred in the afternoon and evening (12:00–22:00) with peaks around 15:00 and 16:00/20:00 for the 10- and 60-min extreme events, respectively (Fig. 3.2). A considerably smaller amount occurs in the first half of the day homogeneously distributed over the early hours. Median values of diurnal timing for individual stations (red marks in Fig. 3.2) vary significantly between individual stations ranging between 9–17:00 (10-min) and 10–20:00 (60-min) storms. Stations can be grouped into three dominant patterns of timing: (1) an accumulation of events over 12 h, emerging predominantly in the afternoon and evening (ten of 22 for 10-min and four of 22 for 60-min); (2) a bimodal distribution of events in the early morning (more than one event) and afternoon with a higher and denser concentration in the afternoon (four of 22 for 10-min and eight of 22 for 60-min); and (3) a

Table 3.1: Large-scale atmospheric CTs and CPs according to Werner and Gerstengarbe (2010). (This table shows patterns identified in this study area only.)

Large-scale atmospheric CT	Atmospheric CP
West	WA: westerly, anticyclonic WZ: westerly, cyclonic WS: westerly, south-shifted
Southwest	SWA: south-westerly, anticyclonic SWZ: south-westerly, cyclonic
Northwest	NWA: north-westerly, anticyclonic NWZ: north-westerly, cyclonic
High Central Europe	HM: high over Central Europe BM: zonal ridge across Central Europe
Low Central Europe	TM: low over Central Europe
North	HNA: Icelandic high, ridge Central Europe HNZ: Icelandic high, trough Central Europe TRM: trough over Central Europe
East	NEZ: north-easterly, cyclonic HFA: Svanidavian high, ridge Central Europe HFZ: Scandinavian high, trough Central Europe HNFZ: high Scandinavian Iceland, trough Central Europe SEA: south-easterly, anticyclonic SEZ: south-easterly, cyclonic
South	SA: southerly, anticyclonic SZ: southerly, cyclonic TB: low over the British Isles TRW: trough over Western Europe

homogenous distribution of events over 24 h (seven of 22 for 10-min and ten of 22 for 60-min).

The spatial distribution across Germany of the three timing patterns (Fig. 3.3) reveals that the north-western region (e.g. Hamburg, Bremen, Hannover, and List auf Sylt) has most of its events in the afternoon and evening, and almost no precipitation in the early hours (blue pie charts in Fig. 3.3). The southern region (e.g. Munich, Freudenstadt, and Groß Arber) is dominated by the second timing pattern with two peaks: the major one being in the evenings (yellow pie charts). More homogenous distribution of events around the clock can be observed in the west and centre of Germany (red pie charts). However, deviations of these spatial patterns of timing were noticeable across the middle section of Germany.

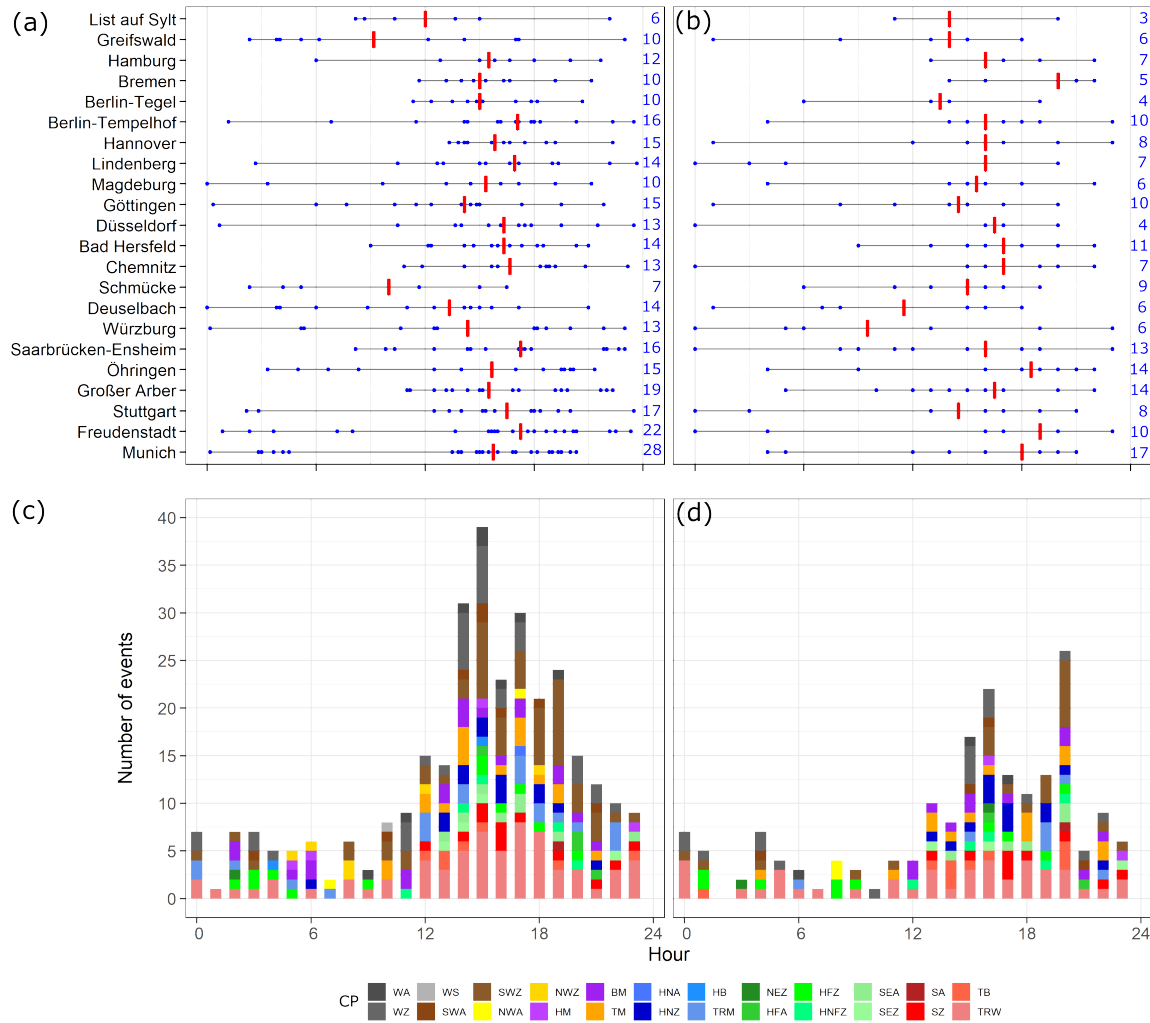


Figure 3.2: Diurnal distribution of short-duration heavy storm events across Germany of (a) 10-min duration (≥ 10 mm) and (b) 60-min duration (≥ 20 mm). Red mark represents the median, and the number of events is given in blue. Hourly frequency distribution, including information about prevailing CTs and CPs, is shown for 10-min events in (c) and 60-min events in (d). All acronyms are explained in Table 3.1.

Diurnal timing cannot be linked directly to specific prevailing atmospheric CTs (presented by colour coding in Fig. 3.2), i.e. none of the CPs dominate during early morning or afternoon storms. Heavy rainstorms co-occurred around the clock with eastern, southern, south-western, and western CTs. However, it is notable that the low central type co-occurred mostly with storms during the afternoon, but not during night and morning hours. For 10-min events, the northwest type only co-occurred during the day, and for the 60-min storms, the north and high central east type only co-occurred in the afternoon and evening.

Storms associated with the most frequent CT, the southwestern circulation, tended to co-occur mostly with the circulation pattern SZ (cyclonic southerly) in the afternoon. However, the TRW (trough over Western Europe) pattern co-occurred with storms around the clock.

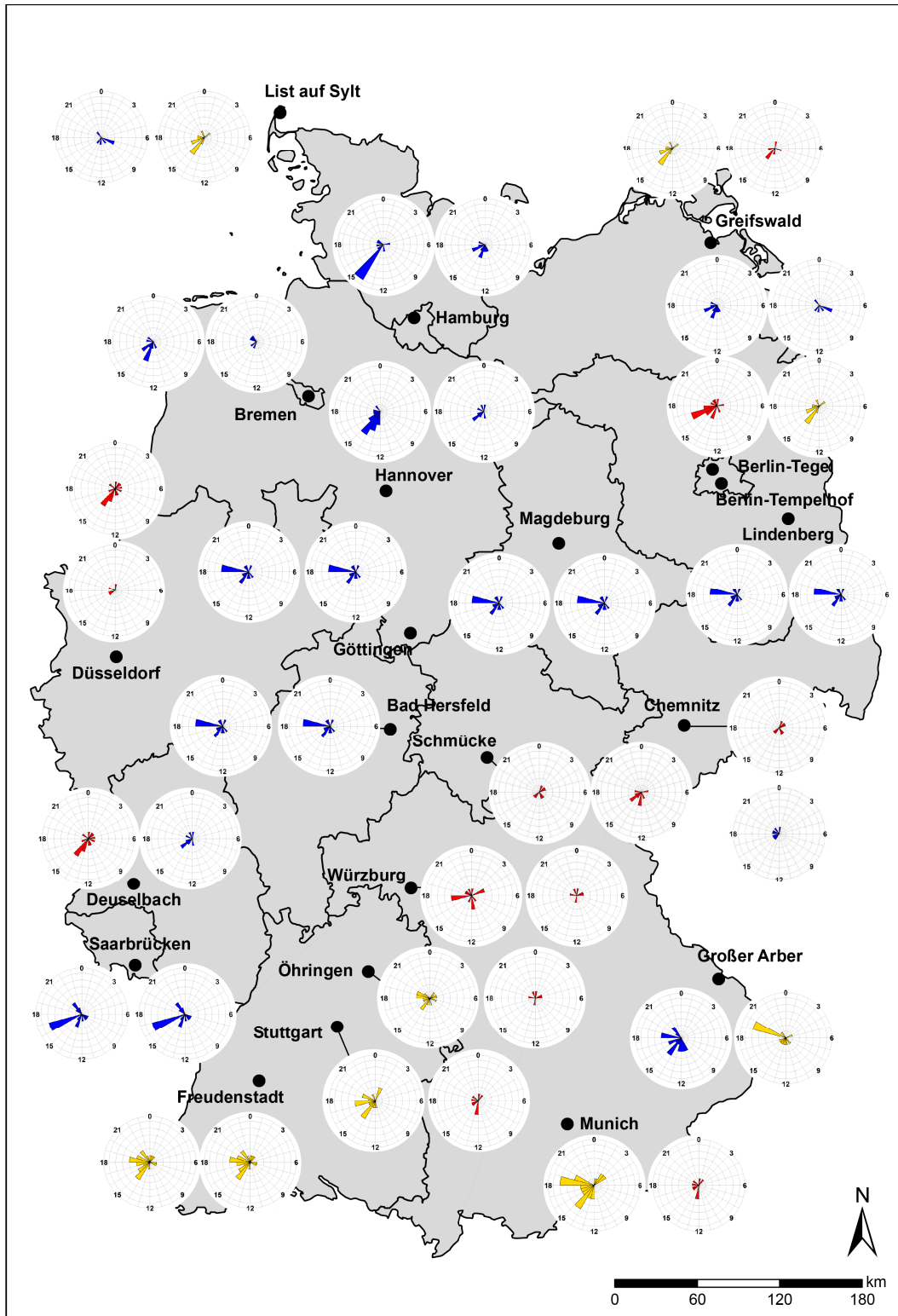


Figure 3.3: Diurnal frequency distribution of short-duration heavy storm events across Germany. The pie chart represents 24-h clock, whereby left pie charts represent 10-min events (≥ 10 mm), and right pie charts represent 60-min events (≥ 20 mm). Colours represent classifications: blue = accumulation of events over 12 h, yellow = bimodal distribution, and red = homogeneous distribution (modified after Paton and Haacke (2021)).

3.4.2 Seasonal distribution of heavy storm events

In total, 58% (10-min) and 83% (60-min) of storms occurred in the summer months (June, July, and August) with a median date on the 9th of July (Julian day 190) and the 11th of August (Julian day 223) for 10- and 60-min events, respectively (Fig. 4.8). Most heavy rainfall events (84% of 10-min and 99% of 60-min events) occurred between May and September, whereas a significantly smaller proportion (for the 60-min event, only one event at the station in Berlin) occurred in the autumn and winter months from October to April. Stations, with a wider seasonal range of the occurrence of 10-min events, are mainly located in the southern part of Germany.

The seasonal timing of heavy rainstorm events shows some interesting co-occurrence patterns with CTs. Outliers, outside the summer months, co-occur mostly with northwestern and high central CTs. For the 10-min event, there exists a strong relation between northern circulation and 10-min events in the autumn months. During the entire summer months, all CTs except the north-western type were detected to co-occur during individual storms; the western type tends to be more pronounced in the second summer half.

3.4.3 Annual distribution of heavy storm events

For the 10-min events, the largest number of storms occurred in the years 2005 and 2017 (23 and 24 storms, respectively). In 2015, the smallest number of storms (six) was identified. The average annual storm number was around 15; no trend was detected over the 20 years of data.

For the 60-min events, the largest number of storms were consecutively detected from 2016, 2017, and 2018 (14, 14, and 19 storms, respectively), whereas in the years 2004 and 2015, only three and two storms occurred (Fig. 3.5). The plot of annual events in Figure 3.5d shows a clear trend. A Mann–Kendall trend test indicated an increase in the occurrence of storm events (Mann–Kendall test statistic τ : 0.491, $p < 0.01$, $N = 20$) with a statistically significant trend slope (after the Theil–Sen approximation) of 0.5%, equivalent to an increase of 0.5 events/year or 10 events over the investigation periods. The trend test was carried out over a short period of 20 years, so care needs to be taken when interpreting these results.

The annual variations of 10- and 60-min events differ notably, not only concerning their trend behaviour but also their annual clustering. In the years with the most 60-min events, we detected average or below-average numbers of 10-min events and *vice versa*. This effect is particularly visible for the year 2004, where twenty 10-min but only three 60-min extreme events were detected. The large number of storms that occurred in 2018 is particularly interesting, as it was a year mostly famous for being particularly dry over the entire summer months throughout Germany.

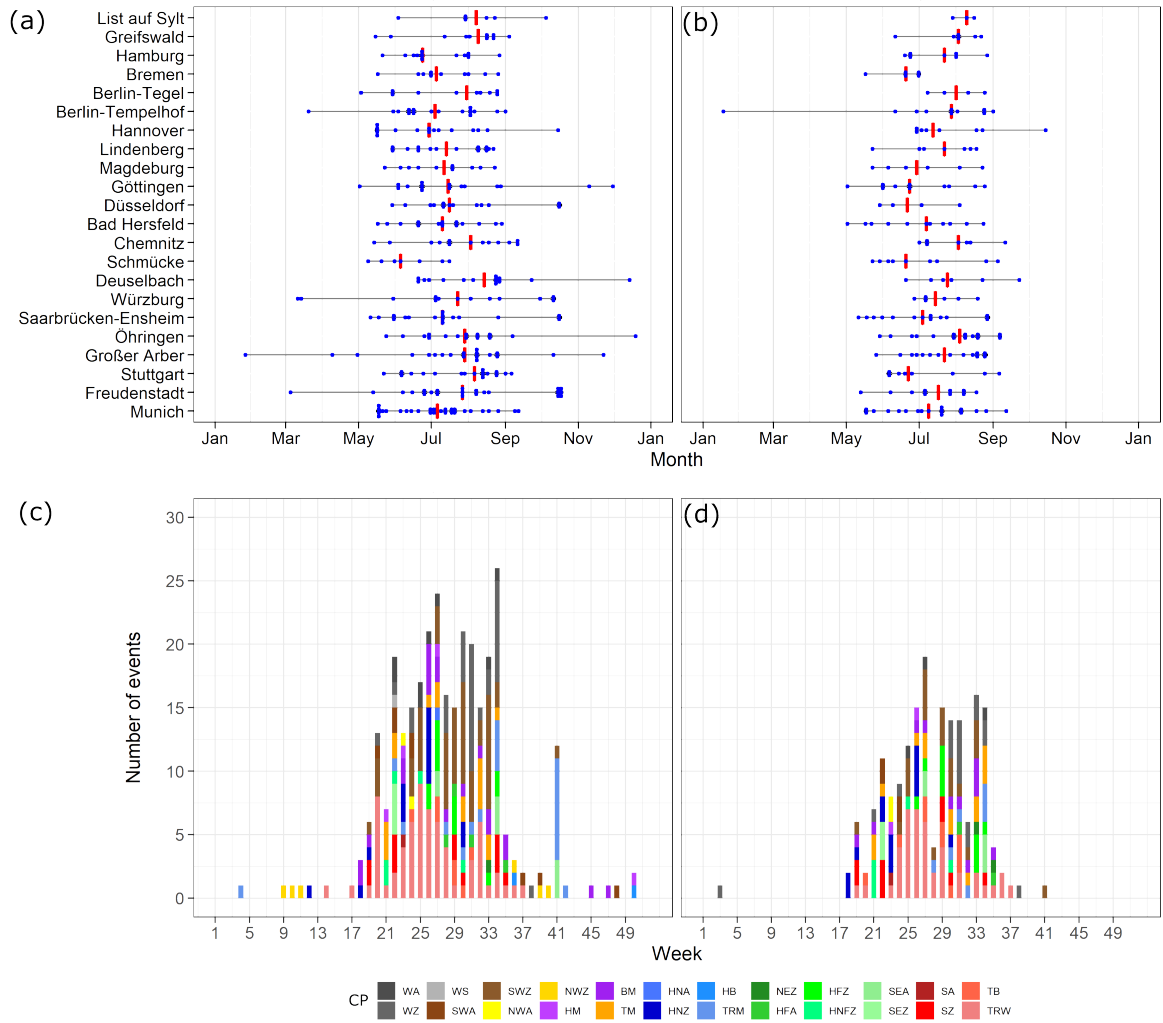


Figure 3.4: Seasonal distribution of short-duration heavy storm events across Germany of (a) 10-min duration (≥ 10 mm) and (b) 60-min duration (≥ 20 mm). Red mark represents the median. Weekly frequency distribution, including information about prevailing CTs and CTs, is shown for 10-min events in (c) and 60-min events in (d). All acronyms are explained in Table 3.1.

In the years with the largest number of storm events, storms were associated with a wide range of different CTs. The 10-min extreme storms in 2005 and 2017 co-occurred mostly with southwest and southern CTs, whereas the 60-min extreme storms in the years 2016, 2017, and 2018 were associated with CTs in all directions.

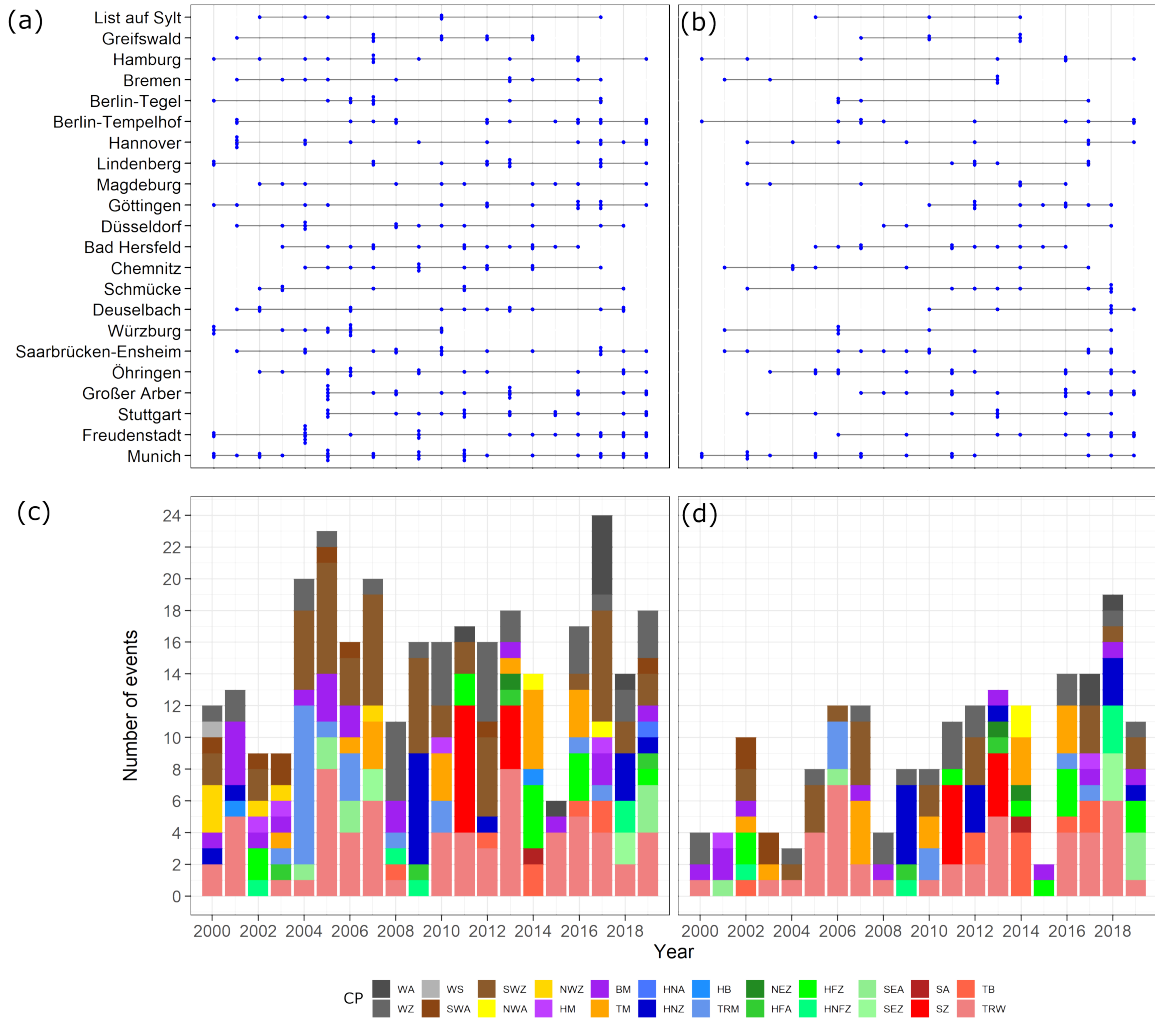


Figure 3.5: Annual distribution of short-duration heavy storm events across Germany of (a) 10-min duration (≥ 10 mm) and (b) 60-min duration (≥ 20 mm). Red mark represents the median. Annual frequency distribution, including information about prevailing CTs and CPs, is shown for 10-min events in (c) and 60-min events in (d). All acronyms are explained in Table 3.1.

3.5 Discussion

3.5.1 Timing of extreme events

The *diurnal* distribution was quantified in this study for extreme events only. In contrast, many previous studies on diurnal distributions quantified the frequency and amount distribution for the entire (hourly) rainfall regime, including low-to-moderate hourly rainfall values (e.g., Yaqub et al. (2011), Mandapaka et al. (2013), and Ghada et al. (2019)). Other studies used a percentile-based approach looking at the most extreme events only (e.g., Meredith et al. (2019)). These studies confirmed a peak in rainfall amount in the late afternoon to late evening hours for study areas in Central Europe. However, a direct comparison of their results with

the here-used peak-over-threshold selection of extreme events is limited. Ghada et al. (2019) investigated the geographical patterns associated with the diurnal cycle across Germany. They did not find differences in peak distributions regarding latitude, longitude, and elevation for average hourly rainfall (but larger differences with rainfall frequency). However, their study included all hourly rainfall amounts >0.2 mm, which does not compare well to our threshold value of 20 mm (for 60-min events) for event selection.

This study showed that the diurnal distribution of extreme events does not follow the diurnal distribution of rainfall if all and not only extreme rainfall events were considered. Instead, we were able to distinguish more complex spatial patterns with distinct timing signatures of storms that differed between the northern (mostly afternoon) and southern regions (a bimodal distribution with a second peak in the early morning) of Germany. The afternoon peaks are caused by classical convection mechanisms (Ghada et al., 2019). Whereas the morning peaks may be attributed to the accumulation of humidity at lower levels during the night and complex topography, for example, as found in southern Bavaria towards the Alps with distinct peaks in early morning storm events in Munich. Proximity to water bodies may result in a similar effect and explain the morning peak in the northeast (e.g., Greifswald at the Baltic Sea), but this explanation is not valid for the diurnal timing in the north-western part of Germany where no pronounced morning peaks were detected in most cases.

Our *seasonal* distribution of extreme events confirmed previous knowledge that storms occurred mainly during the summer months of June–July–August (Darwish et al. (2018) and Ghada et al. (2019) for the UK). At the same time, our study showed that 42% of 10-min events (17% of 60-min events) occurred outside the summer months, most of them in May and September (26% of 10-min and 16% of 60-min events), and a smaller portion in the winter. A recent study by Darwish et al. (2018) identified a shift of extreme events from the summer to autumn months, which might lead to an intensification of event incidents. However, the total number of detected autumn extremes in this study was considered too small for trend analysis to yield reliable results.

To our knowledge, no studies have analysed the *annual* areal distribution of sub-hourly extremes across Germany or Europe over the last decades. A general trend increase of hourly extremes was detected by De Toffol et al. (2009) and Müller and Pfister (2011) for extremes with durations from 1- to 30-min for individual station series, but neither study analysed the concurrence of extremes in specific years. We found a statistically significant trend increase of the 60-min storm events across Germany; however, this result should not be overvalued as the analysis was based on only 20 years of data, considered too short for climate-relevant trend analysis.

The fact that the annual variations and trend behaviour of 10- and 60-min extreme

events differed notably suggests that the sub-hourly temporal scaling cannot be neglected. Distinctively different annual behaviours, as we detected for several years, for example for 2004, when nearly seven times more 10-min events occurred, confirm that the 10- and 60-min extremes are far from running continuously. The large number of storms that were detected in 2018 are particularly interesting. According to Thompson et al. (2020), the 2018 drought was one of the longest and hottest recent European droughts with spring and summer precipitation falling below 40% of normal amounts. Concurrently, a higher-than-average number for the 10-min and the largest number of 60-min extremes occurred in this year. In similar hot and dry summers of 2004, 2010, 2013, and 2015 (Hanel et al., 2018), no increased numbers of storm events were detected; the opposite was true for 2015, with the smallest overall number of events. A detailed explanation of the underlying process mechanisms is pending.

3.5.2 Atmospheric CTs and extreme events

Atmospheric CTs govern rainfall emergence. However, the correlations between CTs and rainfall incident and timing are more pronounced for low-to-moderate rainfall events rather than extreme events (Ghada et al., 2019). Our findings partly confirmed the results by Brier and Hoy (2019). They found that sub-hourly extremes (15-min events) in Central Germany are frequently generated by warm, humid continental air from Southern and Eastern Europe as well as trough conditions over Western Europe. Beyond that, we saw that CTs from any wind direction might prevail during the selected extreme events, which suggests that other dominant factors influence the convective precipitation occurrence of short extremes as well.

The occurrence of specific CTs did not dominate the timing of extreme events on the diurnal, seasonal, and annual scales. Heavy storms in the afternoon frequently occurred with warm and moist air from south-western directions, as was estimated in the study by Ghada et al. (2019) for any hourly rainfall intensities. Some distinct patterns exist between the co-occurrence of northern and central CTs during the day and night storms and for autumn storms, but the number of those cases was too small to derive a clear connection.

The diverse co-occurrence of CTs with identified 10- and 60-min extreme events is remarkable and requires further investigation. High-resolution (convection-permitting) regional climate models, such as those used in Meredith et al. (2019) or the analysis of atmospheric circulation anomalies versus soil moisture–temperature coupling as done by Liu et al. (2020), could be employed to study the overall extreme climatic behaviour, for example, for the year 2018, which was particularly dry and hot, and to show the largest areal number of 60-min storms. Only a process-based approach, beyond the scope of this study, will allow the identification of the underlying mechanisms that led to the generation of

multiple CT-storm combinations that occurred in that year.

3.5.3 Future research and way forward

Three major areas of research on the timing of extremes remain: the modulation of extreme event occurrence due to CTs, orography, large water bodies, and urban influences (e.g. reported by Lorenz et al. (2019)); a potential change of timing due to climate change; and the temporal scaling of sub-hourly rainfall.

The modulation of extreme event occurrence cannot be addressed using the available rainfall point data from individual stations. Especially for large cities, which are considered to have an effect on rainfall distribution, more than one point data is required. In this study, two stations were selected for the city of Berlin. Differences can be seen at all timescales; however, a radar-based time-series analysis as described by Mandapaka et al. (2013) or Panziera et al. (2018) would be better to assess urban and regional signals as a function of storm timing. Currently, homogeneous precipitation time series from radar systems are only available for a period of 16 years in Germany (Lengfeld et al., 2019).

For a stringent analysis of changes in extreme timing, much longer time series than 20 years are required, but normally not available in the necessary resolution. Longer rainfall series should also be analysed in uniform with other climate drivers of rainstorms, which showed a clear trend over the last one to two decades and are highly sensitive to convective dynamics such as increasing temperatures with more frequent heatwaves during the summer months (Fenner et al., 2019) and increasing the occurrence of westerly CTs (Plavcová and Kyselý, 2013). If and how the changing dynamics affect the timing of extremes is not yet clear and beyond the scope of this study.

Finally, the temporal scaling of sub-hourly data needs further research. Whereas the diurnal timing of 10- and 60-min extremes was relatively similar, dissimilarities emerged regarding their annual and seasonal clustering. The distinct differences in timing indicate that the behaviour of hourly and sub-hourly extremes cannot simply be lumped together but need to be analysed separately.

During this analysis, it emerged that the selection of fixed time intervals of sub-hourly extremes may not be an adequate way of dealing with convective storms, as it also does not capture the essence of the entire storm behaviour. For subsequent analysis of short rainstorms relevant for a risk assessment of urban flash floods, we suggest against simply filtering for sub-hourly time steps with extreme intensities, but rather including the entire course of the precipitation hydrograph in the storm selection. Beside the average intensity, the categorisation of such sub-hourly extreme events should also include information on hydrograph shape, peak intensity and duration, and total rainfall amount. Furthermore, further research could include

the investigation of changes in the timing of extreme rainfall in urbanised areas in comparison to rural areas.

3.6 Conclusion

This study sheds new light on the temporal distribution of short heavy rainfall extremes, whose timing cannot be simplified to summer afternoons. However, a complex spatial signature of storms regarding diurnal timing was discovered that differed between the northern (mostly afternoon) and southern regions (a bimodal distribution with a second peak in the early morning) of Germany. Although the most frequent occurrence of events was identified in summer, a significant number occurred between May and September depending on the region. Therefore, the traditional seasonal division of summer (June–July–August) may not be appropriate when analysing extreme events. We identified annual clusters for years with a particularly small and large number of events, but they were not identical for the two aggregation times. This discrepancy and the diverse co-occurrence of CTs require further research on the underlying mechanisms and driving forces of convective storm generation and initiation using, for example, high-resolution convection-permitting regional models for different geographic settings. For future work on the temporal scaling of convective extremes, we hypothesise that the 60-min events share more similarities with daily extremes than with 10-min extremes. We further suggest including the rainfall hydrograph of short extremes in future analysis to capture the essence of the entire convective storm behaviour.

Acknowledgements

This work was supported by the Deutsche Forschungsgemeinschaft as part of the Research Training Group Urban Water Interfaces (GRK 2032). I thank Dr. Nehls and Dr. Otto for useful critiques and for reviewing this study.

Data availability statement

All relevant data are included in the paper or its Supplementary Information.

Chapter 4

Impact-based classification of extreme rainfall events using a simplified overland flow model

This study was submitted to Urban Water Journal as:

Haacke, N. & Paton, E.N.: Impact-based classification of extreme rainfall events using a simplified overland flow model. *Urban Water Journal*, submitted for publication on May 25, 2022, resubmitted with advised corrections on October 26, 2022

This is the original manuscript of an article submitted to Taylor & Francis in *Urban Water Journal*.

4.1 Abstract

In this study, we present a new approach to rainfall classification that uses a simplified overland flow model to facilitate impact assessments of heavy rainstorms. Conventional rainfall classification approaches using peak intensities or rainfall sums can lead to misjudgements of the impact of rainfall event, as they do not explicitly consider the potential of rain to generate and sustain substantial amounts of overland flow on typically sealed, urban surfaces. The new method of impact-based rainfall classification proposed here comprises three steps: Identification of rainfall events from high-resolution time series, computation of overland flow depths for each event, and impact-based classification of rainfall events as a function of the magnitude of overland flow. The accuracy of this approach was evaluated with respect to its ability to describe seasonal and annual occurrences of and variations in rainstorm impacts for high-resolution series at three different urban stations in Germany.

4.2 Introduction

Urban pluvial floods are caused by extreme rainstorms, with rainfall rates exceeding the capacity of urban drainage systems, and causing severe damage to urban infrastructure (Rözer et al., 2021). They are seen by many as invisible hazards (Forzieri et al., 2018; Jacobs et al., 2018; Moftakhari et al., 2018; Suarez et al., 2005), as they can often strike with little warning in areas with no recent record of flooding. The instances of pluvial flooding are rising due to a combination of global climate change, urbanisation, and a lack of investment in sewer and drainage infrastructure (Westra et al., 2014). Although many modelling software packages are available to simulate pluvial flooding in urban catchments (e.g. InfosWorks ICM (Innovyze, 2020), SWMM (Rossman, 2010), MOUSE (DHI, 2000)), and many methods exist to describe the underlying hydrological processes (c.f. Salvatore et al. (2015)), predicting the extent and severity of pluvial floods remains challenging. This is due to an incomplete understanding of the interactions between urban and natural hydrological systems, as well as the high degree of uncertainty (Salvatore et al., 2015).

Local information about urban drainage systems, topographic data, land use and soil moisture preconditions, and precipitation data with high spatial and temporal resolutions are needed to realistically reproduce complex hydrological processes. However, considering that it is time-consuming and costly to develop and run hydrological models, and- perhaps most decisively, the paucity of available data- the utility and applicability of such models to urban pluvial flooding remains limited. In recent years, the improvement of geographic information systems (GIS) and the availability of remote sensing data at higher resolutions have helped to link hydrologic processes and topography so that we may finally identify and map areas that are the most prone to flooding (Di Salvo et al., 2017). For example, a topography-based urban flooding index, the topographic wetness index (TWI), was developed and has increasingly been applied to urban settings via the Blue Spots method; this approach is focused specifically on identifying the surface depressions that are most prone to fill during high-intensity storms (Balstrøm and Crawford, 2018).

While there has been great progress in the representation of surface characteristics, it is still common to represent rainfall events by design rainfalls with characteristics based on conventional rainfall classifications using time-aggregated data. For pluvial flooding, the focus has only been on extremes selected by either a percentile approach (99th and 95th percentiles (Brieber and Hoy (2019), Jacobeit et al. (2017), and Schär et al. (2016) and citations therein) or on events exceeding a certain threshold (peak-over-threshold method; Acero et al. (2011), Agilan et al. (2021), Anagnostopoulou and Tolika (2012), Beguería et al. (2011), and Haacke and Paton (2021)), both of which are based on averaged intensities; the most commonly used intensities are mm/1 h, mm/6 h, and mm/24 h. However, recent studies have shown that averaged rainfall intensities do not accurately represent the specific hydrography of extreme

rainfall events and lead to the over- or underestimation of rainfall characteristics and to an incomplete understanding of the overland flow generated (as discussed in detail by Dunkerley (2020)). A better approach would be to consider the actual lengths of rainfall events as event characteristics, such that the precipitation amount, mean rainfall rate, surface runoff volume and flow depth generated are defined in relation to it (Dunkerley, 2008). The most intense periods of rainfall within a given event are thought to affect the flux, depth of overland flow, and infiltrability in different ways; for instance: a late peak event shows higher runoff ratios and lower infiltration depths than an early peak event (Dunkerley, 2017). The rainfall pattern (also termed ‘event profile’, which is defined as the time-varying sequence of rainfall intensities, including any intermittency) heavily controls the amount of infiltration and runoff (in addition to surface characteristics).

Recent studies have critiqued the fact that little attention has been paid to events resulting in low levels of flooding (Moftakhari et al., 2018). Such events are often thought to be less harmful; however, they are still able to generate substantial overland flow, causing minor to moderate flooding, which may be amplified in highly sealed urban environments. Compared to extreme pluvial flooding, these events do not pose significant threats to public safety or cause major property damage; nevertheless, they can disrupt daily activities, add strain to infrastructure systems, and cause minor property damage (Moftakhari et al., 2018). They also trigger diffuse pollution transport processes on urban surfaces (Paton and Haacke, 2021). Hence, we argue that rainstorm events should be evaluated and classified by their potential to generate overland flow on urban surfaces and not exclusively by their average or maximal intensities. We suggest applying an approach that is commonly used in soil erosion studies, especially on rural hillslopes, where overland flow depth has been successfully used to evaluate the impact of heavy rainfall on the incipient motion of unconsolidated sediments and adsorbed nutrients or pollutants (Abrahams et al., 1998; Parsons and Stromberg, 1998; Yuan et al., 2019). The goal of this study was to present a new rainfall classification method based on the potential of individual rainstorm events to generate and sustain overland flow, defined as flow depth per time unit, on a simplified urban model surface, considering fluctuations in intensity and intermittency to represent rainstorm characteristics as accurately as possible. To illustrate the potential of the proposed method, it was additionally compared to a conventional method. We then applied this method to three stations across Germany to demonstrate its ability to describe the seasonal and annual occurrence of and variations in rainstorm impacts using high resolution data compiled over the last three decades.

4.3 Impact-based rainfall classification method

The new method for impact-based rainfall classification proposed here comprises three consecutive steps: rainfall event delineation, overland flow depth computation for each event,

and impact-based classification of rainfall events as a function of overland flow. For event delineation, individual rainfall events were derived from continuous, long-term, high-resolution rainfall series with a temporal resolution of at least 10 min using a fixed inter-event time (IET). The overland flow depth generated by the delineated rainfall events was calculated for a typical urban sealed surface and used as an indicator of the magnitude of surface runoff and pluvial flooding. For impact-based classification, the same fixed flow depth thresholds were used to classify individual rainfall events according to the flow depth they were able to generate and sustain for a specific period of time. The method was applied and evaluated for three stations across a south-north transect through Germany (Würzburg, Potsdam, Hamburg); interim results were shown for the station Würzburg for illustration only.

4.3.1 Event delineation

Individual rainfall events were delineated from continuous rainfall time series with a 10-min time step or higher. Rain data of less than 0.1 mm per 10 min were disregarded, as they were considered artefacts of condensation or funnel drainage at the end of events and increased their duration while minimally increasing the rainfall depth (Gaál et al., 2014). To extract rainfall events, an IET of one hour was used to define rainless intervals between rainfall events (Fig. 4.1a), which was considered short enough to capture convective rainstorms events in the study region. For different climatic settings, the IET might have to be adjusted to identify typical IETs, as reviewed here by Dunkerley (2008).

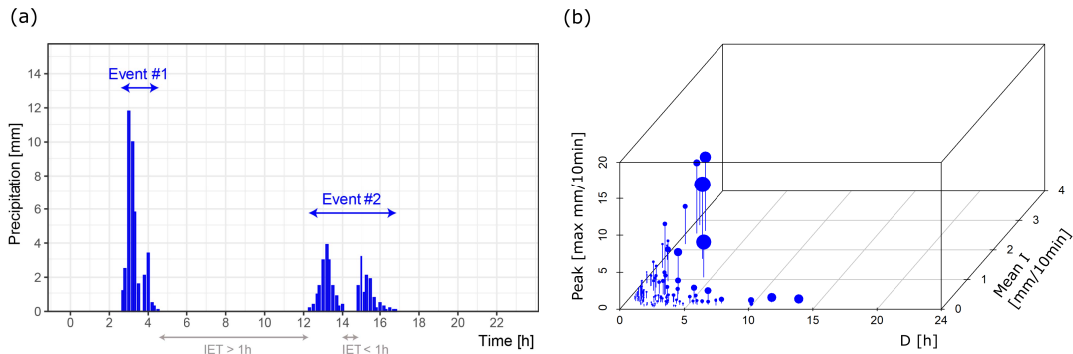


Figure 4.1: (a) Schematic showing the identification of individual rainfall events. (b) Delineated rainfall events in 2010 for the station Würzburg. Point sizes represent precipitation amounts.

Each delineated rainfall event was characterised and visualised by four summary values in a multi-dimensional scatterplot containing information on total rainfall depth (P), peak intensity, mean intensity and event duration (D). In particular, the last three characteristics represented critical drivers of overland flow (Fang et al., 2012; Sen et al., 2010) but have often been neglected or averaged in recent rainstorm classifications (Jo et al., 2020; Yoo and Park,

2012). As an example of the delineation and characteristics of rainfall events, Figure 4.1b shows 105 delineated events for a rainfall series of the station Würzburg in Germany.

4.3.2 Overland flow model

An overland flow model after that of Scoging (1992) was used to calculate the flow depth as an indicator of the magnitude of surface runoff for a typical asphalt street surface for each delineated rainfall event (Fig. 4.2). The flow depth was chosen as an indicator of the impact of rainfall events, as it was successfully employed in a previous study (Yuan et al., 2019) as a proxy for incipient motion in unconsolidated sediments. The magnitude of the flow depth indicated that a significant amount of overland was generated, resulting in pluvial flooding and the redistribution of pollutants.

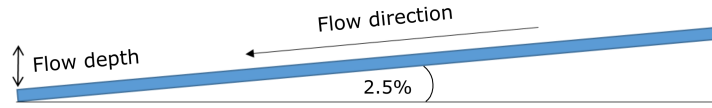


Figure 4.2: Schematic representation of the model street.

The overland flow model was based on a one-dimensional kinematic approximation of the dynamic St. Venant equation for the computation of flow depth. The continuity equation is given by:

$$\frac{\partial q(x, t)}{\partial x} + \frac{\partial D(x, t)}{\partial t} = ex(x, t) \quad (4.1)$$

where q is the discharge per unit width [mm^2s^{-1}], D is the flow depth [mm], and ex is the rainfall excess [mm s^{-1}].

Equation 4.1 can be expressed in finite-difference form, where Δt time is increment in seconds:

$$\frac{q(x, t - \Delta t) - q(x - \Delta x, t - \Delta t)}{\Delta x} + \frac{D(x, t) - D(x, t - \Delta t)}{\Delta t} = ex(x, t - \Delta t) \quad (4.2)$$

Rearranging, and solving for $D(x, t)$, the unknown:

$$D(x, t) = (ex(x, t)\Delta t) + D(x, t - \Delta t) + \frac{\Delta t}{\Delta x}[q(x - \Delta x, t - \Delta t) - q(x, t - \Delta t)]. \quad (4.3)$$

Initially depth at $t = t_0 + \Delta t$ is determined entirely by $ex(x, t)$ since inflow discharge is zero.

The infiltration rate, interception and depression storage of a typical sealed urban surface were assumed to have constant values as given in Table 4.1, derived from a recent review after Rammal and Berthier (2020) and from terrestrial laser scan experiments on sealed surfaces by Nehls et al. (2015). The flow velocity v was calculated using the Darcy-Weisbach flow equation in infinite form:

$$v(x, t) = \sqrt{\frac{8gD(x, t)s(x)}{ff(x, t)}} \quad (4.4)$$

and

$$q(x, t) = D(x, t)v(x, t) \quad (4.5)$$

where v is the flow velocity [mm^2s^{-1}], g is the gravitational constant [mm/s^2], s in the sine slope gradient [m/m] and ff in the Darcy-Weisbach friction factor [-].

Rainfall excess ex [mm s^{-1}] was defined as the amount of rainfall at a given time that could not infiltrate the surface and thus exceeded the interception and depression storage capacities:

$$ex(x, t) = r(x, t) - i(x, t) - loss(x, t) \quad (4.6)$$

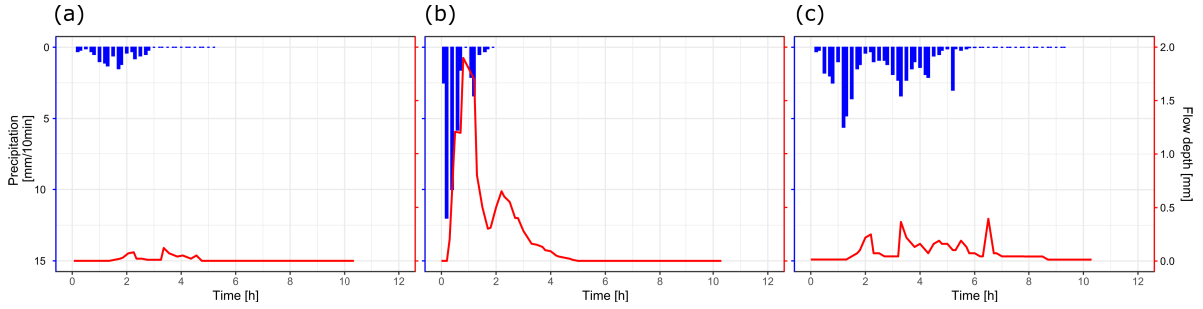
where r is the rainfall intensity [mm s^{-1}], i is the infiltration rate [mm s^{-1}], and $loss$ is the loss due to interception and depression storage [mm s^{-1}]; once the loss storage is filled during a rain event, the loss term is set to zero.

The model street surface was represented by a 100-metre long and 10-metre wide model domain (total area = 1000 m^2), with a low slope and high degree of sealing; thus, the surface had a low infiltration rate and small interception and depression storage. Table 4.1 gives some typical parameter values for the street surfaces. The model time step was set to 10 s to ensure computational stability.

Figure 4.3 shows example outputs of the overland flow model for rainfall events with very low intensities (drizzle) and medium intensities over long periods (continual rain), resulting in no or minimal overland flow, as well as for rainfall events with high intensities of convection that generated substantial overland flow.

Table 4.1: Typical parameterisation of a street surface.

Parameter	Values
Slope (s)	2.5%
Friction factor (ff)	0.1
Infiltration rate (i)	0.36 mm/h (Nehls et al. 2015)
Interception and depression storage ($loss$)	0.46 mm (Rammal and Berthier 2020)

**Figure 4.3:** Example flow depth dynamics of three rainfall types: (a) drizzle, (b) convective, and (c) continuous rainfall.

4.3.3 Impact-based classification of rainfall events

Most delineated rainfall events did not generate any overland flow, as their rainfall intensity and/or durations were too small (Fig. 4.3a & c); therefore, most rainfall either infiltrated or filled the interception and depression storage. Using this classification approach, the remaining rain events that generated and sustained certain overland flow depths over a specific time were categorised into four classes of severity. The severity of the impact that caused pluvial flooding and pollution transfer was defined with fixed thresholds for the flow depths (low, medium, high, or very high) and a specific minimum flow duration. When selecting a minimum flow duration, it should correspond to the temporal resolution of the rainfall series to avoid any artefacts of downscaling.

Figure 4.4 shows the process by which rainfall events were classified according to their ability to generate significant overland flow, and the simulated hydrographs of flow depths from multiple delineated rainfall events (Fig. 4.4a) are classified into four impact categories with flow depths of 1 to >4 mm for at least 10 min (Fig. 4.4b).

4.3.4 Data requirement and test stations

Our classification method required the use of high-resolution rainfall data, with a temporal resolution of at least 10 min. The method was tested with rainfall data collected at intervals of 1 and 10 min and, a lower resolution is not advised because time-averaged rainfall intensities

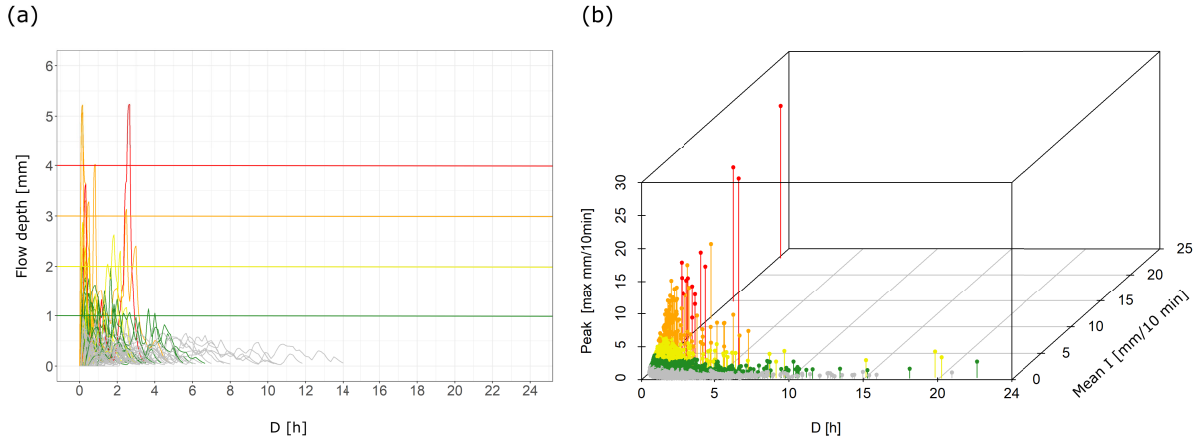


Figure 4.4: (a) Flow depths dynamics of multiple delineated rainfall events; (b) classification of rainfall events corresponding to flow depth categories in a three-dimensional scatterplot (output for Würzburg). Colour coding: grey: events generating no overland flow, green: class 1, yellow: class 2, orange: class 3, red: class 4 (see Tab. 4.2 for threshold values).

will result in an incorrect reproduction of flow depth rates. High-quality time series of climate stations in Würzburg (ID = 5707), Hamburg (ID = 1975) and Potsdam (ID = 3987) (Climate Data Centre) were used to evaluate and present the classification method. Hamburg is located on the northwest coast, Potsdam in the north-western lowlands, and Würzburg in the central low-elevation mountains of Germany. The datasets covered a period of three decades from 1990 to 2020 (1993 – 2020 for Potsdam) and were selected because of their availability and high quality.

4.4 Evaluation of impact-based rainfall classification method

4.4.1 Evaluation of event delineation

The main challenge facing event delineation methods for rainfall series is the identification of the minimum number of hours with no or negligible rainfall to separate the time series into individual events. According to a review by Dunkerley (2008), the duration of the IET can range widely – from 3 min to 24 h for different seasons and climatic settings – thus, regional analyses of the optimal IETs are essential. Three different statistical approaches exist to identify the dry periods between two rainfall events: autocorrelation analysis (AutoA), average annual number of events analysis (AAEA) and coefficient of variation analysis (CVA). In AutoA, events are delineated by finding the IET at which the autocorrelation coefficient is no longer significantly different from zero, such that the rainfall event can be regarded as independent (Wenzel and Voorhees, 1981). In AAEA, the IET is defined based on the average number of events annually, wherein an increasing IET is accompanied by a decrease in the average number of events. Finally, in CVA, it is assumed that IETs are represented well by an

exponential distribution (Adams and Papa, 2000; Restrepo-Posada and Eagleson, 1982). All three approaches were tested for the period from 1990 – 2020 for the study stations Würzburg, Potsdam and Hamburg using the ‘IETD’ package (Duque, 2020) in R version (4.1.1; R Core Team (2020)). While the AAEA approach only presented the influence of potential IETs on rain event selection, the AutoA and CVA approaches calculated IETs between 1 h 23 min – 2 h 35 min and 13 h 42 min – 17 h 30 min at a significance level of 10% for the whole period, respectively. Smallest IETs were achieved in summer season (AutoA: 50 min – 1 h 35 min, CVA: 10 h 18 min – 15 h 18 min), longest IETs in winter (AutoA: 2 h – 8 h, CVA: 14 h 15 min – 20 h). In comparison, the CVA approach calculated much longer IETs for both the entire period and individual seasons. Considering the wide ranges stemming from different delineation methods, no “correct” value for IET can be extracted. Restrepo-Posada and Eagleson (1982) and Dunkerley (2010) found that a longer IET may prove helpful in ensuring the identification of subsequent independent events. However, it adversely affects event properties, such as the duration and intensity of short-duration, convective rainstorms, which are known to occur mostly in the summer months in the study area (Haacke and Paton, 2021). Based on the derived IET specifically for the summer season by using AutoA (Fig. 4.5), an IET of 1 h was considered the most appropriate IET to ensure the detection of shorter events and used for further analysis. In total, 2969 events for Würzburg, 4304 events for Hamburg, and 2747 events for Potsdam were delineated for the study period 1990 – 2020.

4.4.2 Evaluation of overland flow model

Computed flow depths depend strongly on the size of the model domain: the larger the model area, the higher the maximum flow depth. Figure 4.6 shows the exponential development of maximal flow depth with increasing model size for several delineated rainfall events from Würzburg station, where the rainfall maxima ranged from 1 – 14 mm/10 min. Maximum flow depths varied greatly between 1.7 and 24.9 mm, 0.5 and 6.4 mm, 0.3 and 2.9 mm, and 0.1 and 1.4 mm for a model size of 1.000.000 m² (edge length dx = 1000 m), 10.000 m² (dx = 100 m), 1.000 m² (dx = 31.62 m), and 100 m² (dx = 10 m), respectively. To represent an accurate size and to have reasonable computing times, we chose a model size of 1000 m², which was represented by 10 cells lined up and dx = 10 m.

The time series from Würzburg station from 1990 – 2020 was chosen as an example, and the overland flow model was used to compute runoff depths for all 2969 delineated rainfall events (Fig. 4.4b). More than two-thirds of the events (71%) did not generate any overland flow, while ~29% generated overland flow that lasted for at least 10 min and had flow depths ranging between 1 and 5 mm.

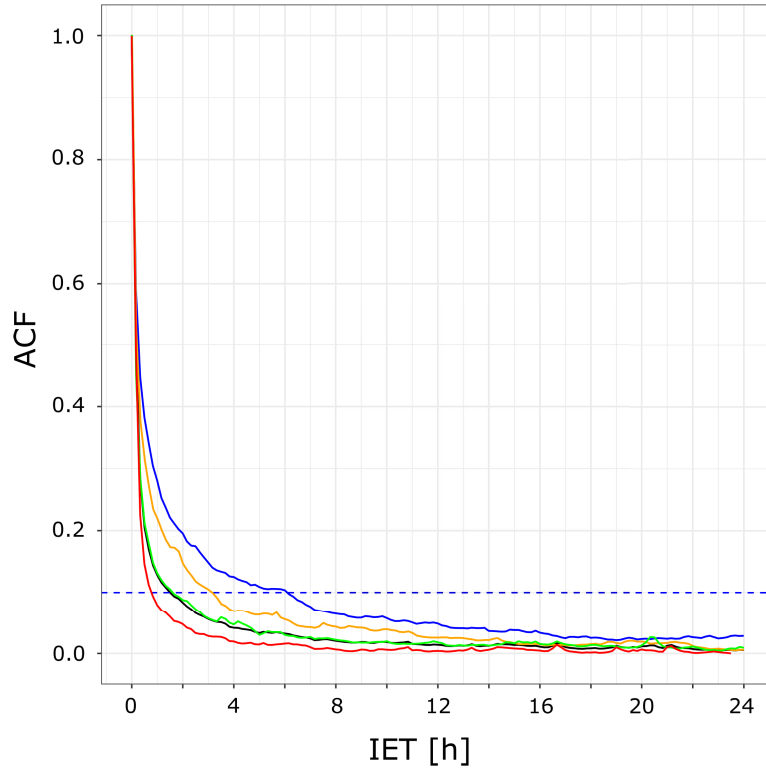


Figure 4.5: Output of the autocorrelation analysis (AutoA method) for Würzburg station for the whole period (1990 – 2020) and all four seasons. The x-axis is in 10 min time steps. Abbreviations: ACF: autocorrelation function. Lines show the mean of ACF for 1990 – 2020 (black), summer (June – August; red), autumn (September – November; orange), winter (December – February; blue), and spring (March – May; green). The dashed horizontal line is the critical correlation for a significance level of 10%.

4.4.3 Evaluation of impact-based classification

The proposed impact-based classification method was evaluated for all three stations, respectively, with Würzburg station shown as an example (Fig. 4.4, Tab. 4.2). The three-dimensional (3D) scatterplot in Figure 4.4b shows that only certain quadrants of the plots contained rainfall events that generated overland flow, with a high concentration appearing in the first quadrant (duration: < 5 h, mean intensity: < 5 mm/10 min). While 867 events met at least the criterion of class 1 (flow depth $df \geq 1$ mm/10 min), only 14 events generated an overland flow of at least 4 mm in 10 min (class 4, see Tab. 4.2). Classes 1 and 2 included events of both short and long durations (ranging from 10 min to 22.4 h), whereas events in classes 3 and 4 were generally much shorter, with durations up to seven hours.

The associated mean and peak intensities of the rainfall events increased from class 1 to 4 and the spans of the intensities became considerably larger with increasing class numbers (e.g., maximum intensity for class 1: 0.9 – 2.7 mm/10 min, class 4: 8.4 – 29 mm/10 min, Tab. 4.2). There was only a small degree of overlap between the four classes with regard to maximum intensity, but there was substantial overlap between the mean intensity and rainfall amount.

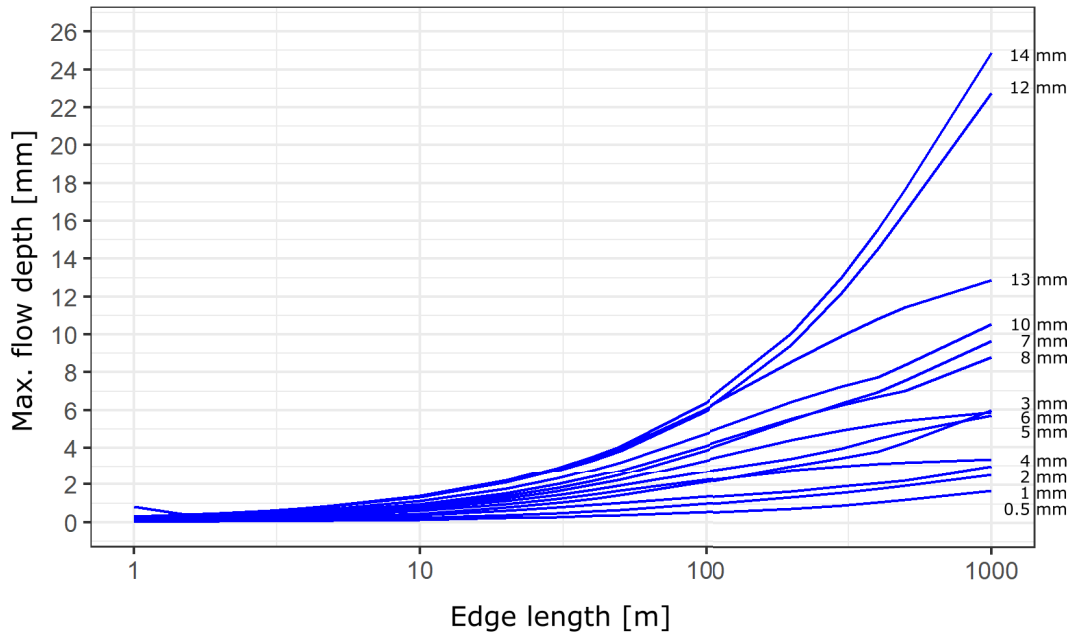


Figure 4.6: Development of flow depths with increasing model domain. Each line represents a single rainfall event. Events were chosen with regard to peak intensity, which ranged between 1 and 14 mm/10 min.

Figure 4.4b clearly shows that using only peak intensities to describe the magnitude of impact cannot adequately reflect the complexity of runoff responses, particularly for class 3 and 4 events. In contrast, it appears necessary to include all information available for the delineated rainfall model to classify the resulting impacts accordingly. The proposed classification of rainfall events based on simulating overland flow behaviour fills this gap by including the entire sequence of individual rainfall events.

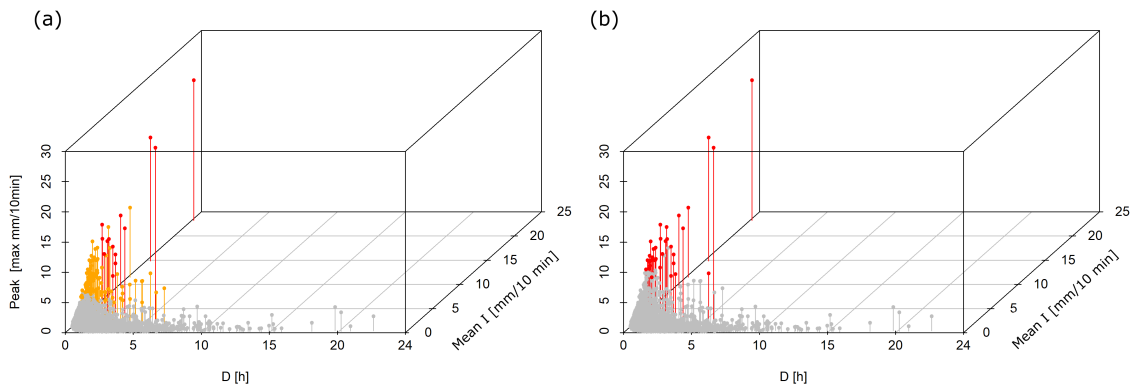
To illustrate the potential of the proposed impact-based classification method, it was compared to a conventional method after the Deutscher Wetterdienst (DWD) (n.d.[a],[b], Tab. 4.3), which uses rainfall intensity as the only classification parameter. The DWD classification scheme categorises rainstorms into three severity levels and includes intensity thresholds for 10 min, 1 and 6 h, but only for the highest severity level storm durations below 1 h are considered. In this comparison, we only used the highest DWD severity level (as summarised in Tab. 4.2), as otherwise, the comparison would be statistically flawed. Using the DWD categorisation, 33 events were categorised as extreme events for the Würzburg station (Tab. 4.2); in comparison, 91 and 14 events were assigned to our high-impact classes 3 and 4, respectively. The scatterplots in Figure 4.7 show that not all DWD extreme events were detected in class 4 by the impact-based approach, but more than half of them were assigned to class 3. There appears to be more consistency between the impact-based and the conventional method in event identification for longer storm durations, whereas for shorter durations below 1 h, a much larger spectrum of equally extreme events is identified by the impact-based method.

Table 4.2: Classification of the delineated rainfall events for Würzburg station from 1990 – 2020.

Traits	Class 1	Class 2	Class 3	Class 4	DWD
Threshold [mm/10 min]	1	2	3	4	
Impact level	low	middle	high	very high	extreme rainfall
Number of events (%)	590 (19.9)	172 (5.8)	91 (3.1)	14 (0.47)	33 (1.1)
Event duration [min]	10-1350	10-1210	10-410	10-350	10-360
Longest event duration [h]	22.4	20.2	6.8	5.8	6.0
Precipitation amount [mm]	1.6-56.2	2.8-51.3	4.9-47.0	18.7-69.6	8.7-69.6
Maximum intensity [mm/10 min]	0.91-2.7	2.5-4.5	4.5-13.1	8.4-29.0	8.3-29.0
Mean intensity [mm/10 min]	0.1-2.7	0.2-4.1	0.4-11.5	1.2-23.2	0.7-23.2

Table 4.3: Extreme rainfall events and their threshold values according to DWD (n.d. a, b).

Time-resolution	10 min	60 min (1 h)	360 min (6 h)
Rainfall intensity	≥ 8.3 mm	≥ 40 mm	≥ 60 mm

**Figure 4.7:** Comparison of detected extreme events between (a) the proposed impact-based classification method (red: events of class 4, orange: events of class 3, grey: all other events), and (b) a conventional classification method using rainfall intensity thresholds (red: events selected by using thresholds according to Tab. 4.3, grey: all other events).

4.5 Application of the impact-based classification method: A time-series analysis

The classification method described and evaluated here was used for an impact-based time-series analysis of rainstorm events, which we examined at both seasonal and annual scales (Figs. 4.8 and 4.9) for three example urban stations on a north–south transect across Germany (Hamburg, Potsdam, Würzburg).

Rainfall events generating relevant overland flow (by our definition, class 1 – 4) occurred throughout the year, with the number of events decreasing considerably with increases in the threshold for flow depth/10 min, ultimately being limited to the summer season (May – September) (Fig. 4.8).

Up to 50% of all rainfall events in summer generated overland flow, of which 60 – 80% was due to events in class 1 and 20 – 40% of class 2 – 4 (Fig. 4.8). With very few exceptions, class 4 events occurred between May and September in Hamburg, and between June and August in Potsdam and Würzburg. In winter, only approximately 7 – 20% of the monthly rainfall events generated substantial overland flow (mainly class 1). The mean annual number of rainstorms with significant impacts varied between 40 for Hamburg and 28 for Würzburg and Potsdam, of which, on average, 67% were from class 1, 18% from class 2, 9% from class 3, and 6% from class 4 (Fig. 4.9). The greatest number of rainstorm events classified annually (48 – 58) was detected in 2007, while the fewest events were detected in 1995 for Hamburg (19) and 2018 for Potsdam (14) and Würzburg (18).

Over a period of 31 years, no significant annual trends were observed in the total number of rainfall events or rainfall events of individual classes. However, a decadal comparison (1990 – 1999, 2000 – 2009 and 2010 – 2019) showed a substantial increase in rainstorm impacts: In Hamburg, the number of class 4 events increased from 13 to 25 to 31, while those of class 3 events increased from 10 to 29 to 39 per decade. In Würzburg, the number of class 3 events increased from 24 to 32 to 35 per decade, though no increase was detected for class 4 events. Potsdam station was not considered for decadal comparison due to missing data.

Our classification method provided new insights into the similarities and dissimilarities of different time series regarding the temporal distribution of rainstorm impacts. The next step in analysis will include a systematic review of multiple stations and, where possible, for longer time series; however, the latter will necessarily be limited because of the lack of high-resolution series that extend for longer than 30 years.

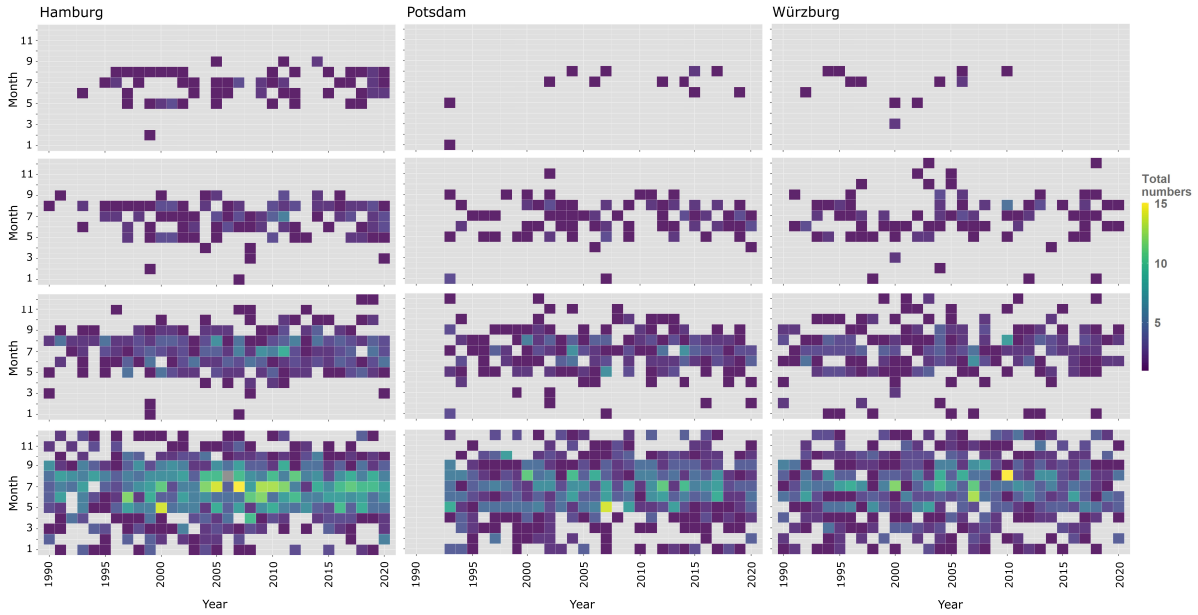


Figure 4.8: Seasonal rainfall frequency distribution of class 4 (first row), class 3 (second row), class 2 (third row), and class 1 (fourth row) events in Würzburg, Hamburg, and Potsdam.

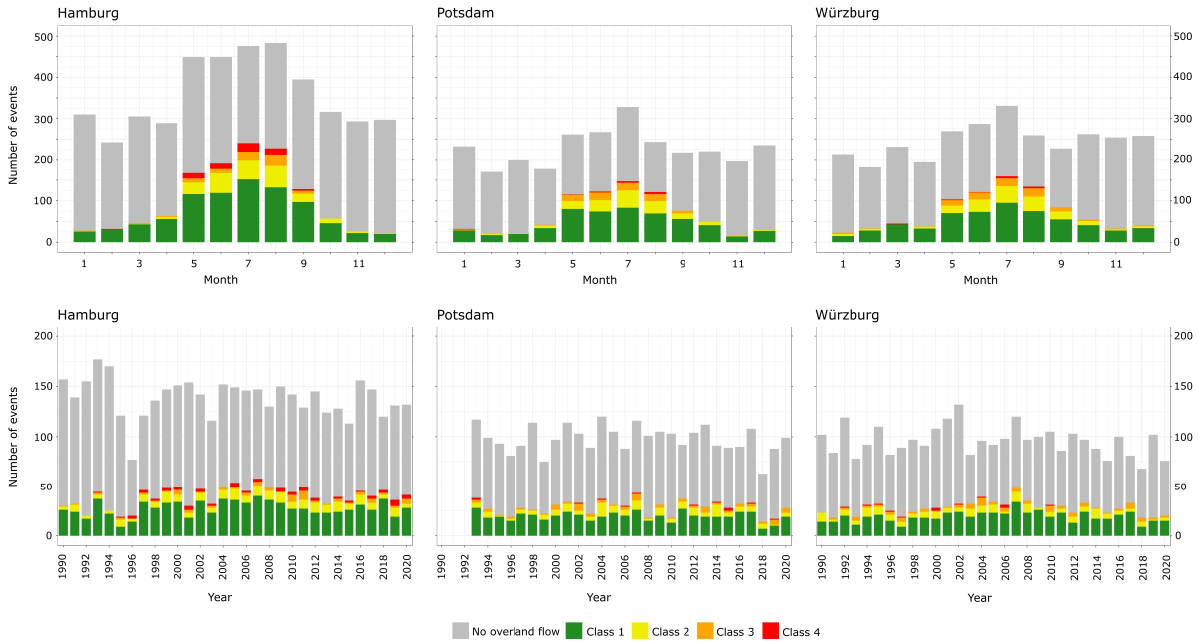


Figure 4.9: Seasonal (first row) and annual (second row) number of classified storm events for a period of 31 years for Würzburg and Hamburg (1990 – 2020) and for 28 years for Potsdam (1993 – 2020). Colours show events of classes with: no overland flow (grey), class 1 (green), class 2 (yellow), class 3 (orange), and class 4 (red, see Tab. 4.2 for thresholds).

4.6 Discussion

The primary purpose of this study was to present a new impact-based rainstorm classification method to complement the current classification of heavy rainstorms. The proposed method can be readily applied to high-resolution rainfall series, and we showcased its ability to filter events according to rainfall impacts in order to analyse seasonal and annual variations in rainfall intensity.

We also explained the necessity of the new classification approach by the fact that conventional classification approaches (as used by Haacke and Paton (2021), Hofstätter et al. (2017), Jacobeit et al. (2017), and Lorenz et al. (2019)) normally only characterise the severity of rainstorm events based on averaged values, such as the total amount of rainfall or maximum intensity of fixed time intervals. Additionally, conventional classifications employ hourly or daily resolutions, even though higher-resolution data are often locally available. However, the use of aggregated rainfall data poses a risk of mischaracterising the impacts of rainfall events. The 3D-scatterplots of classified events (Fig. 4.4b) demonstrated that those with very similar rainstorm characteristics were assigned to different impact classes, supporting the need to include more temporal dynamics when evaluating rainstorms. Furthermore, the comparison between a conventional method and the proposed method showed that using rainfall intensities as a classification parameter only is not sufficient to describe an events impact. A better representation of rainstorm characteristics was achieved by our approach, considering both the intermittency of rainfall and the entire course of individual rainfall events, thus enabling the precise computation of the flow depth profile, which ultimately allows events to be classified according to their impacts.

However, using high-resolution data is a limiting factor for the applicability of the proposed method as they are often not available in all regions. Data sets covering a short period of a few years can still be used for an initial assessment, but data for at least 30 years is strongly recommended for time series analysis. Although our approach can be adapted to data of coarser resolution (e.g. hourly data), we would not recommend this as the presentation of extreme events will be skewed. Furthermore, the four impact classes were derived for the three selected stations in Germany and might need to be adapted for stations elsewhere.

Our approach includes several uncertainties, which we addressed in the evaluation of the three classification steps: event delineation, overland flow computation, and event-based classification. First, event delineation depends on the choice of IET, which needs to be adjusted to regional rainfall patterns, as discussed by Dunkerley (2010) and Duque (2020). Second, higher-resolution (e.g. 1 min) rainfall data may be employed, which will result in a better reproduction of overland flow hydrographs and may cause higher peak flow depths for extreme rainfall intensities. Third, our default setting of 10 min, for which a rain event generated and sustained a certain overland flow depth, was arbitrary to some extent, and it

was deemed to represent a reasonable baseline for the on-set of pluvial flooding and pollution transfer, but regional characteristics might necessitate changes to this time setting.

Finally, our classification relies on a simplification of a sealed, typical urban surface for which the overland flow model was parameterised using fixed values for slope, infiltration rate, interception, and depression storage, and antecedent moisture conditions were neglected. No runoff concentration, which is normally associated with pluvial flooding and pollution transfer, was modelled, but only overland flow was generated on the model surface. This approach accounts for the micro-topography of sealed surfaces by including interception and depression storage, as experimentally quantified by Nehls et al. (2015) and Rammal and Berthier (2020).

A more realistic, but also more complex representation of urban surfaces would include the reproduction of the meso-topography of street surfaces such as kerbside features and larger depressions and drain channels or the reproduction of entire street canyon features (GebreEgziabher and Demissie, 2020; Li et al., 2008; Xing et al., 2019). The latter model surface would require the definition of multiple typical street canyon types for different city structures. By doing this, runoff concentrations could be reproduced much more accurately, and the actual impact of pluvial flooding for all delineated rainfall events could be quantified more accurately. At the same time, different street canyon types will result in different impact-based rainfall classifications. A supra-regional analysis of rainfall characteristics, as carried out here for the simplified urban surface for Hamburg, Potsdam and Würzburg, would not be feasible any more, as too many very different canyon types would need to be considered simultaneously. We therefore suggest keeping the overland flow model simplistic for analysing general behavioural trends in extremes; however, one may want to consider using a much more complex representation of urban layouts when preparing rainfall classifications for regional studies or individual cities.

4.7 Conclusion

Up to this point, extreme rainfalls were merely categorised based on their maximum rainfall intensity, amount or return period. We proposed a new classification method for extreme rains that used their potentials to generate overland flow on a typical urban asphalt surface as a filter to categorise their extremeness. Besides the maximum rainfall intensity, this approach considers the full dynamics of the rainstorm event including actual length of rainfall events and other characteristics such as precipitation amount, mean intensity and flow depths.

The evaluation of this method including a comparison with a conventional classification method showed that it is appropriate to use flow depth per time as an indicator of the generated impacts of overland flow in order to classify rainfall events. Rainfall events generating substantial overland flow were assigned to several impact classes indicating

increasing flow depths and thus stronger impact. We found that events with similar rainstorm intensities were assigned to different impact classes. This observation supports the assumption of a higher risk of misjudging the impact of events based on rainstorm intensities alone. Therefore, improved characterisation and classification of rainfall events can be achieved using the approach proposed here. In a further step, a temporal analysis was carried out for all four classes for three different locations in Germany. Results showed that events with the greatest impacts mainly occurred in summer, and there was a clear increase in the number of events over the last three decades.

However, this method is limited by its need of high-resolution data. Furthermore, flow depth distributions may vary for other regions or other surface layouts so that impact classes may need adaptation. Further analysis may include the analysis of spatial variations as well as the investigation of surface characteristics and varying class thresholds.

Data availability statement

All data, models, and code generated or used during the study appear in the submitted article.

Acknowledgements

This work was supported by the Deutsche Forschungsgemeinschaft as part of the Research Training Group Urban Water Interfaces (GRK 2032).

Chapter 5

Pilot study: Depression storage capacities of different real urban surfaces quantified by a terrestrial laser scanning-based method

5.1 Introduction

5.1.1 State of research

Urban catchments are patchworks of pervious and impervious areas, with the latter accounting for up to 66% of the city's ground area (Shuster et al., 2007). Impervious surfaces reduce the infiltration capacity of a catchment and increase the volume of stormwater runoff (Akbari et al., 2003; Nehls et al., 2021). Excessive urban runoff often has detrimental impacts on society and infrastructure by increasing the likelihood of pluvial flooding and on ecosystems by being discharged into surface water bodies. Thus, managing the quantity and quality of runoff from urban areas is an increasingly important environmental issue for urban communities.

The interest in a better understanding of the dynamics of urban runoff inundation and pollution transport has increased the development of methods to accurately model and mitigate its consequences. However, models still fail to reliably simulate surface flow processes for the whole range of rainfall intensities (Maksimović et al., 2009). One reason for that is that little attention has been given to a thorough understanding of rainfall-runoff partitioning and the role of urban topography (in particular, in submeter scale, hereafter called meso-topography).

The rainfall-runoff partitioning is governed by the surface storage V_S , the maximum volume that can be filled with water at the pavement surface (McGraw-Hill, 2002). It comprises the

pore system storage V_P and the depression storage V_D . Whether it is a pore or a depression depends on the diameter of the cavity. Cavities with diameters smaller than 0.3 mm can be considered pores (Jarvis, 2007). Water within these pores is immobile due to capillary force and thus reduces the hydraulic potential of stored water. However, cavities greater than 0.3 mm in diameter are too large to have the capillary force and thus store “free” water that can drain. In the urban water budget, meso-topographic elements like terrain depressions and sinks are characterised by V_D . For sealed and partially sealed surfaces, V_D plays a crucial role: compared to the pore system, more water can be stored in meso-topographic elements in less time, thus significantly reducing the contribution to surface runoff (Mansell and Rollet, 2009). V_D is, therefore, an essential component for calculating the discharge capacities of catchments in urban flood modelling and the water availability in process-based models, as proposed by Rim (2011). However, model simulations use estimated and spatially and temporally fixed values for V_D (Mansell and Rollet, 2009) due to the lack of a database for V_D based on field measurements.

5.1.2 Aims of the study

This study aims to fill this research gap by quantifying V_D for three differently paved real urban study sites and describing the spatial distribution of individual depressions. In detail, the following questions are going to be answered for each study site:

1. What is the total and the average storage capacity?
2. How much of the total area contributes to the total storage capacity?
3. How much do individual depressions contribute to the total storage capacity?

A terrestrial laser scanner (TLS) was used to collect high-resolution (millimetre range) morphological data from three study areas in Berlin. This method was tested and validated for eleven ideal pavements on a plot scale in a previous study by Nehls et al. (2015).

5.2 Materials and Methods

5.2.1 Study sites

Three differently sealed urban areas were scanned in the city centre of Berlin, Germany, in September 2021. The city centre is the area with the highest sealing degree and densest housing development (Döllefeld, 2020). The study sites are about 100 m² in size, respectively, and are sealed with typical pavements for this city area, i.e., concrete and brick pavers (Fig. 5.1).

Study sites represent parts of sidewalks, free spaces and parking lots and are constantly used by pedestrians, cars, and bikes. Additionally, surfaces are considerably shaped and altered by nearby trees and vegetation and contain depressions and fractures in varying degrees.

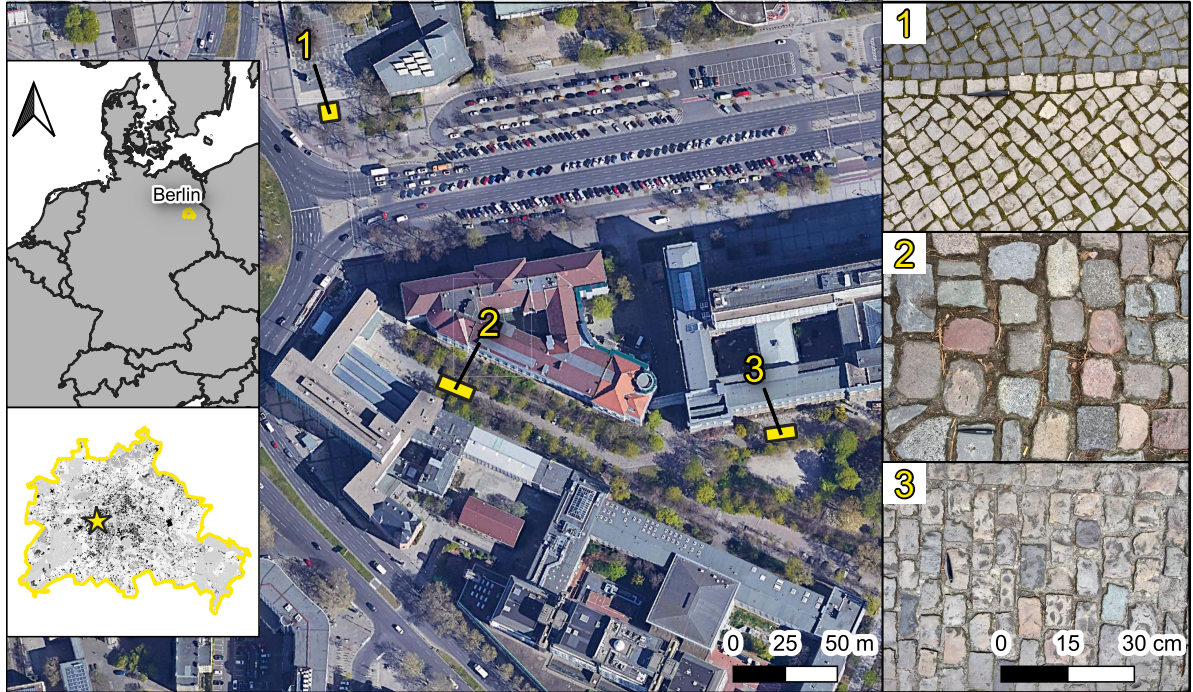


Figure 5.1: Overview map of study sites (yellow boxes) in the centre of Berlin (yellow star), Germany. Pavement designs are shown in boxes on the right: (1) small concrete pavers, (2) old brick pavers, (3) new brick pavers.

5.2.2 Morphological survey through terrestrial laser scanning

The areas were scanned with a scan resolution of 6.3 mm/10 m (high level), a laser beam diameter of < 1.5 mm at 1.5 m, and a vertical scanning speed of 12.5 rps (scanning time approx. 7 min; Z+F IMAGER©5010C, Zoller + Fröhlich GmbH, Germany). The areas were scanned from four different positions to ensure full detection of all morphological features and to avoid shading. To subsequently register scans into a single scene, eight target points were placed at different heights and angles around each site. Here, at least three identical target points were detected from two different scan positions to obtain well-matched scans.

5.2.3 Data processing

The first step of data processing was to merge the four scans of one area into a scene using Z+F LaserControl©9.0, a scan processing software provided by the Z+F company (Z+F LaserControl, 2017). To simplify and accelerate further processing, an area of 100 m² was cut out and exported in an ASCII format. For generating a high-resolution surface, a Geographic

Information System (GIS) was used for the next step. The advantages of using GIS are handling big data sets and processing georeferenced scans. The open-source software QGIS complemented by GRASS (GRASS Development Team, 2022) and SAGA (Conrad et al., 2015) plugins for advanced geographical and geoscientific analyses were used for this study. The data were processed in a meter-based coordinate reference system for surface generation (i.e., ERTS89 UTM zone 32N). Rasterization of the heterogeneously distributed data points was done using the Delaunay Triangulated Irregular Network (TIN) algorithm implemented in SAGA (0.005x0.005 m grid). Subsequently, depressions in all three surface areas were identified by filling the sinks using the package *terrain analysis-hydrology* (SAGA fill sinks; Wang and Liu (2006)). This package outputs a filled depression raster. To calculate the depression water depth within the entire study area, the filled depression raster needed to be subtracted from the original topography via the raster volume processing tool by SAGA. In a final step, single depressions were identified by the contour polygons algorithm from Gdal (depression water depth of ≥ 1.4 mm according to the uncertainty of the method in the z-direction (Nehls et al., 2015)). The depression storage capacity of every depression was calculated using the *sample-raster-values* algorithm supplied by QGIS. Depressions with an area of $15 \cdot 10^{-6}$ m² and a volume of $2.1 \cdot 10^{-8}$ m³ were excluded as they do not fit the uncertainty criteria according to Nehls et al. (2015). Statistical analysis was conducted in Microsoft Excel.

5.3 Results and Discussion

5.3.1 Spatial distribution of depressions

Study site 1 shows an elevation distribution between 0 m and 0.1 m, with low values in the lower half of the site (Fig. 5.2a), interrupted by a local high (0.1 m) in the lower-left corner. The site's upper part depicts generally higher values with two local depressions in the upper left and upper right (0.05 m). Depressions are heterogeneously distributed and were probably created when the floor was laid or due to subsoil settling. However, the local elevation in the lower-left corner was most probably formed due to the root growth of a nearby tree. Considering the uncertainty criteria as cut-off points, the number of identified depressions amounts to 3022, covering 18.05% of the total area (Tab. 5.1).

Study site 2 depicts elevation values between 0 m and 0.25 m (Fig. 5.3a), with the lowest values in the right centre, marked by two major depressions, and highest values in the left centre and one major depression in the very left. Many depressions were also identified related to wide and partially merged joints. The total number of depressions is 2610, covering 13.53% of the total area (Tab. 5.1).

For study site 3, the elevation ranges between 0 m and 0.25 m (Fig. 5.4a). The highest

Table 5.1: Data of dimension, depression storage capacity, sink area of depressions, and the number of identified depressions for the different real paving system designs analysed using terrestrial laser scanning.

Study site	Dimension [m x m]	Depression storage capacity/average depth [L]/[mm]	Sink area of depressions [%]	Number of identified depressions
Site 1	10 x 10	105.45/1.05	18.05	3022
Site 2	5.3 x 17.8	103.70/1.03	13.53	2610
Site 3	12.5 x 8	9.00/0.09	3.64	2398

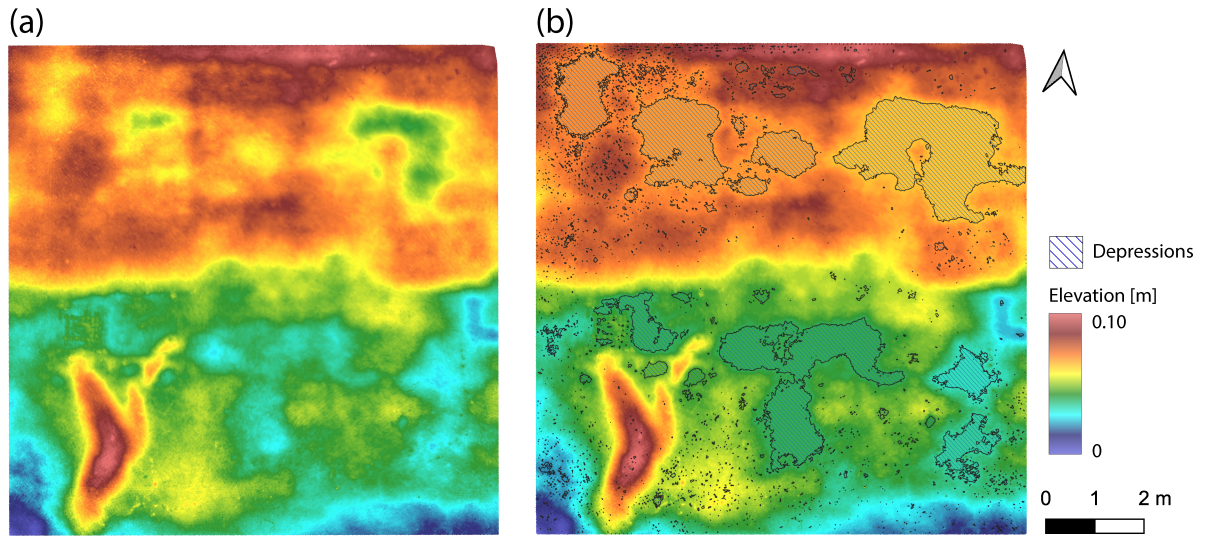


Figure 5.2: Elevation and depression distribution map of study site 1 with (a) unfilled and (b) filled depressions.

values are found along the left and right border of the site, with one major depression in the middle dropping slightly towards the upper middle. This site represents a typical drainage area, where runoff is forced to flow from the sides to the centre and then towards the gully located in the top centre. This construction leads to a hydrologically well-connected area with no big depressions. 2398 depressions were identified, covering an area of 3.64% (Tab. 5.1).

5.3.2 Storage capacities of real urban surfaces

For calculating the storage capacities, identified depressions were filled (see workflow described above), leading to filled depression elevation distribution maps (Figs. 5.2b, 5.3b, 5.4b). The largest elevation modifications can be found where major depressions are located

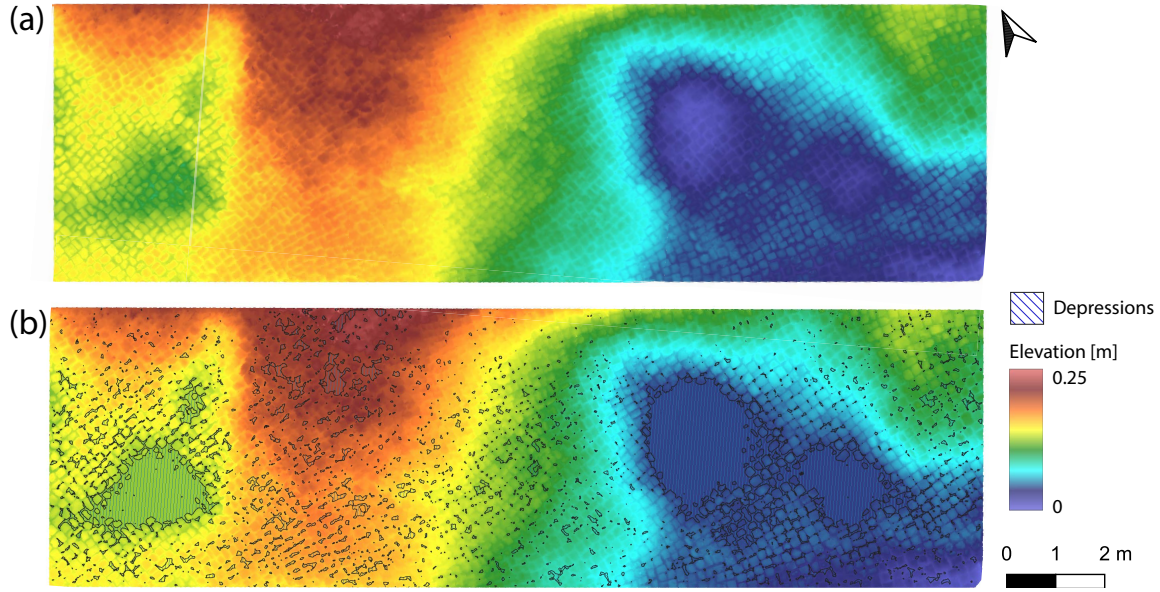


Figure 5.3: Elevation and depression distribution map of study site 2 with (a) unfilled and (b) filled depressions.

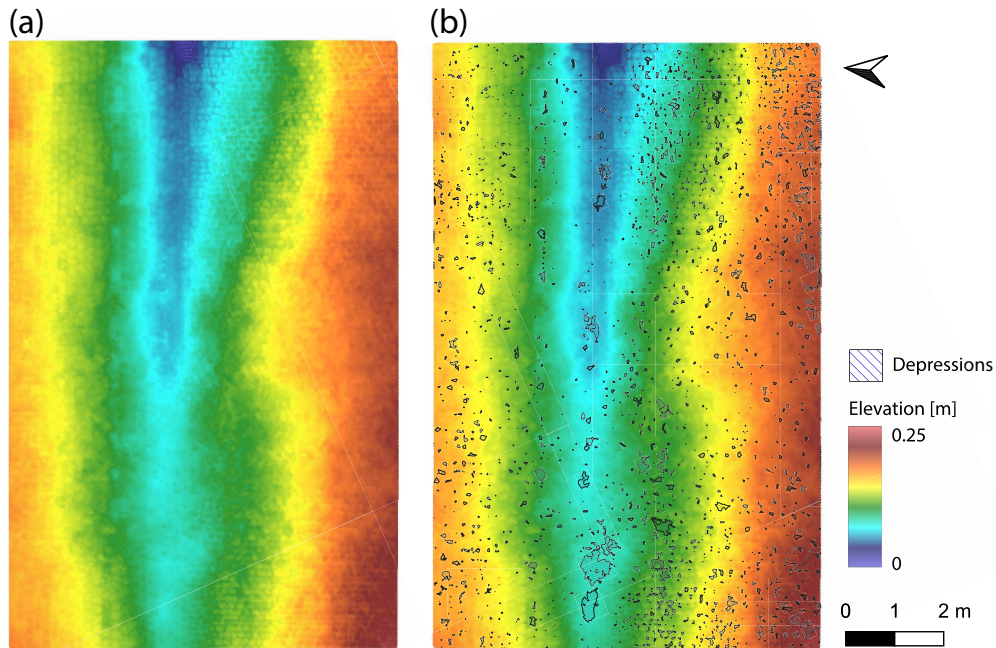


Figure 5.4: Elevation and depression distribution map of study site 3 with (a) unfilled and (b) filled depressions.

in the topographic input distributions, which are the lower centre, the upper left corner and the upper right corner for the first study site, the top corner for the second study site, and the right centre and very left of the third study site. To better illustrate the value of change, that is, the water depth d_w , the latter was plotted in Figure 5.5. Here, values range between 0.0015 m and 0.0225 m, and 0.0015 m and 0.0323 m, for study sites 1 and 2, with a mean d_w of 0.002 m, respectively. Study site 3 has a quantified d_w range of 0.0015 m to 0.0328 m;

however, the maximum d_w represents the inlet into the gully and was therefore excluded. The maximum d_w resulting from depressions is 0.010 m.

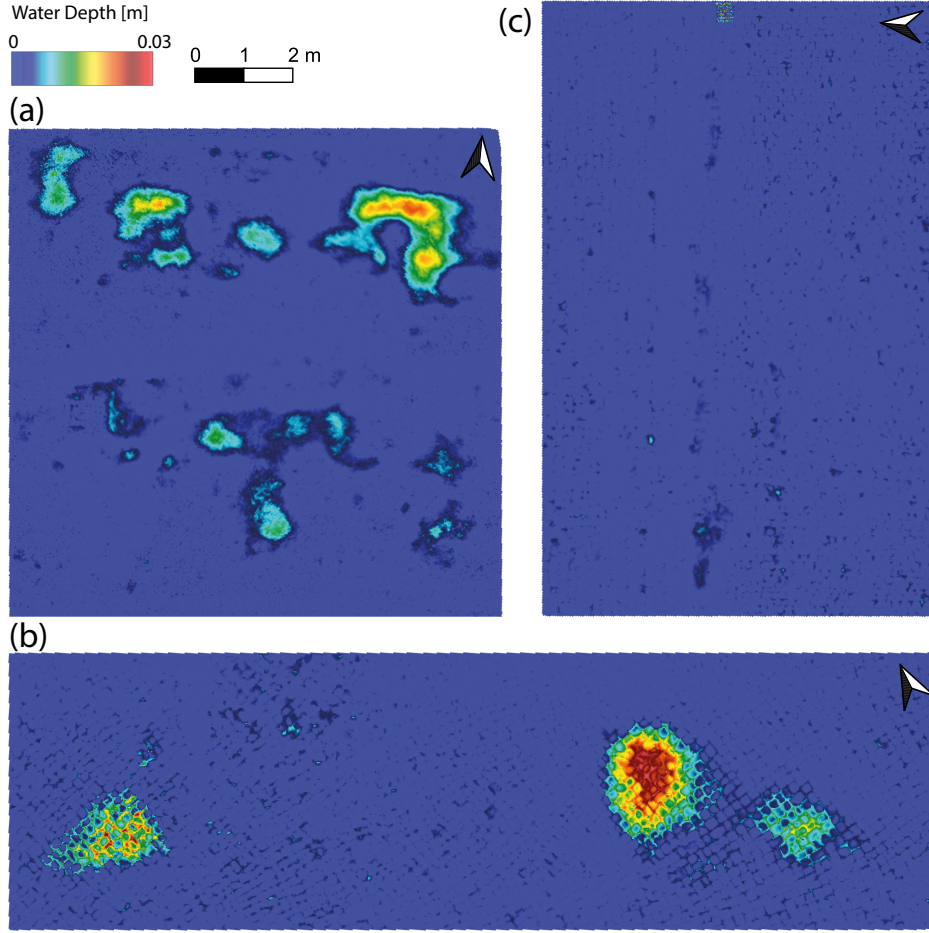


Figure 5.5: Water depth distribution of all study sites: (a) study site 1, (b) study site 2, and (c) study site 3.

Study site 1 has an accumulated depression volume of $10.5 \cdot 10^{-2} \text{ m}^3$ on a reference area of 100 m^2 , resulting in an average depression storage depth V_D of 1.05 mm. 95% of it is covered by the most prominent eight depressions, of which the biggest one has a volume of $4.24 \cdot 10^{-2} \text{ m}^3$ and a depression surface area of 4.98 m^2 ($V_{Di} = 8.51 \text{ mm}$) (Fig. 5.6). In comparison, study site 2 has a total depression volume of $10.37 \cdot 10^{-2} \text{ m}^3$ (reference area = 94 m^2 , average $V_D = 1.03 \text{ mm}$), 95% of it is covered by the biggest 164 depressions, of which the biggest depression has a volume of $6.83 \cdot 10^{-2} \text{ m}^3$ and a depression surface area of 6.60 m^2 ($V_{Di} = 10.35 \text{ mm}$). Here, the most extensive two depressions cover 91%. Study site 3 has an accumulated volume of $9.0 \cdot 10^{-3} \text{ m}^3$ (reference area = 100 m^2 , average $V_D = 0.09 \text{ mm}$), 95% of it is covered by the biggest 944 depressions, of which the most significant depression has a volume of $7.8 \cdot 10^{-4} \text{ m}^3$ and a depression surface area of 0.25 m^2 ($V_{Di} = 3.12 \text{ mm}$).

When comparing the three study sites, the highest number of depressions, the highest volume, and the most extensive total area of depressions were identified for study site 1,

leading to the highest average V_D (Tab. 5.1). This can be explained by the micro-texture of the small concrete pavers, the pavement-design related depression storage (Nehls et al., 2015), and the relatively shallow topography leading to larger hydrologically connected areas. A similar V_D but considerably smaller number of depressions in study site 2 can be explained by the depressions formed between the brick pavers and the smoother paver surface, leading to a lower pavement surface storage capacity than the small concrete pavers (Timm et al., 2018). The smallest number of depressions, lowest V_D , and smallest total depression area were identified for study site 3 due to the construction of the whole area.

Nehls et al. (2015) studied different ideal pavements and found averaged V_D varying from 0.07 to 1.40 mm, which is in accordance with our findings. However, unlike ideal pavements, depressions identified in this study were spatially heterogeneously distributed and showed significantly higher individual depression storage depths V_{Di} than the averaged V_D . These differences demonstrate the importance of irregular structures for the surface storage depth of pavements.

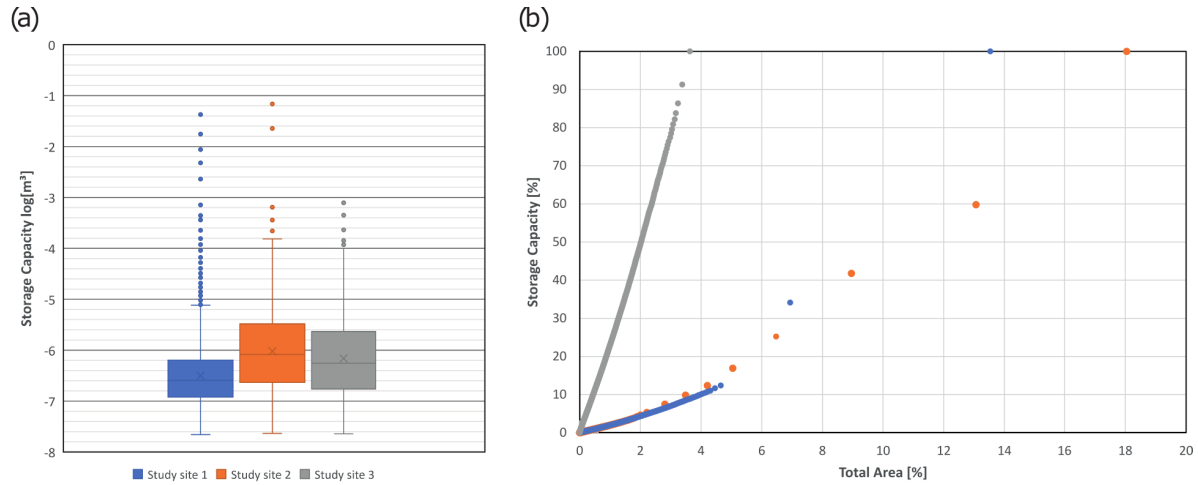


Figure 5.6: (a) Storage capacity ($\log[m^3]$) of individual depressions for each study site and (b) Cumulative storage capacity (%) plotted against the total area (%). Points in both graphs show individual depressions.

5.3.3 Conclusion and Outlook

This study has shown that quantifying the depression storage of real urban surfaces is crucial for better understanding the impact of cracks, ruts and puddles on the urban water balance and runoff and pollutant transport dynamics. The overlaying depression pattern mainly results from subsoil consolidation, uplifting due to roots of trees, or ruts from use or age. These depression patterns contribute the most to the total depression storage capacity. Results have shown that depressions on real urban surfaces vary significantly in space, size, and volume, so averaged depression storage depths should not be used to characterise the

respective pavement design. However, to derive representative depression storage depths, more urban sites of the same pavement design need to be studied. Further investigations may also include the measure of statistical dispersion intended to represent the spatially heterogeneous distribution of depressions by calculating the Gini coefficient. This dispersion index can also derive a more detailed description of the spatial distribution of depressions, a measure quantifying whether a set of observed occurrences are clustered or dispersed compared to a standard statistical model.

The terrestrial laser scanning method has proven to be a suitable tool for analysing the morphology of urban surfaces of large areas, which can be acquired in a time-efficient manner. Based on the results, a high scan resolution does not seem necessary to identify the most relevant depressions and, therefore, can be decreased. Additionally, more pavement designs should be included in an extended study.

Chapter 6

Synthesis

This final chapter summarises and discusses the main findings and conclusions from Chapters 2 to 5, along with an outlook on the remaining challenges for future research. While the central aspect of the first study lies in the collation of current knowledge on pollution patterns and processes in urban catchments to better understand the interlinked dynamics of source areas and pathways, the other studies focus on the analysis of key drivers of pollutant transport, namely extreme rainfall events and urban surface layouts.

6.1 Main findings and conclusions

Objective 1: Collation of current knowledge regarding patterns and processes of diffuse pollution in urban watersheds, and assessment of urban functional and structural connectivity.

Chapter 2 provided a comprehensive overview of current knowledge about diffuse pollution in urban catchments, focussing mainly on temporal and spatial patterns of diffuse pollution and pollution transport processes on urban surfaces. Based on this, it was shown that patterns and processes of diffuse pollution need to be merged into a process-based connectivity framework to better understand the interlinked dynamics of source areas and pathways to improve future management of urban waters.

A review of diffuse pollution sources showed diverse spatial patterns that dominate or influence diffuse pollution and can become potential critical source areas. However, four patterns can be distinguished: pollution patterns that accumulate or build upon the surface (e.g., atmospheric deposition), static pollution patterns (e.g. street pollution due to cars), management patterns that influence pollution structure (e.g., street cleaning and salt application for de-icing), and hydrological response factors (e.g., type of sealing,

pre-wetness). Furthermore, the emergence of critical source areas of diffuse pollution depends on diffuse pollution's transport and mobilisation processes, which were significantly altered in an urban catchment due to numerous surface configurations and modifications. The buffer, barrier, and booster elements can also affect distribution processes, preventing, disrupting, or accelerating the transfer of pollutants. Other important influencing factors presented are rainfall intensity and pollution accumulation.

To better understand pollution fluxes, connectivity (including structural, hydrological and pollutant connectivity) was introduced to describe the complexity of feedback and interactions of pollutants within urban systems. The authors showed that structural connectivity always affects the hydrological and pollutant connectivity, although the effect may be very dissimilar as pollutant connectivity also depends on the accumulation state of pollutants on urban surfaces.

This study is the first of its kind that conceptually applied connectivity to multiple pollutant patterns across urban surfaces and provides a comprehensive overview of urban diffuse pollution for urban hydrologists, planners and urban drainage managers. Structural and functional connectivity need to be included in urban models to bring the concept to the next level and make it useable for real catchments (identification of critical source areas, finding locations for LIDs). However, this requires more detailed information about the distribution of buffer, barrier, and booster elements, extensive pollution monitoring, monitoring techniques for structural and functional aspects of connectivity, and spatiotemporal understanding of effective rainfall events.

These shortcomings formed the motivation to investigate further the spatiotemporal occurrence and impact of extreme rainfall events and the characteristics of actual urban surfaces in the context of the subsequent analyses.

Objective 2: Analysis of the temporal occurrence of short and heavy rainstorms and categorisation of the prevailing large-scale atmospheric circulation patterns for 22 meteorological stations across Germany.

In Chapter 3, the diurnal, seasonal and annual occurrence of sub-hourly to hourly extreme rainfall events was analysed for 22 meteorological stations across Germany. The co-occurrence of large-scale atmospheric circulation patterns with extreme rainfall events, and their use as a first trend indicator, were also assessed.

The study identified three diurnal distribution patterns across Germany, with extreme events predominantly occurring in the afternoon and evening in the North, in the morning and evening in the South, and throughout the day in the West and Centre. During short-duration extreme rainfall events, no large-scale circulation patterns were identified at diurnal,

seasonal and annual temporal scales. Since formation processes are mainly convective and strongly influenced by prevailing local conditions, such as orography, urban influence, and water bodies, this is perhaps to be expected and implies that extreme rainfall events are highly spatially variable. To capture such events in atmospheric circulation patterns, a dense, high-resolution data network is necessary. Thus, further investigation on the formation of short-term rainfall extremes and large-scale atmospheric circulation patterns is required to facilitate the latter's use as a trend indicator for hourly to sub-hourly extreme rainfall events.

According to the findings of other studies, rainfall extremes were found to occur mainly in the summer season (Ghada et al., 2019; Darwish et al., 2021). Putting these results in context with those presented in Chapter 2, we conclude that hydrological connectivity is expected more frequently in summer. In case of prolonged dry periods between extreme rainfall events, high pollution connectivity is likely to increase the need for intense water and pollution management during this season (June - August). However, a significant number of events were also identified in May and particularly September. Fowler and Kilsby (2003) identified a seasonal shift in the UK of extreme rainfall events from summer to autumn over time (due to a changing climate). A seasonal shift of extreme rainfall would mean that the traditional seasonal division might not be appropriate for analysing changes in such events if warming extends the "convective season". Furthermore, extreme events might co-occur with the abscission of leaves starting in early autumn, leading to more blocked gullies and pluvial flooding. However, changes in the timing of short and extreme rainfall in Germany still need further investigation.

The analysis of the annual distribution of extreme events yielded a surprising finding: Over 20 years, a statistically significant upwards trend was found for hourly rainfall extremes but not for sub-hourly rainfall extremes. According to Lengfeld et al. (2019), as well as similar findings in the UK (Darwish et al., 2018), this would suggest that hourly extremes share more similarities regarding trends with daily than sub-hourly extreme events. However, trends of time-series <30 years need to be treated with caution, given they are considered too short for climate-relevant trend analysis.

This study gives new insights into the timing of short-duration rainfall extremes for Germany, which is rare as high-resolution data are often not available, incomplete, or non-existent. The results also showed that the timing of short extreme rainfall events is complex and spatially different. Knowing the timing is essential for warning systems and monitoring campaigns to quantify floods and the dynamics of diffuse pollution in-situ, which can be used for individually city-adapted water and pollution management strategies. The chosen extreme event selection method (peak-over-threshold) has proven helpful in getting an overview of event distribution (temporally and spatially). However, using fixed thresholds and intervals may lead to difficulties compared to other studies. Furthermore, they do not allow capture of the entire convective storm behavior as the rainfall hydrograph is not considered, which might lead to misjudgments of event impacts. These uncertainties

motivated the delineation of rainfall events and the evaluation of impacts not exclusively based on rainfall intensities in the subsequent study.

Objective 3: Development of a new rainfall classification method based on individual rainfall event impacts of generated overland flow on a simplified urban model surface.

In Chapter 4, a novel rainfall-classification method was presented, classifying rainfall events by generating overland flow depths on an urban surface. The novelty of this method lies in considering not only maximum rainfall intensities but also more temporal information about rainfall events. The motivation of this approach stems from scientific findings showing that the 'event profile' of the time-varying rainfall rate and any periods of no rain significantly affect hydrological responses, such as flood generation, wash-off and transport processes of pollutants and particles. Conventional classification and data processing does not consider this profile. Commonly, rainfall records are converted to an annual series of the maximum rainfall rate or depth for particular time intervals, such as 10 min, 1 h, or 24 h. Thus, short-intensity rainfall events may then be one or two orders of magnitude less intense than their mean hourly intensities, leading to erroneous assessments of their impacts.

The method developed here requires three steps: the identification of rainfall events from high-resolution time series, computation of overland flow depths for each event on a typical urban sealed surface, and impact-based classification of rainfall events as a function of the magnitude of overland flow. Four different impact classes were formed based on the rainfall time-series of three climate stations in Germany. Results were compared to a conventional classification approach and clearly showed that the impact-based approach better represented rainstorm characteristics and inference of impacts. The time-series analyses also showed that rainfall events with the highest potential impact are mainly short and occur in the summer season, according to the results of the previous study.

This method equips urban hydrologists and flood modellers with a tool to better evaluate the impact of rainfall events and analyse the general behavioural trends of extremes. Additionally, the first step requires identification of rainfall events from high-resolution time series, including their length and temporal characteristics. Such events can then be applied to flood simulations instead of designed rainfall. However, there are some limitations, such as the need for high-resolution data. Furthermore, flow depth distributions may vary for other regions or surface layouts, so impact classes may need adaptation. A better representation of the complex urban surface may also affect the results. In this study, only fixed values from the literature have been used for the infiltration, interception, and storage capacity of ideal urban surfaces. The storage capacity of non-ideal, real urban surfaces may have a relevant impact on runoff generation and pollutant transport but has not been analysed or quantified

yet. Therefore, the following study focuses on the analysis and quantification of the storage capacity of different real urban surfaces.

Objective 4: Quantification of the depression storage capacity of different real urban surfaces using a terrestrial laser-based method.

In Chapter 5, the depression storage capacity of different non-ideal, real urban surfaces was analysed and quantified. The method allows a high-resolution surface reproduction to identify single depressions, and calculate their volumes.

The proposed method was tested and validated for different ideal urban surfaces by Nehls et al. (2015), with depression storage capacities determined. Scans from at least four positions are required to make the method viable for real surfaces and larger areas, and more are suggested. The quality of a scan of a real surface taken in an urban catchment also strongly depends on weather conditions (too much sun and wet surfaces are inappropriate) and on the level of activity and crowdedness. After merging all scans into a holistic scene, further data processing and analysis are suggested in Geographic Information Systems (GIS). Depending on the desired resolution, high computational power and computation time may be required. Based on the three analysed study sites, it can be concluded that depression storage capacities for all analysed surface types vary widely in space, size, and volume; thus, averaged depression storage depths should not be considered representative for the respective pavement designs. More sites need to be scanned and included to determine the range of depression storage capacities of each surface type. Contrary to expectations, water held in depressions along joints constituted most of the identified depressions but least of the total depression storage capacity.

The encouraging results of this pilot study indicate that the use of a terrestrial laser scanner coupled with GIS is a promising approach to accurately quantify and analyse meso-topographical features, such as depressions, of real urban surfaces. Algorithms in GIS even allow calculating the catchment areas of individual depressions, which is helpful for better understanding pollutant or particle transport processes. This approach is very straightforward. Once applied to many different surfaces, it equips urban hydrologists and modellers with real values for depression storage capacities and thus contributes to a better surface representation.

6.2 Challenges and future research

The four research objectives of this thesis addressed different aspects of diffuse pollution in urban catchments by focussing on two influencing factors, extreme rainfall and urban surface representation. Thus, it contributes to a better understanding of pollution dynamics and the

formation of critical source areas. However, this thesis does not conclude the studied processes. Research limitations were identified, and new research questions were raised. This section presents limitations and new avenues that could be explored in future studies to practically enhance future pollution management.

6.2.1 Applicability of the connectivity concept in urban areas

The concept of connectivity has been successfully applied to study processes of water and pollutants in rural areas. This, in part, is due to the development of monitoring and modelling tools that explicitly consider structural and functional aspects of connectivity within catchment systems. However, monitoring source areas and pathways of diffuse pollution in urban settings has received little attention (Russell et al., 2019), while monitoring techniques for the urban context or also lacking.

From the overview of urban diffuse pollution patterns and processes in Chapter 2, limited information exists on the temporal variation in the size and pollution intensity of pollutant source areas and the processes driving rainfall-runoff responses on mixed urban surfaces, while there is limited availability of empirical data. To overcome this lack of data, future field studies should focus on data collection within individual street canyons, including road, pavement and tree pit surfaces and building facades, and roofs. Sampling locations should also include different city types (new/old/industrial) and sizes (small town to city scales), building types, central to suburban locations, high to low degrees of sealing, different traffic volumes, and high to low-income areas. Like the data collection in rural catchments, weekly sampling over several seasons will provide a reliable base for further studies.

In addition to the identification and quantification of contributing pollution sources, future research should include the development of control strategies and treatment technologies in collaboration with industry. Future stormwater quality programs should, to a larger extent, reflect societal developments and include emerging pollutants of concern, defined, e.g., in the lists of priority pollutants (such as the Directive 2013/39/EU, 2013) or released with the introduction of new products, materials, or chemicals to the urban environment (Müller et al., 2020).

However, routine monitoring of urban diffuse pollution is challenging, since it comprises a cocktail of pollutants from multiple sources and therefore requires a wide variety of lab techniques, which are often time-consuming, and require sophisticated and costly equipment. Therefore, future research should focus on developing monitoring techniques which enable on-site detection of contaminants, reducing detection times and the complexity of measurements. Microfluidic technology based on colourimetric and chemiluminescent methods offer an exciting opportunity. These methods were successfully applied for fast analysis of phenol (Duffy et al., 2017) and microplastics (Elsayed et al., 2021) in drinking

water. This can be complemented with standard smartphones to ease data transfer to servers for long-term storage and real-time remote access, including GPS data (Bayram et al., 2018; Fang et al., 2017).

For a better understanding of diffuse pollution pathways, future research could include the development of rainfall simulators for lab- and urban field studies, facilitating the evaluation of the spatial distribution of pollutants and rainfall-runoff responses on different urban surface designs. Rainfall simulators are mainly used to study soil erosion (Ries et al., 2009; Menezes Sanchez Macedo et al., 2021), infiltration-runoff processes (Roth et al., 1985; Abudi et al., 2012) and subsurface flow (Kavka et al., 2021) in rural catchments or agricultural fields under extreme rainfall conditions. However, as seen in Chapter 4, rainfall peak intensity is not necessarily the decisive factor when analysing the impact of rainfall in urban catchments, but the whole rainfall events' profile. Therefore, future studies could include constructing a (capillary-based or nozzle-based) rainfall simulator and simulating real rainfall events of all intensities. This includes the simulation of rainfall event appropriate drop sizes and fall velocities and requires preceding analysis and assessment of disdrometer datasets. Once developed, this rainfall simulator could also be applied to assess and quantify different diffuse pollution sources, e.g., biocide or heavy metal release from building materials made from zinc or copper into the environment (Faller and Reiss, 2005; De Buyck et al., 2021; Wicke et al., 2022).

Based on collected data, results can then be scaled up to larger areas and predicted under changing boundary conditions. This includes identifying critical source areas of diffuse pollution by analysing the spatiotemporal overlap of pollution supply and transport potential and setting up a multi-dimensional matrix of relevant source areas where significant amounts of pollution are generated. Furthermore, a multi-scale modelling approach needs to be developed that explicitly considers the structural and functional aspects of diffuse pollution dynamics' in an urban catchment. This approach can then be used to rank the severity of multiple critical source areas and help urban environmental managers to find where connectivity patterns need to be altered (e.g., by implementing water sensitive urban design tools; see Sharma et al., 2016) to generate more targeted pollution control.

6.2.2 Future research in extreme rainfall classification and analysis

Choosing an adequate rainfall classification for rainfall analysis is not trivial. Most common classification approaches classify rainfall events based on intensity threshold exceedance, percentiles or their origin (stratiform and convective) and use either rain gauge (Ghada et al., 2019) or radar (Lengfeld et al., 2019) data, or a combination of both (Baldwin et al., 2005), as well as satellite data (Shukla et al., 2018). This study chose a threshold-based approach for extreme rainfall event selection and successfully applied it to different datasets

for a spatiotemporal analysis across Germany. Regional differences in the temporal occurrence of short and extreme rain events and periods of clustered occurrence were identified, which is of great interest for flood prevention. For more locally precise statements about the temporal occurrence of extreme rainfall events, a further study could focus on the spatial classification of extreme rainfall regions and derivation of region-dependent temporal characteristics (like the study of Jones et al., 2013 for the UK). For better territorial coverage, either a dense rain gauge network (possibly complemented by radar data), or satellite data of high spatial resolution should be used.

Additionally, trend estimations using these extreme rainfall regions can be explored. However, these approaches are subjective: locally defined thresholds or classes can differ on a regional/global scale, making it difficult to compare studies. Therefore, to obtain a universal classification, an objective approach is required. Some recent studies suggest data-driven clustering approaches based on the k-means algorithm (Löwe et al., 2016; Urgilés et al., 2021) or the Bayesian algorithm (Little et al. 2008). Other studies have focused on acoustic rain rate measurements (Nakazato et al., 2018) or raindrop analysis using image processing (Avanzato and Beritelli, 2020) to estimate and classify rainfall intensity. With the spread of artificial intelligence techniques, new approaches to rainfall classification based on image processing and video matching processes based on advanced neural networks, have been introduced (Villarreal Guerra et al., 2018; Avanzato and Beritelli, 2020).

In this study, a novel approach was developed and presented in Chapter 4 and classifies rainfall events based on their impacts (represented by runoff depth) on an impervious asphalt surface. This method could be further developed by generating surface-related classes according to different materials, e.g., cobblestones, concrete slabs and pervious asphalt (Timm et al., 2018). Another idea could be to create a more authentic and heterogeneous surface by including more than one surface type or meso-topographical features like large depressions. This, however, would complicate the model and only makes sense for regional studies or individual cities. As the proposed impact classes were derived for only three stations in Germany, the method could also be applied to more German stations to develop a regional class system and/or to other stations elsewhere. In both cases, classes may need adaptation.

Moreover, future research could investigate changes in the timing of extreme rainfall compared to surrounding rural areas, as urban areas can have a notable impact on the local and regional climate. How rainfall changes are affected by the urban environment which is increasingly important as cities continue to be vulnerable to rainfall extremes, witnessing floods and droughts (Liu and Niyogi, 2019). Furthermore, changing rainfall leads to changing runoff generation processes and thus strongly influences pollution distribution patterns.

Much work, including studies within this thesis, has examined rainfall changes by focusing

on its extremes or its mean. Less work, however, focuses on quantifying the unevenness of precipitation, ultimately due to no existing or intuitive metric. In a study by Pendergrass and Knutti (2018), different methods were presented to overcome this open research gap and quantify the unevenness of daily precipitation and its change. Therefore, in a further study, the proposed methods could be applied to German weather stations using daily and hourly datasets, including comparing them.

Global urbanisation and a predicted increase in pluvial flooding due to climate change will lead to more urban activities, pollution accumulation, and runoff events in many regions. Therefore, only a continuous development of the scientific understanding of how climate change and urbanisation impact the urban water management, a close collaboration between scientists and policy-makers, and increased awareness concerning the environmental impacts of anthropogenic activities among the public, can lead to sustainable and effective adaptation for urban catchments.

Chapter 7

Supplementary contributions

The chapter gives an overview of the supplementary scientific work, which I carried out during my time as a PhD student at the Technical University Berlin.

Co-authored publication:

1. Hinkelmann, R., Kleinschmit, B., Porst, G., **Haacke, N.** & Pacheco Fernández, M.: Summary of abstracts. In: Conference Contributions. UWI Urban Water Interfaces, 2020; doi.org/10.24407/KXP:1733879374.

Conference posters (in chronological order):

1. **Haacke, N.** & Paton, E.N.: Identification of intra-city variation of urban flash floods by statistical analysis of extreme rainfall events in Berlin, Germany, Proceedings of the 10th Novatech Conference, Lyon, France, 2019.
2. **Haacke, N.** & Paton, E.N.: Heavy precipitation in Germany – An analysis to identify spatiotemporal patterns. Scientific discussion meeting about "Intensification of short-duration rainfall extremes and implications for flash flood risks" (The Royal Society), London, 03-04 February 2020.
3. **Haacke, N.** & Paton, E.N.: Spatiotemporal patterns of short-duration heavy precipitation in Germany, EGU General Assembly 2020, Online, 4–8 May 2020, EGU2020-9391, 2020; doi.org/10.5194/egusphere-egu2020-9391.

Presentations (in chronological order):

1. Tügel, F. & **Haacke, N.**: Sintfluten – von Mythen zur Wissenschaft, Exhibition „Sintflut heute“ organised by Group Global 3000, 2019.

2. Nehls, T., Rim, Y.N., **Haacke, N.** & Kluge, B.: Pores, seams, puddles - the surface storage and the water balance of paved urban soils (a sythesis), 10th Conference on Soils of Urban, Industrial, Traffic, Mining and Military Areas (SUITMA10), Seoul, South Korea, 16-21 June 2019.
3. **Haacke, N.**, Ladwig, R., Tügel, F., Matta, E. & Hinkelmann, R.: Behandlung von Extremwetterereignissen und Klimawandel im DFG Graduiertenkolleg Urban Water Interfaces, Dritte Forschungswerkstatt Wasser, Forschungskolleg Future Water, Universität Duisburg-Essen, 23 January 2020.
4. **Haacke, N.** & Paton, E.N.: Survey of rain events: how to categorise and analyse individual storm events in high-resolution precipitation time series, 1st International Conference on Urban Water Interfaces (UWI), Online, 22-24 September 2020.
5. Tügel, F., **Haacke, N.**, Hassan, A. & Hinkelmann, R.: Investigating the suitability of the Green-Ampt model with tabulated parameter values from literature by using a 2D hydrodynamic rainfall-runoff model and field experiments with rainfall simulator, 1st International Conference on Urban Water Interfaces (UWI), Online, 22-24 September 2020.

Bibliography

- Abrahams, A. D., Li, G., Krishnan, C., and Atkinson, J. F. (1998). "Predicting Sediment Transport by Interrill Overland Flow on Rough Surfaces". In: *Earth Surface Processes and Landforms* 23.12, pp. 1087–1099. DOI: 10.1002/(SICI)1096-9837(199812)23:12<1087::AID-ESP934>3.0.CO;2-4.
- Abudi, I., Carmi, G., and Berliner, P. (2012). "Rainfall Simulator for Field Runoff Studies". In: *Journal of Hydrology* 454–455, pp. 76–81. DOI: 10.1016/j.jhydrol.2012.05.056.
- Acero, F. J., García, J. A., and Gallego, M. C. (2011). "Peaks-over-Threshold Study of Trends in Extreme Rainfall over the Iberian Peninsula". In: *Journal of Climate* 24.4, pp. 1089–1105. DOI: 10.1175/2010JCLI3627.1.
- Adams, B. J. and Papa, F. (2000). *Urban Stormwater Management Planning with Analytical Probabilistic Models*. New York: John Wiley & Sons. 376 pp.
- Agilan, V., Umamahesh, N., and Mujumdar, P. (2021). "Influence of Threshold Selection in Modeling Peaks over Threshold Based Nonstationary Extreme Rainfall Series". In: *Journal of Hydrology* 593, p. 125625. DOI: 10.1016/j.jhydrol.2020.125625.
- Ahiablame, L. M., Engel, B. A., and Chaubey, I. (2012). "Effectiveness of Low Impact Development Practices: Literature Review and Suggestions for Future Research". In: *Water, Air, & Soil Pollution* 223.7, pp. 4253–4273. DOI: 10.1007/s11270-012-1189-2.
- Akbari, H., Shea Rose, L., and Taha, H. (2003). "Analyzing the Land Cover of an Urban Environment Using High-Resolution Orthophotos". In: *Landscape and Urban Planning* 63.1, pp. 1–14. DOI: 10.1016/S0169-2046(02)00165-2.
- Alexander, L. V., Zhang, X., Peterson, T. C., Caesar, J., Gleason, B., Klein Tank, A. M. G., Haylock, M., Collins, D., Trewin, B., Rahimzadeh, F., Tagipour, A., Rupa Kumar, K., Revadekar, J., Griffiths, G., Vincent, L., Stephenson, D. B., Burn, J., Aguilar, E., Brunet, M., Taylor, M., New, M., Zhai, P., Rusticucci, M., and Vazquez-Aguirre, J. L. (2006). "Global Observed Changes in Daily Climate Extremes of Temperature and Precipitation". In: *Journal of Geophysical Research: Atmospheres* 111.D5. DOI: 10.1029/2005JD006290.
- Alexander, L. V., Fowler, H. J., Bador, M., Behrangi, A., Donat, M. G., Dunn, R., Funk, C., Goldie, J., Lewis, E., Rogé, M., Seneviratne, S. I., and Venugopal, V. (2019). "On the Use of Indices to Study Extreme Precipitation on Sub-Daily and Daily Timescales". In: *Environmental Research Letters* 14.12, p. 125008. DOI: 10.1088/1748-9326/ab51b6.

- Alfieri, L., Burek, P., Feyen, L., and Forzieri, G. (2015). “Global Warming Increases the Frequency of River Floods in Europe”. In: *Hydrology and Earth System Sciences* 19.5, pp. 2247–2260. DOI: 10.5194/hess-19-2247-2015.
- Allan, R. P., Barlow, M., Byrne, M. P., Cherchi, A., Douville, H., Fowler, H. J., Gan, T. Y., Pendergrass, A. G., Rosenfeld, D., Swann, A. L. S., Wilcox, L. J., and Zolina, O. (2020). “Advances in Understanding Large-scale Responses of the Water Cycle to Climate Change”. In: *Annals of the New York Academy of Sciences* 1472.1, pp. 49–75. DOI: 10.1111/nyas.14337.
- Amundsen, C., Haland, S., French, H., Roseth, R., Kitterød, N.-O., Pedersen, P., and Riise, G. (2010). *Salt SMART- Environmental Damages Caused by Road Salt -A Literature Review*. 2587. Norwegian Institute for Agricultural and Environmental Research, p. 98.
- Anagnostopoulou, C. and Tolika, K. (2012). “Extreme Precipitation in Europe: Statistical Threshold Selection Based on Climatological Criteria”. In: *Theoretical and Applied Climatology* 107.3-4, pp. 479–489. DOI: 10.1007/s00704-011-0487-8.
- Arnbjerg-Nielsen, K. (2006). “Significant Climate Change of Extreme Rainfall in Denmark”. In: *Water Science and Technology* 54.6-7, pp. 1–8. DOI: 10.2166/wst.2006.572.
- Arnbjerg-Nielsen, K., Willems, P., Olsson, J., Beecham, S., Pathirana, A., Gregersen, I., Madsen, H., and Nguyen, V.-T.-V. (2013). “Impacts of Climate Change on Rainfall Extremes and Urban Drainage Systems”. In: *Water Science & Technology* 68.1, pp. 16–28. DOI: 10.2166/wst.2013.251.
- Arnell, N. W. and Gosling, S. N. (2016). “The Impacts of Climate Change on River Flood Risk at the Global Scale”. In: *Climatic Change* 134.3, pp. 387–401. DOI: 10.1007/s10584-014-1084-5.
- Aryal, R. K., Furumai, H., Nakajima, F., and Jinadasa, H. (2007). “The Role of Inter-Event Time Definition and Recovery of Initial/Depression Loss for the Accuracy in Quantitative Simulations of Highway Runoff”. In: *Urban Water Journal* 4.1, pp. 53–58. DOI: 10.1080/15730620601145873.
- Aschonitis, V., Gavioli, A., Lanzoni, M., Fano, E., Feld, C., and Castaldelli, G. (2018). “Proposing Priorities of Intervention for the Recovery of Native Fish Populations Using Hierarchical Ranking of Environmental and Exotic Species Impact”. In: *Journal of Environmental Management* 210, pp. 36–50. DOI: 10.1016/j.jenvman.2018.01.006.
- Ashley, W. S., Bentley, M. L., and Stallins, J. A. (2012). “Urban-Induced Thunderstorm Modification in the Southeast United States”. In: *Climatic Change* 113.2, pp. 481–498. DOI: 10.1007/s10584-011-0324-1.
- Avanzato, R. and Beritelli, F. (2020). “A CNN-based Differential Image Processing Approach for Rainfall Classification”. In: *Advances in Science, Technology and Engineering Systems Journal* 5.4, pp. 438–444. DOI: 10.25046/aj050452.
- Bailey, A., Deasy, C., Quinton, J., Silgram, M., Jackson, B., and Stevens, C. (2013). “Determining the Cost of In-Field Mitigation Options to Reduce Sediment and

- Phosphorus Loss”. In: *Land Use Policy* 30.1, pp. 234–242. DOI: 10.1016/j.landusepol.2012.03.027.
- Baldwin, M. E., Kain, J. S., and Lakshmivarahan, S. (2005). “Development of an Automated Classification Procedure for Rainfall Systems”. In: *Monthly Weather Review* 133.4, pp. 844–862. DOI: 10.1175/MWR2892.1.
- Balstrøm, T. and Crawford, D. (2018). “Arc-Malstrøm: A 1D Hydrologic Screening Method for Stormwater Assessments Based on Geometric Networks”. In: *Computers & Geosciences* 116, pp. 64–73. DOI: 10.1016/j.cageo.2018.04.010.
- Barbero, R., Fowler, H. J., Lenderink, G., and Blenkinsop, S. (2017). “Is the Intensification of Precipitation Extremes with Global Warming Better Detected at Hourly than Daily Resolutions?” In: *Geophysical Research Letters* 44.2, pp. 974–983. DOI: 10.1002/2016GL071917.
- Barbero, R., Fowler, H. J., Blenkinsop, S., Westra, S., Moron, V., Lewis, E., Chan, S., Lenderink, G., Kendon, E., Guerreiro, S., Li, X.-F., Villalobos, R., Ali, H., and Mishra, V. (2019). “A Synthesis of Hourly and Daily Precipitation Extremes in Different Climatic Regions”. In: *Weather and Climate Extremes* 26, p. 100219. DOI: 10.1016/j.wace.2019.100219.
- Barjenbruch, M. (2018). “RAU – Reducing the Environmental Impact of Microplastics from Car Tires”. In: *Plastics in the Environment, Sources-Sinks-Solutions*. Ed. by S. Ziemann, T. Nguyen, and A. Gunkel. Bonn, Germany: Federal Ministry of Education and Research (BMBF).
- Bayram, A., Horzum, N., Metin, A., Kilic, V., and Solmaz, M. (2018). “Colorimetric Bisphenol-A Detection With a Portable Smartphone-Based Spectrometer”. In: *IEEE Sensors Journal* PP, pp. 1–1. DOI: 10.1109/JSEN.2018.2843794.
- Beguiría, S., Angulo-Martínez, M., Vicente-Serrano, S. M., López-Moreno, J. I., and El-Kenawy, A. (2011). “Assessing Trends in Extreme Precipitation Events Intensity and Magnitude Using Non-Stationary Peaks-over-Threshold Analysis: A Case Study in Northeast Spain from 1930 to 2006”. In: *International Journal of Climatology* 31.14, pp. 2102–2114. DOI: 10.1002/joc.2218.
- Bentley, M. L., Ashley, W. S., and Stallins, J. A. (2010). “Climatological Radar Delineation of Urban Convection for Atlanta, Georgia”. In: *International Journal of Climatology* 30.11, pp. 1589–1594. DOI: 10.1002/joc.2020.
- Berg, P., Moseley, C., and Haerter, J. O. (2013). “Strong Increase in Convective Precipitation in Response to Higher Temperatures”. In: *Nature Geoscience* 6.3, pp. 181–185. DOI: 10.1038/ngeo1731.
- Berliner Stadtreinigung (2018). *Städtliche Leistung. Mit Vollem Einsatz Für Ein Sauberes Berlin*. URL: <https://www.bsr.de/strassenreinigung-20471.php>.
- Björklund, K. (2010). “Substance Flow Analyses of Phthalates and Nonylphenols in Stormwater”. In: *Water Science and Technology* 62.5, pp. 1154–1160. DOI: 10.2166/wst.2010.923.

- Blanco-Canqui, H. and Lal, R. (2010). "Buffer Strips". In: *Principles of Soil Conservation and Management*. Dordrecht: Springer.
- Blenkinsop, S., Lewis, E., Chan, S. C., and Fowler, H. J. (2017). "Quality-Control of an Hourly Rainfall Dataset and Climatology of Extremes for the UK". In: *International Journal of Climatology* 37.2, pp. 722–740. DOI: 10.1002/joc.4735.
- Blocken, B., Derome, D., and Carmeliet, J. (2013). "Rainwater Runoff from Building Facades: A Review". In: *Building and Environment* 60, pp. 339–361. DOI: 10.1016/j.buildenv.2012.10.008.
- Blomqvist, G. (1998). *Impact of De-Icing Salt on Roadside Vegetation - A Literature Review*. 427A. Swedish National Road and Transport Research Institute, p. 43.
- Bloomfield, J. P., Williams, R. J., Gooddy, D. C., Cape, J. N., and Guha, P. (2006). "Impacts of Climate Change on the Fate and Behaviour of Pesticides in Surface and Groundwater—A UK Perspective". In: *The Science of the Total Environment* 369.1-3, pp. 163–177. DOI: 10.1016/j.scitotenv.2006.05.019. pmid: 16914182.
- Bollmann, U. E., Minelgaite, G., Schlüsener, M., Ternes, T., Vollertsen, J., and Bester, K. (2016). "Leaching of Terbutryn and Its Photodegradation Products from Artificial Walls under Natural Weather Conditions". In: *Environmental Science & Technology* 50.8, pp. 4289–4295. DOI: 10.1021/acs.est.5b05825.
- Borga, M. and Morin, E. (2014). "Characteristics of Flash Flood Regimes in the Mediterranean Region". In: *Storminess and Environmental Change: Climate Forcing and Responses in the Mediterranean Region*. Ed. by N. Diodato and G. Bellocchi. Advances in Natural and Technological Hazards Research. Dordrecht: Springer Netherlands, pp. 65–76. DOI: 10.1007/978-94-007-7948-8_5.
- Bracken, L., Wainwright, J., Ali, G., Tetzlaff, D., Smith, M., Reaney, S., and Roy, A. (2013). "Concepts of Hydrological Connectivity: Research Approaches, Pathways and Future Agendas". In: *Earth-Science Reviews* 119, pp. 17–34. DOI: 10.1016/j.earscirev.2013.02.001.
- Bracken, L. J. and Croke, J. (2007). "The Concept of Hydrological Connectivity and Its Contribution to Understanding Runoff-Dominated Geomorphic Systems". In: *Hydrological Processes* 21.13, pp. 1749–1763. DOI: 10.1002/hyp.6313.
- Bracken, L. J., Turnbull, L., Wainwright, J., and Bogaart, P. (2015). "Sediment Connectivity: A Framework for Understanding Sediment Transfer at Multiple Scales". In: *Earth Surface Processes and Landforms* 40.2, pp. 177–188. DOI: 10.1002/esp.3635.
- Brieber, A. and Hoy, A. (2019). "Statistical Analysis of Very High-Resolution Precipitation Data and Relation to Atmospheric Circulation in Central Germany". In: *Advances in Science and Research* 16, pp. 69–73. DOI: 10.5194/asr-16-69-2019.
- Brierley, G., Fryirs, K., and Jain, V. (2006). "Landscape Connectivity: The Geographic Basis of Geomorphic Applications". In: *Area* 38.2, pp. 165–174.

- Bromley, L. B. of (2019). *Street Cleaning*. URL: https://www.bromley.gov.uk/info/200089/street_care_and_cleaning/1038/street_cleaning/2 (visited on 02/15/2020).
- Burian, S. J. and Shepherd, J. M. (2005). "Effect of Urbanization on the Diurnal Rainfall Pattern in Houston". In: *Hydrological Processes* 19.5, pp. 1089–1103. DOI: 10.1002/hyp.5647.
- Burkhardt, M., Zuleeg, S., Vonbank, R., Schmid, P., Hean, S., Lamani, X., Bester, K., and Boller, M. (2011). "Leaching of Additives from Construction Materials to Urban Storm Water Runoff". In: *Water Science and Technology* 63.9, pp. 1974–1982. DOI: 10.2166/wst.2011.128.
- Bürgel, B., Burkhardt, M., Duester, L., Fitz, M., Frühlich, R., Fuchs, S., Göbel, P., Nehls, T., Schiedek, T., Starke, P., Uhl, M., Welker, A., and Hillenbrand, T. (2016). *Diffuse Stoffeinträge in Gewässer Aus Siedlungs- Und Verkehrsflächen, DWA Themen*. Hennef: Deutsche Vereinigung für Wasserwirtschaft, Abwasser und Abfall e.V., p. 24.
- Calvillo, S. J., Williams, E. S., and Brooks, B. W. (2015). "Street Dust: Implications for Stormwater and Air Quality, and Environmental through Street Sweeping." In: *Reviews of environmental contamination and toxicology* 233, pp. 71–128. DOI: 10.1007/978-3-319-10479-9_3. pmid: 25367134.
- Campbell, N., D'Arcy, B., Frost, A., Novotny, V., and Sampson, A. (2004). *Diffuse Pollution: An Introduction to the Problems and Solutions*.
- Chang, Y, Chou, C, Su, K, and Tseng, C (2004). "Effectiveness of Street Sweeping and Washing for Controlling Ambient TSP". In: *Atmospheric Environment* 39.10, pp. 1891–1902. DOI: 10.1016/j.atmosenv.2004.12.010.
- Charron, D., Thomas, M., Waltner-Toews, D., Aramini, J., Edge, T., Kent, R., Maarouf, A., and Wilson, J. (2004). "Vulnerability of Waterborne Diseases to Climate Change in Canada: A Review". In: *Journal of Toxicology and Environmental Health. Part A* 67.20-22, pp. 1667–1677. DOI: 10.1080/15287390490492313. pmid: 15371208.
- Chocat, B., Ashley, R., Marsalek, J., Matos, M., Rauch, W., Schilling, W., and Urbonas, B. (2007). "Toward the Sustainable Management of Urban Storm-Water". In: *Indoor and Built Environment* 16.3, pp. 273–285. DOI: 10.1177/1420326X07078854.
- Christianthiel.net (2017). *Three Women with Umbrellas Walking through Water in Berlin Streets, Flooded after Days of Heavy Rainfalls*. shutterstock. URL: <https://www.shutterstock.com/de/image-photo/berlin-germany-06-29-2017-three-1010690893> (visited on 03/12/2022).
- City of Boston (2018). *Street Sweeping in the City*. URL: <https://www.boston.gov/departments/public-works/all-a> (visited on 02/20/2020).
- Clark, S., Field, R., and Pitt, R. (2002). "Wet-Weather Pollution Prevention by Product Substitution". In: *Linking Stormwater BMP Designs and Performance to Receiving Water Impact Mitigation*. Engineering Foundation Conference 2001. Snowmass Village, Colorado, United States: American Society of Civil Engineers, pp. 266–283. DOI: 10.1061/40602(263)19.

- Clark, S. E., Steele, K. A., Spicher, J., Siu, C. Y., Lalor, M. M., Pitt, R., and Kirby, J. T. (2008). “Roofing Materials’ Contributions to Storm-Water Runoff Pollution”. In: *Journal of Irrigation and Drainage Engineering* 134.5, pp. 638–645. DOI: 10.1061/(ASCE)0733-9437(2008)134:5(638).
- Climate Data Center (n.d.). *Open Data*. URL: https://opendata.dwd.de/climate_environment/CDC/ (visited on 10/19/2020).
- Climate Data Center (2021). *CDC-Portal*. Deutscher Wetterdienst. URL: <https://opendata.dwd.de/> (visited on 12/06/2021).
- Coles, S. (2001). *An Introduction to Statistical Modeling of Extreme Values*. Springer Series in Statistics. London: Springer London. DOI: 10.1007/978-1-4471-3675-0.
- Collins, M., Knutti, R., Arblaster, J., Dufresne, J.-L., Fichefet, T., Friedlingstein, P., Gao, X., Gutowski, W. J., Johns, T., Krinner, G., Shongwe, M., Tebaldi, C., Weaver, A. J., Wehner, M. F., Allen, M. R., Andrews, T., Beyerle, U., Bitz, C. M., Bony, S., and Booth, B. B. B. (2013). “Long-Term Climate Change: Projections, Commitments and Irreversibility”. In: *Climate Change 2013 - The Physical Science Basis: Contribution of Working Group I to the Fifth Assessment Report of the Intergovernmental Panel on Climate Change*, pp. 1029–1136. URL: <https://research.monash.edu/en/publications/long-term-climate-change-projections-commitments-and-irreversibil> (visited on 05/09/2022).
- Comarazamy, D. E., González, J. E., Luvall, J. C., Rickman, D. L., and Mulero, P. J. (2010). “A Land–Atmospheric Interaction Study in the Coastal Tropical City of San Juan, Puerto Rico”. In: *Earth Interactions* 14.16, pp. 1–24. DOI: 10.1175/2010EI309.1.
- Connecteur WG 1 (2018). *Cost Action ES 1306: Connecting Euro- Pean Connectivity Research: WG Theory Development*. URL: <http://connecteur.info/wiki/connectivity-wiki/> (visited on 12/17/2021).
- Conrad, O., Bechtel, B., Bock, M., Dietrich, H., Fischer, E., Gerlitz, L., Wehberg, J., Wichmann, V., and Böhner, J. (2015). “System for Automated Geoscientific Analyses (SAGA) v. 2.1.4”. In: *Geoscientific Model Development* 8.7, pp. 1991–2007. DOI: 10.5194/gmd-8-1991-2015.
- Corada-Fernández, C., Candela, L., Torres-Fuentes, N., Pintado-Herrera, M. G., Paniw, M., and González-Mazo, E. (2017). “Effects of Extreme Rainfall Events on the Distribution of Selected Emerging Contaminants in Surface and Groundwater: The Guadalete River Basin (SW, Spain)”. In: *Science of The Total Environment* 605–606, pp. 770–783. DOI: 10.1016/j.scitotenv.2017.06.049.
- Corcoran, E., C. Nellemann, E. Baker, R. Bos, D. Osborn, and H. Savelli, eds. (2010). *Sick Water? The Central Role of Wastewater Management in Sustainable Development: A Rapid Response Assessment*. Norway: United Nations Environment Programme, UN-HABITAT, GRID-Arenal.

- Crabtree, B., Dempsey, P., Johnson, I., and Whitehead, M. (2008). “The Development of a Risk-Based Approach to Managing the Ecological Impact of Pollutants in Highway Runoff”. In: *Water Science and Technology* 57.10, pp. 1595–1600. DOI: 10.2166/wst.2008.269.
- Cristiano, E., ten Veldhuis, M.-C., and van de Giesen, N. (2017). “Spatial and Temporal Variability of Rainfall and Their Effects on Hydrological Response in Urban Areas – a Review”. In: *Hydrology and Earth System Sciences* 21.7, pp. 3859–3878. DOI: 10.5194/hess-21-3859-2017.
- Curriero, F. C., Patz, J. A., Rose, J. B., and Lele, S. (2001). “The Association between Extreme Precipitation and Waterborne Disease Outbreaks in the United States, 1948-1994”. In: *American Journal of Public Health* 91.8, pp. 1194–1199. DOI: 10.2105/ajph.91.8.1194. pmid: 11499103.
- Dare, R. and Davidson, N. (2015). *Seasonal Distributions of Daily Heavy Rain Events over Australia*. Bureau Research Report 6. Melbourne, Australia: Bureau of Meteorology.
- Darwish, M. M., Fowler, H. J., Blenkinsop, S., and Tye, M. R. (2018). “A Regional Frequency Analysis of UK Sub-Daily Extreme Precipitation and Assessment of Their Seasonality”. In: *International Journal of Climatology* 38.13, pp. 4758–4776. DOI: 10.1002/joc.5694.
- Darwish, M. M., Tye, M. R., Prein, A. F., Fowler, H. J., Blenkinsop, S., Dale, M., and Faulkner, D. (2021). “New Hourly Extreme Precipitation Regions and Regional Annual Probability Estimates for the UK”. In: *International Journal of Climatology* 41.1, pp. 582–600. DOI: 10.1002/joc.6639.
- De Buyck, P.-J., Van Hulle, S., Dumoulin, A., and Rousseau, D. (2021). “Roof Runoff Contamination : A Review on Pollutant Nature, Material Leaching and Deposition”. In: *Reviews in Environmental Science and Biotechnology* 20.2 (2), pp. 549–606. DOI: 10.1007/s11157-021-09567-z.
- De Toffol, S., Laghari, A. N., and Rauch, W. (2009). “Are Extreme Rainfall Intensities More Frequent? Analysis of Trends in Rainfall Patterns Relevant to Urban Drainage Systems”. In: *Water Sci. Technol.* 59.9, pp. 1769–1776. DOI: 10.2166/wst.2009.182. pmid: 19448312.
- Deletic, A., Zhang, K., Jamali, B., Castonguay, A., Kuller, M., Prodanovic, V., and Bach, P. (2019). “Modelling to Support the Planning of Sustainable Urban Water Systems: UDM 2018”. In: *New Trends in Urban Drainage Modelling*. Ed. by G. Mannina. New York, USA: Springer International Publishing. URL: <https://doi.org/10.1007/978-3-319-99867-1>.
- Deumlich, D. and Gericke, A. (2020). “Frequency Trend Analysis of Heavy Rainfall Days for Germany”. In: *Water* 12.7, p. 1950. DOI: 10.3390/w12071950.
- Deutscher Wetterdienst (DWD) (n.d.[a]). *Wetter- und Klimalexikon: Niederschlagsintensität*. URL: <https://www.dwd.de/DE/service/lexikon/Functions/glossar.html?lv2=101812&lv3=101906> (visited on 01/20/2022).

- Deutscher Wetterdienst (DWD) (n.d.[b]). *Wetter- und Klimalexikon: Starkregen*. URL: <https://www.dwd.de/DE/service/lexikon/Functions/glossar.html?nn=103346&lv2=102248&lv3=102572> (visited on 01/20/2022).
- DHI (2000). *MOUSE Surface Runoff Models - Reference Manual*. Hørsholm, Denmark: DHI Water & Environment.
- Di Salvo, C., Ciotoli, G., Pennica, F., and Cavinato, G. P. (2017). “Pluvial Flood Hazard in the City of Rome (Italy)”. In: *Journal of Maps* 13.2, pp. 545–553. DOI: 10.1080/17445647.2017.1333968.
- Diem, J. E. and Brown, D. P. (2003). “Anthropogenic Impacts on Summer Precipitation in Central Arizona, U.S.A”. In: *The Professional Geographer* 55.3, pp. 343–355. DOI: 10.1111/0033-0124.5503011.
- DigitalGlobe (2006). *QuickBird Imagery Products*. URL: http://glcf.umd.edu/library/guide/QuickBird_Product_Guide.pdf.
- Directive 2008/105/EC (2008). “Directive 2008/105/EC of the European Parliament and of the Council of 16 December 2008 on Environmental Quality Standards in the Field of Water Policy, Amending and Subsequently Repealing Council Directives 82/176/EEC, 83/513/EEC, 84/156/EEC, 84/491/EEC, 86/280/EEC and Amending Directive 2000/60/EC of the European Parliament and of the Council”. In: *Official Journal of the European Union* 348, pp. 84–97.
- Directive 2013/39/EU (2013). “Directive 2013/39/EU of the European Parliament and of the Council of 12 August 2013 Amending Directives 2000/60/EC and 2008/105/EC as Regards Priority Substances in the Field of Water Policy”. In: *Official Journal of the European Union* L226, pp. 1–17.
- Dressing, S. (2018). *Critical Source Area Identification And BMP Selection: Supplement To Watershed Planning Handbook*. Washington: United States Environmental Protection Agency, p. 70.
- Driscoll, C., Eger, C., Chandler, D., Roodsari, B., Davidson, C., Flynn, C., Lambert, K., Bettez, N., and Groffmann, P. (2015). “Green Infrastructure: Lessons from Science and Practice”. In: *A publication of the Science Policy Exchange*, p. 32.
- Duffy, E., Padovani, R., He, X., Gorkin, R., Vereshchagina, E., Ducrée, J., Nesterenko, E., Nesterenko, P. N., Brabazon, D., Paull, B., and Vázquez, M. (2017). “New Strategies for Stationary Phase Integration within Centrifugal Microfluidic Platforms for Applications in Sample Preparation and Pre-Concentration”. In: *Analytical Methods* 9.13, pp. 1998–2006. DOI: 10.1039/C7AY00127D.
- Duncan, H. (1995). *A Review of Urban Stormwater Quality Processes*. 95/9. Clayton: Cooperative Research Centre for Catchment Hydrology.
- Dunkerley, D. (2008). “Identifying Individual Rain Events from Pluviograph Records: A Review with Analysis of Data from an Australian Dryland Site”. In: *Hydrological Processes* 22.26, pp. 5024–5036. DOI: 10.1002/hyp.7122.

- Dunkerley, D. (2017). “An Approach to Analysing Plot Scale Infiltration and Runoff Responses to Rainfall of Fluctuating Intensity: Plot Scale Infiltration”. In: *Hydrological Processes* 31.1, pp. 191–206. DOI: 10.1002/hyp.10990.
- Dunkerley, D. (2020). “Rainfall Intensity in Geomorphology: Challenges and Opportunities”. In: *Progress in Physical Geography: Earth and Environment* 45.4, pp. 488–513. DOI: 10.1177/0309133320967893.
- Dunkerley, D. L. (2010). “How Do the Rain Rates of Sub-Event Intervals Such as the Maximum 5- and 15-Min Rates (I_5 or I_{30}) Relate to the Properties of the Enclosing Rainfall Event?”. In: *Hydrological Processes*, n/a–n/a. DOI: 10.1002/hyp.7650.
- Dupas, R., Delmas, M., Dorioz, J.-M., Garnier, J., Moatar, F., and Gascuel-Oudou, C. (2015). “Assessing the Impact of Agricultural Pressures on N and P Loads and Eutrophication Risk”. In: *Ecological Indicators* 48, pp. 396–407. DOI: 10.1016/j.ecolind.2014.08.007.
- Duque, L. F. (2020). *Inter-Event Time Definition (Package 'IETD')*, p. 9. URL: <https://cran.r-project.org/web/packages/IETD/index.html>.
- Döllefeld (2020). *Stadtstruktur - Flächentypen differenziert 2020 (Umweltatlas)*. FIS-Broker. URL: <https://fbinter.stadt-berlin.de/fb/index.jsp> (visited on 01/24/2022).
- Ebrahimian, A., Gulliver, J. S., and Wilson, B. N. (2016). “Effective Impervious Area for Runoff in Urban Watersheds: EIA in Urban Watersheds”. In: *Hydrological Processes* 30.20, pp. 3717–3729. DOI: 10.1002/hyp.10839.
- Eggert, B., Berg, P., Haerter, J. O., Jacob, D., and Moseley, C. (2015). “Temporal and Spatial Scaling Impacts on Extreme Precipitation”. In: *Atmospheric Chemistry and Physics* 15.10, pp. 5957–5971. DOI: 10.5194/acp-15-5957-2015.
- Elsayed, A. A., Erfan, M., Sabry, Y. M., Dris, R., Gaspéri, J., Barbier, J.-S., Marty, F., Bouanis, F., Luo, S., Nguyen, B. T. T., Liu, A.-Q., Tassin, B., and Bourouina, T. (2021). “A Microfluidic Chip Enables Fast Analysis of Water Microplastics by Optical Spectroscopy”. In: *Scientific Reports* 11.1 (1), p. 10533. DOI: 10.1038/s41598-021-89960-4.
- Eriksson, E., Baun, A., Scholes, L., Ledin, A., Ahlman, S., Revitt, M., Noutsopoulos, C., and Mikkelsen, P. (2007). “Selected Stormwater Priority Pollutants — a European Perspective”. In: *Science of The Total Environment* 383.1-3, pp. 41–51. DOI: 10.1016/j.scitotenv.2007.05.028.
- European Commission (2021). *A European Green Deal*. URL: https://ec.europa.eu/info/strategy/priorities-2019-2024/european-green-deal_en (visited on 11/20/2021).
- European Environment Agency (2019). *Heavy Precipitation in Europe*. URL: <https://www.eea.europa.eu/data-and-maps/indicators/precipitation-extremes-in-europe-3/assessment-1> (visited on 12/12/2021).
- Faller, M. and Reiss, D. (2005). “Runoff behaviour of metallic materials used for roofs and facades – a 5-year field exposure study in Switzerland”. In: *Materials and Corrosion* 56.4, pp. 244–249. DOI: 10.1002/maco.200403835.

- Fang, C., Zhang, X., Dong, Z., Wang, L., Mallavarapu, M., and Naidu, R. (2017). "Smartphone App-Based/Portable Sensor for the Detection of Fluoro-Surfactant of PFOA". In: *Chemosphere* 191. DOI: 10.1016/j.chemosphere.2017.10.057.
- Fang, N.-F., Shi, Z.-H., Li, L., Guo, Z.-L., Liu, Q.-J., and Ai, L. (2012). "The Effects of Rainfall Regimes and Land Use Changes on Runoff and Soil Loss in a Small Mountainous Watershed". In: *CATENA* 99, pp. 1–8. DOI: 10.1016/j.catena.2012.07.004.
- Fenner, D., Holtmann, A., Krug, A., and Scherer, D. (2019). "Heat Waves in Berlin and Potsdam, Germany – Long-term Trends and Comparison of Heat Wave Definitions from 1893 to 2017". In: *International Journal of Climatology* 39.4, pp. 2422–2437. DOI: 10.1002/joc.5962.
- Ferreira, C. S. S., Walsh, R. P. D., de Lourdes Costa, M., Coelho, C. O. A., and Ferreira, A. J. D. (2016). "Dynamics of Surface Water Quality Driven by Distinct Urbanization Patterns and Storms in a Portuguese Peri-Urban Catchment". In: *Journal of Soils and Sediments* 16.11, pp. 2606–2621. DOI: 10.1007/s11368-016-1423-4.
- Fischer, E. M. and Knutti, R. (2016). "Observed Heavy Precipitation Increase Confirms Theory and Early Models". In: *Nature Climate Change* 6.11 (11), pp. 986–991. DOI: 10.1038/nclimate3110.
- Fletcher, T. D., Andrieu, H., and Hamel, P. (2013). "Understanding, Management and Modelling of Urban Hydrology and Its Consequences for Receiving Waters: A State of the Art". In: *Advances in Water Resources*. 35th Year Anniversary Issue 51, pp. 261–279. DOI: 10.1016/j.advwatres.2012.09.001.
- Fletcher, T. D., Shuster, W., Hunt, W. F., Ashley, R., Butler, D., Arthur, S., Trowsdale, S., Barraud, S., Semadeni-Davies, A., Bertrand-Krajewski, J.-L., Mikkelsen, P. S., Rivard, G., Uhl, M., Dagenais, D., and Viklander, M. (2015). "SUDS, LID, BMPs, WSUD and More – The Evolution and Application of Terminology Surrounding Urban Drainage". In: *Urban Water Journal* 12.7, pp. 525–542. DOI: 10.1080/1573062X.2014.916314.
- Forzieri, G., Bianchi, A., Silva, F. B. e, Marin Herrera, M. A., Leblois, A., Laval, C., Aerts, J. C., and Feyen, L. (2018). "Escalating Impacts of Climate Extremes on Critical Infrastructures in Europe". In: *Global Environmental Change* 48, pp. 97–107. DOI: 10.1016/j.gloenvcha.2017.11.007.
- Fowler, H. J. and Kilsby, C. G. (2003). "Implications of Changes in Seasonal and Annual Extreme Rainfall". In: *Geophysical Research Letters* 30.13. DOI: 10.1029/2003GL017327.
- Fowler, H. J., Lenderink, G., Prein, A. F., Westra, S., Allan, R. P., Ban, N., Barbero, R., Berg, P., Blenkinsop, S., Do, H. X., Guerreiro, S., Haerter, J. O., Kendon, E. J., Lewis, E., Schaer, C., Sharma, A., Villarini, G., Wasko, C., and Zhang, X. (2021). "Anthropogenic Intensification of Short-Duration Rainfall Extremes". In: *Nature Reviews Earth & Environment* 2.2, pp. 107–122. DOI: 10.1038/s43017-020-00128-6.
- Freitag, B. M., Nair, U. S., and Niyogi, D. (2018). "Urban Modification of Convection and Rainfall in Complex Terrain". In: *Geophysical Research Letters* 45.5, pp. 2507–2515. DOI: 10.1002/2017GL076834.

- Fryirs, K. (2013). “(Dis)Connectivity in Catchment Sediment Cascades: A Fresh Look at the Sediment Delivery Problem”. In: *Earth Surface Processes and Landforms* 38.1, pp. 30–46. DOI: 10.1002/esp.3242.
- Fryirs, K., Brierley, G., Preston, N., and Spencer, J. (2007a). “Catchment-Scale (Dis)Connectivity in Sediment Flux in the Upper Hunter Catchment, New South Wales, Australia”. In: *Geomorphology* 84, pp. 297–316. DOI: 10.1016/j.geomorph.2006.01.044.
- Fryirs, K. A., Brierley, G. J., Preston, N. J., and Kasai, M. (2007b). “Buffers, Barriers and Blankets: The (Dis)Connectivity of Catchment-Scale Sediment Cascades”. In: *CATENA* 70.1, pp. 49–67. DOI: 10.1016/j.catena.2006.07.007.
- Ganeshan, M., Murtugudde, R., and Imhoff, M. L. (2013). “A Multi-City Analysis of the UHI-influence on Warm Season Rainfall”. In: *Urban Climate* 6, pp. 1–23. DOI: 10.1016/j.uclim.2013.09.004.
- Gaume, E., Bain, V., Bernardara, P., Newinger, O., Barbuc, M., Bateman, A., Blaškovičová, L., Blöschl, G., Borga, M., Dumitrescu, A., Daliakopoulos, I., Garcia, J., Irimescu, A., Kohnova, S., Koutroulis, A., Marchi, L., Matreata, S., Medina, V., Preciso, E., Sempere-Torres, D., Stancalie, G., Szolgay, J., Tsanis, I., Velasco, D., and Viglione, A. (2009). “A Compilation of Data on European Flash Floods”. In: *Journal of Hydrology* 367.1, pp. 70–78. DOI: 10.1016/j.jhydrol.2008.12.028.
- Gaál, L., Molnar, P., and Szolgay, J. (2014). “Selection of Intense Rainfall Events Based on Intensity Thresholds and Lightning Data in Switzerland”. In: *Hydrology and Earth System Sciences* 18.5, pp. 1561–1573. DOI: 10.5194/hess-18-1561-2014.
- GebreEgziabher, M. and Demissie, Y. (2020). “Modeling Urban Flood Inundation and Recession Impacted by Manholes”. In: *Water* 12.4, p. 1160. DOI: 10.3390/w12041160.
- Ghada, W., Yuan, Y., Wastl, C., Estrella, N., and Menzel, A. (2019). “Precipitation Diurnal Cycle in Germany Linked to Large-Scale Weather Circulations”. In: *Atmosphere* 10.9, p. 545. DOI: 10.3390/atmos10090545.
- Glaser, R. and Stangl, H. (2004). “Climate and Floods in Central Europe since AD 1000: Data, Methods, Results and Consequences”. In: *Surveys in Geophysics* 25, pp. 485–510. DOI: 10.1007/s10712-004-6201-y.
- Golden, H. E. and Hoghooghi, N. (2018). “Green Infrastructure and Its Catchment-scale Effects: An Emerging Science”. In: *WIREs Water* 5.1. DOI: 10.1002/wat2.1254.
- González-Sanchis, M., Murillo, J., Cabezas, A., Vermaat, J. E., Comín, F. A., and García-Navarro, P. (2015). “Modelling Sediment Deposition and Phosphorus Retention in a River Floodplain”. In: *Hydrological Processes* 29.3, pp. 384–394. DOI: 10.1002/hyp.10152.
- GRASS Development Team (2022). *Geographic Resources Analysis Support System (GRASS) Software*. Version 8.0. USA: Open Source Geospatial Foundation. URL: <https://grass.osgeo.org>.
- Great Pics – Ben Heine (2021). *ROCHEFORT, BELGIUM - JULY 13, 2021: Drone View of Some Streets and Houses Heavily Damaged from the Historic Floods in Rochefort, Belgium*

- in July 2021*. shutterstock. URL: <https://www.shutterstock.com/de/image-photo/rochefort-belgium-july-13-2021-drone-2030436347> (visited on 03/12/2022).
- Groisman, P. Y., Knight, R. W., Easterling, D. R., Karl, T. R., Hegerl, G. C., and Razuvaev, V. N. (2005). “Trends in Intense Precipitation in the Climate Record”. In: *J. Climate* 18.9, pp. 1326–1350. DOI: 10.1175/JCLI3339.1.
- Grunwald, L., Heusinger, J., and Weber, S. (2017). “A GIS-based Mapping Methodology of Urban Green Roof Ecosystem Services Applied to a Central European City”. In: *Urban Forestry & Urban Greening* 22, pp. 54–63. DOI: 10.1016/j.ufug.2017.01.001.
- Guerreiro, S., Glenis, V., Dawson, R., and Kilsby, C. (2017). “Pluvial Flooding in European Cities—A Continental Approach to Urban Flood Modelling”. In: *Water* 9.4, p. 296. DOI: 10.3390/w9040296.
- Guerreiro, S. B., Fowler, H. J., Barbero, R., Westra, S., Lenderink, G., Blenkinsop, S., Lewis, E., and Li, X.-F. (2018). “Detection of Continental-Scale Intensification of Hourly Rainfall Extremes”. In: *Nature Climate Change* 8.9, pp. 803–807. DOI: 10.1038/s41558-018-0245-3.
- Gumbel, E. J. (1958). *Statistics of Extremes*. Columbia University Press. DOI: 10.7312/gumb92958.
- Göbel, P., Dierkes, C., and Coldewey, W. (2007). “Storm Water Runoff Concentration Matrix for Urban Areas”. In: *Journal of Contaminant Hydrology* 91.1-2, pp. 26–42. DOI: 10.1016/j.jconhyd.2006.08.008.
- Haacke, N. and Paton, E. N. (2021). “Analysis of Diurnal, Seasonal, and Annual Distribution of Urban Sub-Hourly to Hourly Rainfall Extremes in Germany”. In: *Hydrology Research* 52.2, pp. 478–491. DOI: 10.2166/nh.2021.181.
- Haberlie, A. M., Ashley, W. S., Fultz, A. J., and Eagan, S. M. (2016). “The Effect of Reservoirs on the Climatology of Warm-Season Thunderstorms in Southeast Texas, USA”. In: *International Journal of Climatology* 36.4, pp. 1808–1820. DOI: 10.1002/joc.4461.
- Haerter, J. O., Berg, P., and Hagemann, S. (2010). “Heavy Rain Intensity Distributions on Varying Time Scales and at Different Temperatures”. In: *Journal of Geophysical Research* 115.D17, p. D17102. DOI: 10.1029/2009JD013384.
- Hand, W. H., Fox, N. I., and Collier, C. G. (2004). “A Study of Twentieth-Century Extreme Rainfall Events in the United Kingdom with Implications for Forecasting”. In: *Meteorological Applications* 11, pp. 15–31. DOI: 10.1017/S1350482703001117.
- Hanel, M., Rakovec, O., Markonis, Y., Máca, P., Samaniego, L., Kyselý, J., and Kumar, R. (2018). “Revisiting the Recent European Droughts from a Long-Term Perspective”. In: *Scientific Reports* 8.1, p. 9499. DOI: 10.1038/s41598-018-27464-4.
- Harding, K. J. and Snyder, P. K. (2015). “Using Dynamical Downscaling to Examine Mechanisms Contributing to the Intensification of Central U.S. Heavy Rainfall Events”. In: *Journal of Geophysical Research (Atmospheres)* 120, pp. 2754–2772. DOI: 10.1002/2014JD022819.

- Hass, U., Duennbier, U., and Massmann, G. (2012). “Occurrence and Distribution of Psychoactive Compounds and Their Metabolites in the Urban Water Cycle of Berlin (Germany)”. In: *Water Research* 46.18, pp. 6013–6022. DOI: 10.1016/j.watres.2012.08.025.
- Heathwaite, A., Quinn, P., and Hewett, C. (2005). “Modelling and Managing Critical Source Areas of Diffuse Pollution from Agricultural Land Using Flow Connectivity Simulation”. In: *Journal of Hydrology* 304.1-4, pp. 446–461. DOI: 10.1016/j.jhydro1.2004.07.043.
- Heckmann, T. and Vericat, D. (2018). “Computing Spatially Distributed Sediment Delivery Ratios: Inferring Functional Sediment Connectivity from Repeat High-Resolution Digital Elevation Models: Spatially Distributed Sediment Delivery Ratios from Repeat DEMs”. In: *Earth Surface Processes and Landforms* 43.7, pp. 1547–1554. DOI: 10.1002/esp.4334.
- Hess, P. and Brezowsky, H. (1969). *Katalog der Grosswetterlagen Europas*. Dt. Wetterdienst. 70 pp. Google Books: [tp6qXwAACAAJ](https://books.google.de/books?id=tp6qXwAACAAJ).
- Hettiarachchi, S., Wasko, C., and Sharma, A. (2019). “Can Antecedent Moisture Conditions Modulate the Increase in Flood Risk Due to Climate Change in Urban Catchments?” In: *Journal of Hydrology* 571, pp. 11–20. DOI: 10.1016/j.jhydro1.2019.01.039.
- Hirabayashi, Y., Mahendran, R., Koirala, S., Konoshima, L., Yamazaki, D., Watanabe, S., Kim, H., and Kanae, S. (2013). “Global Flood Risk under Climate Change”. In: *Nature Climate Change* 3.9 (9), pp. 816–821. DOI: 10.1038/nclimate1911.
- Hofstätter, M., Lexer, A., Homann, M., and Blöschl, G. (2017). “Large-Scale Heavy Precipitation over Central Europe and the Role of Atmospheric Cyclone Track Types”. In: *International Journal of Climatology* 38, e497–e517. DOI: 10.1002/joc.5386.
- Hofstätter, M. and Stahl, N. (2018). “Vb-Zugbahnen Und Deren Auftreten Als Serie Mit Bezug Zu Den Resultierenden Hochwassern in Bayern Mit Auswirkungen Auf Rückhalteräume Im Isareinzugsgebiet”. In: *Hydrologie und Wasserbewirtschaftung* 62, pp. 77–97. DOI: 10.5675/HyWa_2018_2_2.
- Hosannah, N. and Gonzalez, J. E. (2014). “Impacts of Aerosol Particle Size Distribution and Land Cover Land Use on Precipitation in a Coastal Urban Environment Using a Cloud-Resolving Mesoscale Model”. In: *Advances in Meteorology* 2014, e904571. DOI: 10.1155/2014/904571.
- Howard, K. and Gerber, R. (2018). “Impacts of Urban Areas and Urban Growth on Groundwater in the Great Lakes Basin of North America”. In: *Journal of Great Lakes Research* 44.1, pp. 1–13. DOI: 10.1016/j.jglr.2017.11.012.
- Hundecha, Y. and Bárdossy, A. (2005). “Trends in Daily Precipitation and Temperature Extremes across Western Germany in the Second Half of the 20th Century”. In: *International Journal of Climatology* 25, pp. 1189–1202. DOI: 10.1002/joc.1182.
- Hunter, P. R. (2003). “Climate Change and Waterborne and Vector-Borne Disease”. In: *Journal of Applied Microbiology* 94 Suppl, 37S–46S. DOI: 10.1046/j.1365-2672.94.s1.5.x. pmid: 12675935.

- Hwang, J., Rhee, D. S., and Seo, Y. (2017). “Implication of Directly Connected Impervious Areas to the Mitigation of Peak Flows in Urban Catchments”. In: *Water* 9.9, p. 696. DOI: 10.3390/w9090696.
- Innovyze (2020). *InfoWorks ICM*. Version 10.5. URL: <https://www.innovyze.com/en-us/products/infoworks-ws-pro>.
- IPCC (2012). *Managing the Risks of Extreme Events and Disasters to Advance Climate Change Adaptation: Special Report of the Intergovernmental Panel on Climate Change*. Ed. by C. B. Field, V. Barros, T. F. Stocker, and Q. Dahe. Cambridge: Cambridge University Press. DOI: 10.1017/CB09781139177245.
- Jackson, L. J., Lauridsen, T. L., Søndergaard, M., and Jeppesen, E. (2007). “A Comparison of Shallow Danish and Canadian Lakes and Implications of Climate Change”. In: *Freshwater biology*. URL: <https://doi.org/10.1111/j.1365-2427.2007.01809.x> (visited on 05/11/2022).
- Jacobeit, J., Homann, M., Philipp, A., and Beck, C. (2017). “Atmospheric Circulation Types and Extreme Areal Precipitation in Southern Central Europe”. In: *Advances in Science and Research* 14, pp. 71–75. DOI: 10.5194/asr-14-71-2017.
- Jacobs, J. M., Cattaneo, L. R., Sweet, W., and Mansfield, T. (2018). “Recent and Future Outlooks for Nuisance Flooding Impacts on Roadways on the U.S. East Coast”. In: *Transportation Research Record: Journal of the Transportation Research Board* 2672.2, pp. 1–10. DOI: 10.1177/0361198118756366.
- Jarvis, N. (2007). “A Review of Non-Equilibrium Water Flow and Solute Transport in Soil Macropores: Principles, Controlling Factors and Consequences for Water Quality”. In: *European Journal of Soil Science* 58, pp. 523–546. DOI: 10.1111/j.1365-2389.2007.00915.x.
- Jenkins, G. J., Perry, M., Prior, J., UKCIP09, and UK Climate Impacts Programme (2009). *The Climate of the United Kingdom and Recent Trends*. Exeter: Met Office Hadley Centre. URL: http://www.ukcip.org.uk/images/stories/08_pdfs/Trends.pdf (visited on 05/12/2022).
- Jo, E., Park, C., Son, S.-W., Roh, J.-W., Lee, G.-W., and Lee, Y.-H. (2020). “Classification of Localized Heavy Rainfall Events in South Korea”. In: *Asia-Pacific Journal of Atmospheric Sciences* 56.1, pp. 77–88. DOI: 10.1007/s13143-019-00128-7.
- Jones, M. R., Fowler, H. J., Kilsby, C. G., and Blenkinsop, S. (2013). “An Assessment of Changes in Seasonal and Annual Extreme Rainfall in the UK between 1961 and 2009”. In: *International Journal of Climatology* 33.5, pp. 1178–1194. DOI: 10.1002/joc.3503.
- Junghänel, T., Bissolli, P., Daßler, J., Fleckenstein, R., Imbery, F., Janssen, W., Lengfeld, K., Leppelt, T., Rauthe, M., Rauthe-Schöch, A., Rocek, M., Walawender, E., and Weigl, E. (2021). *Hydro-klimatologische Einordnung der Stark- und Dauerniederschläge in Teilen Deutschlands im Zusammenhang mit dem Tiefdruckgebiet „Bernd“ vom 12. bis 19. Juli 202*. Offenbach am Main: Deutscher Wetterdienst, p. 16.

- Jurado, A., Vázquez-Suñé, E., Carrera, J., Alda, M. López de, Pujades, E., and Barceló, D. (2012). “Emerging Organic Contaminants in Groundwater in Spain: A Review of Sources, Recent Occurrence and Fate in a European Context”. In: *Science of The Total Environment* 440, pp. 82–94. DOI: 10.1016/j.scitotenv.2012.08.029.
- Kavka, P., Neumann, M., Dostál, T., Zúmr, D., Laburda, T., Rodrigo-Comino, J., and Iserloh, T. (2021). “Chapter 17 - Rainfall Simulation Experiments as a Tool for Process Research in Soil Science, Hydrology, and Geomorphology”. In: *Precipitation*. Ed. by J. Rodrigo-Comino. Elsevier, pp. 395–418. DOI: 10.1016/B978-0-12-822699-5.00015-X.
- Keesstra, S. D., Davis, J., Masselink, R. H., Casali, J., Peeters, E. T. H. M., and Dijkema, R. (2019). “Coupling Hysteresis Analysis with Sediment and Hydrological Connectivity in Three Agricultural Catchments in Navarre, Spain”. In: *Journal of Soils and Sediments* 19.3, pp. 1598–1612. DOI: 10.1007/s11368-018-02223-0.
- Kelleher, C., Golden, H. E., Burkholder, S., and Shuster, W. (2020). “Urban Vacant Lands Impart Hydrological Benefits across City Landscapes”. In: *Nature Communications* 11.1, p. 1563. DOI: 10.1038/s41467-020-15376-9.
- Kendon, E. J., Blenkinsop, S., and Fowler, H. J. (2018). “When Will We Detect Changes in Short-Duration Precipitation Extremes?” In: *Journal of Climate* 31.7, pp. 2945–2964. DOI: 10.1175/JCLI-D-17-0435.1.
- Kendon, E. J., Roberts, N. M., Fowler, H. J., Roberts, M. J., Chan, S. C., and Senior, C. A. (2014). “Heavier Summer Downpours with Climate Change Revealed by Weather Forecast Resolution Model”. In: *Nature Climate Change* 4.7, pp. 570–576. DOI: 10.1038/nclimate2258.
- Kikuchi, K. and Wang, B. (2008). “Diurnal Precipitation Regimes in the Global Tropics”. In: *Journal of Climate* 21.11, pp. 2680–2696. DOI: 10.1175/2007JCLI2051.1.
- Kim, D. and Young, T. M. (2009). “Significance of Indirect Deposition on Wintertime PAH Concentrations in an Urban Northern California Creek”. In: *Environmental Engineering Science* 26.2, pp. 269–278. DOI: 10.1089/ees.2007.0277.
- Kingfield, D. M., Calhoun, K. M., Beurs, K. M. de, and Henebry, G. M. (2018). “Effects of City Size on Thunderstorm Evolution Revealed through a Multiradar Climatology of the Central United States”. In: *Journal of Applied Meteorology and Climatology* 57.2, pp. 295–317. DOI: 10.1175/JAMC-D-16-0341.1.
- Klemas, V. (2015). “Remote Sensing of Floods and Flood-Prone Areas: An Overview”. In: *Journal of Coastal Research* 314, pp. 1005–1013. DOI: 10.2112/JCOASTRES-D-14-00160.1.
- Komatsu, E., Fukushima, T., and Harasawa, H. (2007). “A Modeling Approach to Forecast the Effect of Long-Term Climate Change on Lake Water Quality”. In: *Ecological Modelling* 209.2-4, pp. 351–366. URL: https://www.academia.edu/27097277/A_modeling_approach_to_forecast_the_effect_of_long_term_climate_change_on_lake_water_quality (visited on 05/11/2022).

- Kreibich, H. and Thielen, A. H. (2009). "Coping with Floods in the City of Dresden, Germany". In: *Natural Hazards* 51.3, pp. 423–436. DOI: 10.1007/s11069-007-9200-8.
- Kristoffersen, P., Larsen, S. U., Møller, J., and Hels, T. (2004). "Factors Affecting the Phase-out of Pesticide Use in Public Areas in Denmark". In: *Pest Management Science* 60.6, pp. 605–612. DOI: 10.1002/ps.890.
- Kundzewicz, Z. W., Krysanova, V., Dankers, R., Hirabayashi, Y., Kanae, S., Hattermann, F. F., Huang, S., Milly, P. C. D., Stoffel, M., Driessen, P. P. J., Matczak, P., Quevauviller, P., and Schellnhuber, H.-J. (2017). "Differences in Flood Hazard Projections in Europe – Their Causes and Consequences for Decision Making". In: *Hydrological Sciences Journal*, p. 02626667.2016.1241398. DOI: 10.1080/02626667.2016.1241398.
- Kunkel, K. E., Karl, T. R., Brooks, H., Kossin, J., Lawrimore, J. H., Arndt, D., Bosart, L., Changnon, D., Cutter, S. L., Doesken, N., Emanuel, K., Groisman, P. Y., Katz, R. W., Knutson, T., O'Brien, J., Paciorek, C. J., Peterson, T. C., Redmond, K., Robinson, D., Trapp, J., Vose, R., Weaver, S., Wehner, M., Wolter, K., and Wuebbles, D. (2013). "Monitoring and Understanding Trends in Extreme Storms: State of Knowledge". In: *Bulletin of the American Meteorological Society* 94.4, pp. 499–514. DOI: 10.1175/BAMS-D-11-00262.1.
- LaPoint, S., Balkenhol, N., Hale, J., Sadler, J., and Ree, R. (2015). "Ecological Connectivity Research in Urban Areas". In: *Functional Ecology* 29.7. Ed. by K. Evans, pp. 868–878. DOI: 10.1111/1365-2435.12489.
- Laudan, J., Rözer, V., Sieg, T., Vogel, K., and Thielen, A. H. (2017). "Damage Assessment in Braunsbach 2016: Data Collection and Analysis for an Improved Understanding of Damaging Processes during Flash Floods". In: *Natural Hazards and Earth System Sciences* 17.12, pp. 2163–2179. DOI: 10.5194/nhess-17-2163-2017.
- Lawrence, D. and Vandecar, K. (2015). "Erratum: Effects of Tropical Deforestation on Climate and Agriculture". In: *Nature Climate Change* 5.2 (2), pp. 174–174. DOI: 10.1038/nclimate2502.
- Lenderink, G. and van Meijgaard, E. (2008). "Increase in Hourly Precipitation Extremes beyond Expectations from Temperature Changes". In: *Nature Geoscience* 1.8 (8), pp. 511–514. DOI: 10.1038/ngeo262.
- Lengfeld, K., Winterrath, T., Junghänel, T., Hafer, M., and Becker, A. (2019). "Characteristic Spatial Extent of Hourly and Daily Precipitation Events in Germany Derived from 16 Years of Radar Data". In: *Meteorologische Zeitschrift* 28.5, pp. 363–378. DOI: 10.1127/metz/2019/0964.
- Lenggenhager, S., Croci-Maspoli, M., Brönnimann, S., and Martius, O. (2019). "On the Dynamical Coupling between Atmospheric Blocks and Heavy Precipitation Events: A Discussion of the Southern Alpine Flood in October 2000". In: *Quarterly Journal of the Royal Meteorological Society* 145.719, pp. 530–545. DOI: 10.1002/qj.3449.

- Lewis, E., Fowler, H., Alexander, L., Dunn, R., McClean, F., Barbero, R., Guerreiro, S., Li, X.-F., and Blenkinsop, S. (2019). "GSDR: A Global Sub-Daily Rainfall Dataset". In: *Journal of Climate* 32.15, pp. 4715–4729. DOI: 10.1175/JCLI-D-18-0143.1.
- Li, J. (2018). "Hourly Station-Based Precipitation Characteristics over the Tibetan Plateau". In: *International Journal of Climatology* 38.3, pp. 1560–1570. DOI: 10.1002/joc.5281.
- Li, X.-X., Leung, D. Y. C., Liu, C.-H., and Lam, K. M. (2008). "Physical Modeling of Flow Field inside Urban Street Canyons". In: *Journal of Applied Meteorology and Climatology* 47.7, pp. 2058–2067. DOI: 10.1175/2007JAMC1815.1.
- Li, Y., Schubert, S., Kropp, J. P., and Rybski, D. (2020). "On the Influence of Density and Morphology on the Urban Heat Island Intensity". In: *Nature Communications* 11.1 (1), p. 2647. DOI: 10.1038/s41467-020-16461-9.
- Lim, T. C. (2016). "Predictors of Urban Variable Source Area: A Cross-Sectional Analysis of Urbanized Catchments in the United States: Predictors of Urban Variable Source Area". In: *Hydrological Processes* 30.25, pp. 4799–4814. DOI: 10.1002/hyp.10943.
- Lissemore, L., Hao, C., Yang, P., Sibley, P. K., Mabury, S., and Solomon, K. R. (2006). "An Exposure Assessment for Selected Pharmaceuticals within a Watershed in Southern Ontario". In: *Chemosphere* 64.5, pp. 717–729. DOI: 10.1016/j.chemosphere.2005.11.015. pmid: 16403551.
- Liu, J. and Niyogi, D. (2019). "Meta-Analysis of Urbanization Impact on Rainfall Modification". In: *Scientific Reports* 9. DOI: 10.1038/s41598-019-42494-2.
- Liu, X., He, B., Guo, L., Huang, L., and Chen, D. (2020). "Similarities and Differences in the Mechanisms Causing the European Summer Heatwaves in 2003, 2010, and 2018". In: *Earth's Future* 8.4. DOI: 10.1029/2019EF001386.
- Lloyd, C., Freer, J., Johnes, P., and Collins, A. (2016). "Using Hysteresis Analysis of High-Resolution Water Quality Monitoring Data, Including Uncertainty, to Infer Controls on Nutrient and Sediment Transfer in Catchments". In: *Science of The Total Environment* 543, pp. 388–404. DOI: 10.1016/j.scitotenv.2015.11.028.
- Loague, K. and Corwin, D. L. (2005). "Point and NonPoint Source Pollution". In: *Encyclopedia of Hydrological Sciences*. Ed. by M. G. Anderson and J. J. McDonnell. Chichester, UK: John Wiley & Sons, Ltd, hsa097. DOI: 10.1002/0470848944.hsa097.
- Lochbihler, K., Lenderink, G., and Siebesma, A. P. (2017). "The Spatial Extent of Rainfall Events and Its Relation to Precipitation Scaling". In: *Geophysical Research Letters* 44.16, pp. 8629–8636. DOI: 10.1002/2017GL074857.
- Lorenz, J. M., Kronenberg, R., Bernhofer, C., and Niyogi, D. (2019). "Urban Rainfall Modification: Observational Climatology Over Berlin, Germany". In: *Journal of Geophysical Research: Atmospheres* 124.2, pp. 731–746. DOI: 10.1029/2018JD028858.
- Lundy, L., Ellis, J., and Revitt, D. (2012). "Risk Prioritisation of Stormwater Pollutant Sources". In: *Water Research* 46.20, pp. 6589–6600. DOI: 10.1016/j.watres.2011.10.039.

- Lundy, L. and Wade, R. (2013). *A Critical Review of Methodologies to Identify the Sources and Pathways of Urban Diffuse Pollutants. Stage 1 Contribution to: Wadu, R. et al. (2013). A Critical Review of Urban Diffuse Pollution Control: Methodologies to Identify Sources, Pathways and Mitigation Measures with Multiple Benefits.* Available online at: crew.ac.uk/publications.
- Lynam, M. M., Dvonch, J. T., Barres, J. A., Landis, M. S., and Kamal, A. S. (2016). “Investigating the Impact of Local Urban Sources on Total Atmospheric Mercury Wet Deposition in Cleveland, Ohio, USA”. In: *Atmospheric Environment* 127, pp. 262–271. DOI: 10.1016/j.atmosenv.2015.12.048.
- Löwe, R., Madsen, H., and McSharry, P. (2016). “Objective Classification of Rainfall in Northern Europe for Online Operation of Urban Water Systems Based on Clustering Techniques”. In: *Water* 8.3, p. 87. DOI: 10.3390/w8030087.
- Ma, S., Zhou, T., Dai, A., and Han, Z. (2015). “Observed Changes in the Distributions of Daily Precipitation Frequency and Amount over China from 1960 to 2013”. In: *Journal of Climate* 28.17, pp. 6960–6978. DOI: 10.1175/JCLI-D-15-0011.1.
- Makepeace, D. K., Smith, D. W., and Stanley, S. J. (1995). “Urban Stormwater Quality: Summary of Contaminant Data”. In: *Critical Reviews in Environmental Science and Technology* 25.2, pp. 93–139. DOI: 10.1080/10643389509388476.
- Maksimović, Prodanović, D., Boonya-Aroonnet, S., Leitão, J. P., Djordjević, S., and Allitt, R. (2009). “Overland Flow and Pathway Analysis for Modelling of Urban Pluvial Flooding”. In: *Journal of Hydraulic Research* 47.4, pp. 512–523. DOI: 10.1080/00221686.2009.9522027.
- Mallakpour, I. and Villarini, G. (2015). “The Changing Nature of Flooding across the Central United States”. In: *Nature Climate Change* 5.3 (3), pp. 250–254. DOI: 10.1038/nclimate2516.
- Mandapaka, P. V., Germann, U., and Panziera, L. (2013). “Diurnal Cycle of Precipitation over Complex Alpine Orography: Inferences from High-Resolution Radar Observations: Diurnal Variability of Rainfall: Alps”. In: *Quarterly Journal of the Royal Meteorological Society* 139.673, pp. 1025–1046. DOI: 10.1002/qj.2013.
- Mansell, M. and Rollet, F. (2009). “The Effect of Surface Texture on Evaporation, Infiltration and Storage Properties of Paved Surfaces”. In: *Water Science and Technology* 60.1, pp. 71–76. DOI: 10.2166/wst.2009.323.
- Maraun, D., Osborn, T. J., and Gillett, N. P. (2008). “United Kingdom daily precipitation intensity: improved early data, error estimates and an update from 2000 to 2006”. In: *International Journal of Climatology* 28.6, pp. 833–842. DOI: 10.1002/joc.1672.
- Masselink, R. J. H., Heckmann, T., Temme, A. J. A. M., Anders, N. S., Gooren, H. P. A., and Keesstra, S. D. (2017). “A Network Theory Approach for a Better Understanding of Overland Flow Connectivity: Networks for a Better Understanding of Overland Flow Connectivity”. In: *Hydrological Processes* 31.1, pp. 207–220. DOI: 10.1002/hyp.10993.

- McGrane, S. J. (2016). “Impacts of Urbanisation on Hydrological and Water Quality Dynamics, and Urban Water Management: A Review”. In: *Hydrological Sciences Journal* 61.13, pp. 2295–2311. DOI: 10.1080/02626667.2015.1128084.
- McGraw-Hill (2002). *Dictionary of Scientific and Technical Terms*. 6th ed. New York: McGraw-Hill Professional.
- McPhillips, L. E., Chang, H., Chester, M. V., Depietri, Y., Friedman, E., Grimm, N. B., Kominoski, J. S., McPhearson, T., Méndez-Lázaro, P., Rosi, E. J., and Shafiei Shiva, J. (2018). “Defining Extreme Events: A Cross-Disciplinary Review”. In: *Earth’s Future* 6.3, pp. 441–455. DOI: 10.1002/2017EF000686.
- Mekiffer, B (2008). “Eigenschaften Urbaner Böden Berlins – Statistische Auswertung von Gutachtendaten Und Fallbeispielen”. Berlin: Technische Universität Berlin. 141 pp.
- Mekiffer, B and Wessolek, G (2011). “Trümmerschuttböden Und Sulfatfreisetzung. Boden Des Jahres 2010 – Stadtböden, Berlin Und Seine Böden”. In: *Berliner Geographische Arbeiten* 117, pp. 33–37.
- Menezes Sanchez Macedo, P., Ferreira Pinto, M., Alves Sobrinho, T., Schultz, N., Altamir Rodrigues Coutinho, T., and Carvalho, D. Fonseca de (2021). “A Modified Portable Rainfall Simulator for Soil Erosion Assessment under Different Rainfall Patterns”. In: *Journal of Hydrology* 596, p. 126052. DOI: 10.1016/j.jhydrol.2021.126052.
- Meredith, E. P., Ulbrich, U., and Rust, H. W. (2019). “The Diurnal Nature of Future Extreme Precipitation Intensification”. In: *Geophysical Research Letters* 46.13, pp. 7680–7689. DOI: 10.1029/2019GL082385.
- Miao, C., Sun, Q., Kong, D., and Duan, Q. (2016). “Record-Breaking Heat in Northwest China in July 2015: Analysis of the Severity and Underlying Causes”. In: *Bulletin of the American Meteorological Society* 97.12, S97–S101. DOI: 10.1175/BAMS-D-16-0142.1.
- Miles, B. and Band, L. E. (2015). “Green Infrastructure Stormwater Management at the Watershed Scale: Urban Variable Source Area and Watershed Capacitance: INVITED COMMENTARY”. In: *Hydrological Processes* 29.9, pp. 2268–2274. DOI: 10.1002/hyp.10448.
- Miller, J. D. and Hutchins, M. (2017). “The Impacts of Urbanisation and Climate Change on Urban Flooding and Urban Water Quality: A Review of the Evidence Concerning the United Kingdom”. In: *Journal of Hydrology: Regional Studies* 12, pp. 345–362. DOI: 10.1016/j.ejrh.2017.06.006.
- Moftakhari, H. R., AghaKouchak, A., Sanders, B. F., Allaire, M., and Matthew, R. A. (2018). “What Is Nuisance Flooding? Defining and Monitoring an Emerging Challenge”. In: *Water Resources Research* 54.7, pp. 4218–4227. DOI: 10.1029/2018WR022828.
- Moron, V., Barbero, R., Evans, J. P., Westra, S., and Fowler, H. J. (2019). “Weather Types and Hourly to Multiday Rainfall Characteristics in Tropical Australia”. In: *Journal of Climate* 32.13, pp. 3983–4011. DOI: 10.1175/JCLI-D-18-0384.1.

- Morrison, A., Villarini, G., Zhang, W., and Scoccimarro, E. (2019). “Projected Changes in Extreme Precipitation at Sub-Daily and Daily Time Scales”. In: *Global and Planetary Change* 182, p. 103004. DOI: 10.1016/j.gloplacha.2019.103004.
- Murawski, A., Zimmer, J., and Merz, B. (2016). “High Spatial and Temporal Organization of Changes in Precipitation over Germany for 1951–2006”. In: *International Journal of Climatology* 36.6, pp. 2582–2597. DOI: 10.1002/joc.4514.
- Müller, A., Österlund, H., Marsalek, J., and Viklander, M. (2020). “The Pollution Conveyed by Urban Runoff: A Review of Sources”. In: *Science of The Total Environment* 709, p. 136125. DOI: 10.1016/j.scitotenv.2019.136125.
- Müller, A., Österlund, H., Nordqvist, K., Marsalek, J., and Viklander, M. (2019). “Building Surface Materials as Sources of Micropollutants in Building Runoff: A Pilot Study”. In: *Science of The Total Environment* 680, pp. 190–197. DOI: 10.1016/j.scitotenv.2019.05.088.
- Müller, E. N. and Pfister, A. (2011). “Increasing Occurrence of High-Intensity Rainstorm Events Relevant for the Generation of Soil Erosion in a Temperate Lowland Region in Central Europe”. In: *Journal of Hydrology* 411.3, pp. 266–278. DOI: 10.1016/j.jhydrol.2011.10.005.
- Nakazato, R., Funakoshi, H., Ishikawa, T., Kameda, Y., Matsuda, I., and Itoh, S. (2018). “Rainfall Intensity Estimation from Sound for Generating CG of Rainfall Scenes”. In: *2018 International Workshop on Advanced Image Technology (IWAIT)*. 2018 International Workshop on Advanced Image Technology (IWAIT). Chiang Mai: IEEE, pp. 1–4. DOI: 10.1109/IWAIT.2018.8369692.
- National Geographic Society (2019). *Point Source and Nonpoint Sources of Pollution*. National Geographic Society. URL: <http://www.nationalgeographic.org/encyclopedia/point-source-and-nonpoint-sources-pollution/> (visited on 09/05/2021).
- Nehls, T., Menzel, M., and Wessolek, G. (2015). “Depression Storage Capacities of Different Ideal Pavements as Quantified by a Terrestrial Laser Scanning-Based Method”. In: *Water Science and Technology* 71.6, pp. 862–869. DOI: 10.2166/wst.2015.025.
- Nehls, T., Peters, A., Kraus, F., and Rim, Y. N. (2021). “Water Dynamics at the Urban Soil-Atmosphere Interface—Rainwater Storage in Paved Surfaces and Its Dependence on Rain Event Characteristics”. In: *Journal of Soils and Sediments* 21.5, pp. 2025–2034. DOI: 10.1007/s11368-020-02762-5.
- Nehls, T., Rokia, S., Mekiffer, B., Schwartz, C., and Wessolek, G. (2013). “Contribution of Bricks to Urban Soil Properties”. In: *Journal of Soils and Sediments* 13.3, pp. 575–584. DOI: 10.1007/s11368-012-0559-0.
- New York City Soil Survey (2021). *New York City Soil & Water Conservation District, New York, USA*. URL: <https://www.soilandwater.nyc/urban-soils.html>.
- Niyogi, D., Holt, T., Zhong, S., Pyle, P., and Basara, J. (2006). “Urban and Land Surface Effects on the 30 July 2003 Mesoscale Convective System Event Observed in the

- Southern Great Plains”. In: *Journal of Geophysical Research* 111.D19107. DOI: 10.1029/2005JD006746.
- Nunes, J. P., Wainwright, J., Biëdiers, C. L., Darboux, F., Fiener, P., Finger, D., and Turnbull, L. (2018). “Better Models Are More Effectively Connected Models: Better Models Are More Effectively Connected Models”. In: *Earth Surface Processes and Landforms* 43.6, pp. 1355–1360. DOI: 10.1002/esp.4323.
- Oke, T. R. (1982). “The Energetic Basis of the Urban Heat Island”. In: *Quarterly Journal of the Royal Meteorological Society* 108.455, pp. 1–24. DOI: 10.1002/qj.49710845502.
- Oppel, J., Broll, G., Löffler, D., Meller, M., Römbke, J., and Ternes, T. (2004). “Leaching Behaviour of Pharmaceuticals in Soil-Testing-Systems: A Part of an Environmental Risk Assessment for Groundwater Protection”. In: *The Science of the Total Environment* 328.1-3, pp. 265–273. DOI: 10.1016/j.scitotenv.2004.02.004. pmid: 15207589.
- Osborn, T. J. and Hulme, M. (2002). “Evidence for Trends in Heavy Rainfall Events over the UK”. In: *Philosophical Transactions of the Royal Society of London. Series A: Mathematical, Physical and Engineering Sciences* 360.1796. Ed. by D. Cox, J. Hunt, P. Mason, H. Wheeler, and P. Wolf, pp. 1313–1325. DOI: 10.1098/rsta.2002.1002.
- Pachauri, R. K., L. Mayer, and I. P. on Climate Change, eds. (2015). *Climate Change 2014: Synthesis Report*. Geneva, Switzerland: Intergovernmental Panel on Climate Change. 151 pp.
- Pagenkopf, A. (2011). “Urbane Niederschlagsbeeinflussung”. PhD thesis. Humboldt-Universität zu Berlin, Mathematisch-Naturwissenschaftliche Fakultät II. DOI: 10.18452/16421.
- Pal, A., He, Y., Jekel, M., Reinhard, M., and Gin, K. Y.-H. (2014). “Emerging Contaminants of Public Health Significance as Water Quality Indicator Compounds in the Urban Water Cycle”. In: *Environment International* 71, pp. 46–62. DOI: 10.1016/j.envint.2014.05.025.
- Palta, M. M., Grimm, N. B., and Groffman, P. M. (2017). ““Accidental” Urban Wetlands: Ecosystem Functions in Unexpected Places”. In: *Frontiers in Ecology and the Environment* 15.5, pp. 248–256. DOI: 10.1002/fee.1494.
- Panziera, L., Gabella, M., Germann, U., and Martius, O. (2018). “A 12-Year Radar-Based Climatology of Daily and Sub-Daily Extreme Precipitation over the Swiss Alps”. In: *International Journal of Climatology* 38.10, pp. 3749–3769. DOI: 10.1002/joc.5528.
- Parsons, A. J. and Stromberg, S. G. L. (1998). “Experimental Analysis of Size and Distance of Travel of Unconstrained Particles in Interrill Flow”. In: *Water Resources Research* 34.9, pp. 2377–2381. DOI: 10.1029/98WR01471.
- Paton, E. and Haacke, N. (2021). “Merging Patterns and Processes of Diffuse Pollution in Urban Watersheds: A Connectivity Assessment”. In: *WIREs Water* 8.4, e1525. DOI: 10.1002/wat2.1525.

- Paulat, M., Frei, C., Hagen, M., and Wernli, H. (2008). “A Gridded Dataset of Hourly Precipitation in Germany: Its Construction, Climatology and Application”. In: *Meteorologische Zeitschrift* 17.6, pp. 719–732. DOI: 10.1127/0941-2948/2008/0332.
- Pendergrass, A. G. and Knutti, R. (2018). “The Uneven Nature of Daily Precipitation and Its Change”. In: *Geophysical Research Letters* 45.21, pp. 11,980–11,988. DOI: 10.1029/2018GL080298.
- Peterson, T. C. (2005). “Climate Change Indices”. In: *World Meteorological Organization Bulletin* 54.2, pp. 83–86.
- Peterson, T. C. and Manton, M. J. (2008). “Monitoring Changes in Climate Extremes: A Tale of International Collaboration”. In: *Bulletin of the American Meteorological Society* 89.9, pp. 1266–1271. DOI: 10.1175/2008BAMS2501.1.
- Pitt, R., Bannerman, R., Clark, S., and Williamson, D. (2004a). “Sources of Pollutants in Urban Areas (Part 1) - Older Monitoring Projects”. In: *Journal of Water Management Modeling*. DOI: 10.14796/JWMM.R223-23.
- Pitt, R. E., Bannerman, R., Clark, S., and Williamson, D. (2004b). “Sources of Pollutants in Urban Areas (Part 2) - Recent Sheetflow Monitoring”. In: *Journal of Water Management Modeling*. DOI: 10.14796/JWMM.R223-24.
- Plavcová, E. and Kyselý, J. (2013). “Projected Evolution of Circulation Types and Their Temperatures over Central Europe in Climate Models”. In: *Theoretical and Applied Climatology* 114.3-4, pp. 625–634. DOI: 10.1007/s00704-013-0874-4.
- Ploshay, J. J. and Lau, N.-C. (2010). “Simulation of the Diurnal Cycle in Tropical Rainfall and Circulation during Boreal Summer with a High-Resolution GCM”. In: *Monthly Weather Review* 138.9, pp. 3434–3453. DOI: 10.1175/2010MWR3291.1.
- Poschlod, B. and Ludwig, R. (2021). “Internal Variability and Temperature Scaling of Future Sub-Daily Rainfall Return Levels over Europe”. In: *Environmental Research Letters* 16.6, p. 064097. DOI: 10.1088/1748-9326/ac0849.
- Poudyal, S., Cochrane, T. A., and Bello-Mendoza, R. (2016). “First Flush Stormwater Pollutants From Carpark in Different Urban Settings”. In: Canterbury: Water New Zealand Conference Paper Nov/Dez, pp. 24–27.
- Pryor, S. C., Howe, J. A., and Kunkel, K. E. (2009). “How Spatially Coherent and Statistically Robust Are Temporal Changes in Extreme Precipitation in the Contiguous USA?” In: *International Journal of Climatology* 29.1, pp. 31–45. DOI: 10.1002/joc.1696.
- R Core Team (2020). *R: A Language and Environment for Statistical Computing*. Vienna: R Foundation for Statistical Computing. URL: <https://www.R-project.org>.
- R Development Core Team (2018). *R: A Language and Environment for Statistical Computing*. Vienna, Austria.
- Ragab, R., Rosier, P., Dixon, A., Bromley, J., and Cooper, J. D. (2003). “Experimental Study of Water Fluxes in a Residential Area: 2. Road Infiltration, Runoff and Evaporation”. In: *Hydrological Processes* 17.12, pp. 2423–2437. DOI: 10.1002/hyp.1251.

- Ramakrishna, D. M. and Viraraghavan, T. (2005). “Environmental Impact of Chemical Deicers – A Review”. In: *Water, Air, and Soil Pollution* 166.1-4, pp. 49–63. DOI: 10.1007/s11270-005-8265-9.
- Rammal, M. and Berthier, E. (2020). “Runoff Losses on Urban Surfaces during Frequent Rainfall Events: A Review of Observations and Modeling Attempts”. In: *Water* 12.10, p. 2777. DOI: 10.3390/w12102777.
- Rauthe, M., Steiner, H., Riediger, U., Mazurkiewicz, A., and Gratzki, A. (2013). “A Central European Precipitation Climatology? Part I: Generation and Validation of a High-Resolution Gridded Daily Data Set (HYRAS)”. In: *Meteorologische Zeitschrift* 22.3, pp. 235–256. DOI: 10.1127/0941-2948/2013/0436.
- Restrepo-Posada, P. J. and Eagleson, P. S. (1982). “Identification of Independent Rainstorms”. In: *Journal of Hydrology* 55.1-4, pp. 303–319. DOI: 10.1016/0022-1694(82)90136-6.
- Revitt, D. M., Lundy, L., Coulon, F., and Fairley, M. (2014). “The Sources, Impact and Management of Car Park Runoff Pollution: A Review”. In: *Journal of Environmental Management* 146, pp. 552–567. DOI: 10.1016/j.jenvman.2014.05.041.
- Ries, J. B., Seeger, M., Iserloh, T., Wistorf, S., and Fister, W. (2009). “Calibration of Simulated Rainfall Characteristics for the Study of Soil Erosion on Agricultural Land”. In: *Soil and Tillage Research* 106.1, pp. 109–116. DOI: 10.1016/j.still.2009.07.005.
- Rim, Y.-N. (2011). “Analyzing Runoff Dynamics of Paved Soil Surface Using Weighable Lysimeters”. PhD thesis. Berlin: Technische Universität Berlin.
- Rim, Y. N., Litz, N., Nehls, T., Trinks, S., and Wessolek, G. (2010). “Studying Water Budget of Paved Urban Sites Using Weighable Lysimeter”. In: *Soil Solutions for a Changing World*. 19th World Congress of Soil Science. Brisbane, Australia, p. 5.
- Roder Green, A. L., Putschew, A., and Nehls, T. (2014). “Littered Cigarette Butts as a Source of Nicotine in Urban Waters”. In: *Journal of Hydrology* 519, pp. 3466–3474. DOI: 10.1016/j.jhydrol.2014.05.046.
- Rojas, R., Feyen, L., Bianchi, A., and Dosio, A. (2012). “Assessment of Future Flood Hazard in Europe Using a Large Ensemble of Bias-Corrected Regional Climate Simulations”. In: *Journal of Geophysical Research: Atmospheres* 117.D17. DOI: 10.1029/2012JD017461.
- Rojas, R., Feyen, L., Dosio, A., and Bavera, D. (2011). “Improving Pan-European Hydrological Simulation of Extreme Events through Statistical Bias Correction of RCM-driven Climate Simulations”. In: *Hydrology and Earth System Sciences* 15.8, pp. 2599–2620. DOI: 10.5194/hess-15-2599-2011.
- Rossman, L. (2010). *Storm Water Management Model User’s Manual Version 5.0*. Cincinnati, OH: National Risk Management Research Laboratory, p. 295.
- Roth, C. H., Meyer, B., and Frede, H. G. (1985). “A Portable Rainfall Simulator for Studying Factors Affecting Runoff, Infiltration and Soil Loss”. In: *CATENA* 12.1, pp. 79–85. DOI: 10.1016/S0341-8162(85)80006-0.

- Roudier, P., Andersson, J. C. M., Donnelly, C., Feyen, L., Greuell, W., and Ludwig, F. (2016). “Projections of Future Floods and Hydrological Droughts in Europe under a +2°C Global Warming”. In: *Climatic Change* 135.2, pp. 341–355. DOI: 10.1007/s10584-015-1570-4.
- Rui, Y., Fu, D., Do Minh, H., Radhakrishnan, M., Zevenbergen, C., and Pathirana, A. (2018). “Urban Surface Water Quality, Flood Water Quality and Human Health Impacts in Chinese Cities. What Do We Know?” In: *Water* 10.3, p. 240. DOI: 10.3390/w10030240.
- Russell, K. L., Vietz, G. J., and Fletcher, T. D. (2019). “Urban Sediment Supply to Streams from Hillslope Sources”. In: *Science of The Total Environment* 653, pp. 684–697. DOI: 10.1016/j.scitotenv.2018.10.374.
- Rözer, V., Peche, A., Berkahn, S., Feng, Y., Fuchs, L., Graf, T., Haberlandt, U., Kreibich, H., Sämman, R., Sester, M., Shehu, B., Wahl, J., and Neuweiler, I. (2021). “Impact-Based Forecasting for Pluvial Floods”. In: *Earth’s Future* 9.2. DOI: 10.1029/2020EF001851.
- Salvadore, E., Bronders, J., and Batelaan, O. (2015). “Hydrological Modelling of Urbanized Catchments: A Review and Future Directions”. In: *Journal of Hydrology* 529, pp. 62–81. DOI: 10.1016/j.jhydrol.2015.06.028.
- Schiff, K., Tiefenthaler, L., Bay, S., and Greenstein, D. (2016). “Effects of Rainfall Intensity and Duration on the First Flush from Parking Lots”. In: *Water* 8.8, p. 320. DOI: 10.3390/w8080320.
- Schmid, P. E. and Niyogi, D. (2017). “Modeling Urban Precipitation Modification by Spatially Heterogeneous Aerosols”. In: *Journal of Applied Meteorology and Climatology* 56.8, pp. 2141–2153. DOI: 10.1175/JAMC-D-16-0320.1.
- Schär, C., Ban, N., Fischer, E. M., Rajczak, J., Schmidli, J., Frei, C., Giorgi, F., Karl, T. R., Kendon, E. J., Tank, A. M. G. K., O’Gorman, P. A., Sillmann, J., Zhang, X., and Zwiers, F. W. (2016). “Percentile Indices for Assessing Changes in Heavy Precipitation Events”. In: *Climatic Change* 137.1-2, pp. 201–216. DOI: 10.1007/s10584-016-1669-2.
- Scoging, H. (1992). “Modelling Overland-Flow Hydrology for Dynamic Hydraulics.” In: *Overland Flow. Hydraulics and Erosion Mechanics*. London: UCL Press.
- Sen, S., Srivastava, P., Dane, J. H., Yoo, K. H., and Shaw, J. N. (2010). “Spatial–Temporal Variability and Hydrologic Connectivity of Runoff Generation Areas in a North Alabama Pasture—Implications for Phosphorus Transport”. In: *Hydrological Processes* 24.3, pp. 342–356. DOI: 10.1002/hyp.7502.
- Seneviratne, S. I., Nicholls, N., Easterling, D., Goodess, C. M., Kanae, S., Kossin, J., Luo, Y., Marengo, J., McInnes, K., Rahimi, M., Reichstein, M., Sorteberg, A., Vera, C., Zhang, X., Rusticucci, M., Semenov, V., Alexander, L. V., Allen, S., Benito, G., Cavazos, T., Clague, J., Conway, D., Della-Marta, P. M., Gerber, M., Gong, S., Goswami, B. N., Hemer, M., Huggel, C., van den Hurk, B., Kharin, V. V., Kitoh, A., Tank, A. M. K., Li, G., Mason, S., McGuire, W., van Oldenborgh, G. J., Orłowsky, B., Smith, S., Thiaw, W., Velegrakis, A., Yiou, P., Zhang, T., Zhou, T., and Zwiers, F. W. (2012). “Changes in Climate Extremes and Their Impacts on the Natural Physical Environment”. In: *Managing the Risks of Extreme*

- Events and Disasters to Advance Climate Change Adaptation*. Ed. by C. B. Field, V. Barros, T. F. Stocker, and Q. Dahe. Cambridge: Cambridge University Press, pp. 109–230. DOI: 10.1017/CB09781139177245.006.
- Sharma, A., Pezzaniti, D., Myers, B., Cook, S., Tjandraatmadja, G., Chacko, P., Chavoshi, S., Kemp, D., Leonard, R., Koth, B., and Walton, A. (2016). “Water Sensitive Urban Design: An Investigation of Current Systems, Implementation Drivers, Community Perceptions and Potential to Supplement Urban Water Services”. In: *Water* 8.7, p. 272. DOI: 10.3390/w8070272.
- Shepherd, J. M., Carter, M., Manyin, M., Messen, D., and Burian, S. (2010). “The Impact of Urbanization on Current and Future Coastal Precipitation: A Case Study for Houston”. In: *Environment and Planning B: Planning and Design* 37.2, pp. 284–304. DOI: 10.1068/b34102t.
- Sherriff, S. C., Rowan, J. S., Fenton, O., Jordan, P., and Ó hUallacháin, D. (2018). “Sediment Fingerprinting as a Tool to Identify Temporal and Spatial Variability of Sediment Sources and Transport Pathways in Agricultural Catchments”. In: *Agriculture, Ecosystems & Environment* 267, pp. 188–200. DOI: 10.1016/j.agee.2018.08.023.
- Shore, M., Jordan, P., Mellander, P.-E., Kelly-Quinn, M., Wall, D., Murphy, P., and Melland, A. (2014). “Evaluating the Critical Source Area Concept of Phosphorus Loss from Soils to Water-Bodies in Agricultural Catchments”. In: *Science of The Total Environment* 490, pp. 405–415. DOI: 10.1016/j.scitotenv.2014.04.122.
- Shukla, A. K., Ojha, C., and Garg, R. D. (2018). “Comparative Study of Trmm Satellite Predicted Rainfall Data with Rain Gauge Data over Himalayan Basin”. In: *IGARSS 2018 - 2018 IEEE International Geoscience and Remote Sensing Symposium*. IGARSS 2018 - 2018 IEEE International Geoscience and Remote Sensing Symposium. Valencia: IEEE, pp. 9347–9350. DOI: 10.1109/IGARSS.2018.8651413.
- Shuster, W. D., Bonta, J., Thurston, H., Warnemuende, E., and Smith, D. R. (2007). “Impacts of Impervious Surface on Watershed Hydrology: A Review”. In: *Urban Water Journal* 2.4, pp. 263–275. DOI: 10.1080/15730620500386529.
- Siler, N. and Durran, D. (2016). “What Causes Weak Orographic Rain Shadows? Insights from Case Studies in the Cascades and Idealized Simulations”. In: *Journal of the Atmospheric Sciences* 73.10, pp. 4077–4099. DOI: 10.1175/JAS-D-15-0371.1.
- Siler, N. and Roe, G. (2014). “How Will Orographic Precipitation Respond to Surface Warming? An Idealized Thermodynamic Perspective”. In: *Geophysical Research Letters* 41.7, pp. 2606–2613. DOI: 10.1002/2013GL059095.
- Simpson, I. R. and Jones, P. D. (2014). “Analysis of UK Precipitation Extremes Derived from Met Office Gridded Data: Analysis of UK Precipitation Extremes”. In: *International Journal of Climatology* 34.7, pp. 2438–2449. DOI: 10.1002/joc.3850.
- Smith, B. K., Smith, J. A., Baeck, M. L., Villarini, G., and Wright, D. B. (2013). “Spectrum of Storm Event Hydrologic Response in Urban Watersheds: Spectrum of Urban Storm Event

- Hydrologic Response”. In: *Water Resources Research* 49.5, pp. 2649–2663. DOI: 10.1002/wrcr.20223.
- Stachelek, J. and Soranno, P. A. (2019). “Does Freshwater Connectivity Influence Phosphorus Retention in Lakes?” In: *Limnology and Oceanography* 64.4, pp. 1586–1599. DOI: 10.1002/lno.11137.
- Stephens, E., Day, J. J., Pappenberger, F., and Cloke, H. (2015). “Precipitation and Floodiness”. In: *Geophysical Research Letters* 42.23. DOI: 10.1002/2015GL066779.
- Stephenson, D. B. (2008). “Definition, Diagnosis, and Origin of Extreme Weather and Climate Events”. In: *Climate Extremes and Society*. Ed. by H. F. Diaz and R. J. Murnane. Cambridge: Cambridge University Press, pp. 11–23. DOI: 10.1017/CB09780511535840.004.
- Steuer, J., Selbig, W., Hornewer, N., and Prey, J. (1997). *Sources of Contamination in an Urban Basin in Marquette, Michigan and an Analysis of Concentrations, Loads, and Data Quality*. U.S. Geological Survey Water-Resources Investigations Report 97-4242. DOI: 10.3133/wri974242.
- Strauss, P., Leone, A., Ripa, M. N., Turpin, N., Lescot, J.-M., and Laplana, R. (2007). “Using Critical Source Areas for Targeting Cost-Effective Best Management Practices to Mitigate Phosphorus and Sediment Transfer at the Watershed Scale”. In: *Soil Use and Management* 23.s1, pp. 144–153. DOI: 10.1111/j.1475-2743.2007.00118.x.
- Suarez, P., Anderson, W., Mahal, V., and Lakshmanan, T. (2005). “Impacts of Flooding and Climate Change on Urban Transportation: A Systemwide Performance Assessment of the Boston Metro Area”. In: *Transportation Research Part D: Transport and Environment* 10.3, pp. 231–244. DOI: 10.1016/j.trd.2005.04.007.
- Sulikowska, A. and Wypych, A. (2020). “Summer Temperature Extremes in Europe: How Does the Definition Affect the Results?” In: *Theoretical and Applied Climatology* 141.1-2, pp. 19–30. DOI: 10.1007/s00704-020-03166-8.
- Sun, Q., Miao, C., and Duan, Q. (2017). “Changes in the Spatial Heterogeneity and Annual Distribution of Observed Precipitation across China”. In: *Journal of Climate* 30.23, pp. 9399–9416. DOI: 10.1175/JCLI-D-17-0045.1.
- Tabari, H. (2020). “Climate Change Impact on Flood and Extreme Precipitation Increases with Water Availability”. In: *Scientific Reports* 13768.1, p. 10. DOI: 10.1038/s41598-020-70816-2.
- Tedoldi, D., Chebbo, G., Pierlot, D., Kovacs, Y., and Gromaire, M.-C. (2017). “Assessment of Metal and PAH Profiles in SUDS Soil Based on an Improved Experimental Procedure”. In: *Journal of Environmental Management* 202, pp. 151–166. DOI: 10.1016/j.jenvman.2017.06.063.
- Thielen, A., Kemter, M., Vorogushyn, S., Berghäuser, L., Sieg, T., Natho, S., Mohor, G. S., Petrow, T., Merz, B., and Bronstert, A. (2021). *Extreme Hochwasser bleiben trotz integriertem Risikomanagement eine Herausforderung*. Potsdam, Germany: University Potsdam, pp. 1–10.

- Thomas, I., Jordan, P., Mellander, P.-E., Fenton, O., Shine, O., Ó hUallacháin, D., Creamer, R., McDonald, N., Dunlop, P., and Murphy, P. (2016). “Improving the Identification of Hydrologically Sensitive Areas Using LiDAR DEMs for the Delineation and Mitigation of Critical Source Areas of Diffuse Pollution”. In: *Science of The Total Environment* 556, pp. 276–290. DOI: 10.1016/j.scitotenv.2016.02.183.
- Thompson, R. L., Broquet, G., Gerbig, C., Koch, T., Lang, M., Monteil, G., Munassar, S., Nickless, A., Scholze, M., Ramonet, M., Karstens, U., van Schaik, E., Wu, Z., and Rödenbeck, C. (2020). “Changes in Net Ecosystem Exchange over Europe during the 2018 Drought Based on Atmospheric Observations”. In: *Philosophical Transactions of the Royal Society B: Biological Sciences* 375.1810, p. 20190512. DOI: 10.1098/rstb.2019.0512.
- Timm, A., Kluge, B., and Wessolek, G. (2018). “Hydrological Balance of Paved Surfaces in Moist Mid-Latitude Climate – A Review”. In: *Landscape and Urban Planning* 175, pp. 80–91. DOI: 10.1016/j.landurbplan.2018.03.014.
- Trenberth, K., Jones, P., Ambenje, P., Bojariu, R., Easterling, D., Klein Tank, A., Parker, D., Rahimzadeh, F., Renwick, J., Rusticucci, M., Soden, B., and Zhai, P. (2007). “Observations: Surface and Atmospheric Climate Change”. In: *Climate Change 2007: The Physical Science Basis. Contribution of Working Group I to the Fourth Assessment Report of the Intergovernmental Panel on Climate Change*. Cambridge, United Kingdom and New York, NY, USA: Cambridge University Press.
- Trenberth, K. E., Dai, A., Rasmussen, R. M., and Parsons, D. B. (2003). “The Changing Character of Precipitation”. In: *Bulletin of the American Meteorological Society* 84.9, pp. 1205–1218. DOI: 10.1175/BAMS-84-9-1205.
- Tu, M.-C. and Smith, P. (2018). “Modeling Pollutant Buildup and Washoff Parameters for SWMM Based on Land Use in a Semiarid Urban Watershed”. In: *Water, Air, & Soil Pollution* 229.4, p. 121. DOI: 10.1007/s11270-018-3777-2.
- Tuomela, C., Sillanpää, N., and Koivusalo, H. (2019). “Assessment of Stormwater Pollutant Loads and Source Area Contributions with Storm Water Management Model (SWMM)”. In: *Journal of Environmental Management* 233, pp. 719–727. DOI: 10.1016/j.jenvman.2018.12.061.
- Turnbull, L., Wainwright, J., and Brazier, R. E. (2008). “A Conceptual Framework for Understanding Semi-Arid Land Degradation: Ecohydrological Interactions across Multiple-Space and Time Scales”. In: *Ecohydrology* 1.1, pp. 23–34. DOI: 10.1002/eco.4.
- Turnbull, L., Hütt, M.-T., Ioannides, A. A., Kininmonth, S., Poepl, R., Tockner, K., Bracken, L. J., Keesstra, S., Liu, L., Masselink, R., and Parsons, A. J. (2018). “Connectivity and Complex Systems: Learning from a Multi-Disciplinary Perspective”. In: *Applied Network Science* 3.1, p. 11. DOI: 10.1007/s41109-018-0067-2.
- Umweltatlas Berlin (2021). *Senatsverwaltung Für Stadtentwicklung Und Wohnen, Berlin, Germany*. URL: <https://www.stadtentwicklung.berlin.de/umwelt/umweltatlas/>.

- United Nations, Department of Economic and Social Affairs, and Population Division (2019). *World Population Prospects 2019: Highlights (ST/ESA/SER.A/423)*.
- Urgilés, G., Céleri, R., Trachte, K., Bendix, J., and Orellana-Alvear, J. (2021). “Clustering of Rainfall Types Using Micro Rain Radar and Laser Disdrometer Observations in the Tropical Andes”. In: *Remote Sensing* 13.5, p. 991. DOI: 10.3390/rs13050991.
- Vet, R., Artz, R. S., Carou, S., Shaw, M., Ro, C.-U., Aas, W., Baker, A., Bowersox, V. C., Dentener, F., Galy-Lacaux, C., Hou, A., Pienaar, J. J., Gillett, R., Forti, M. C., Gromov, S., Hara, H., Khodzher, T., Mahowald, N. M., Nickovic, S., Rao, P., and Reid, N. W. (2014). “A Global Assessment of Precipitation Chemistry and Deposition of Sulfur, Nitrogen, Sea Salt, Base Cations, Organic Acids, Acidity and pH, and Phosphorus”. In: *Atmospheric Environment* 93, pp. 3–100. DOI: 10.1016/j.atmosenv.2013.10.060.
- Villarreal Guerra, J. C., Khanam, Z., Ehsan, S., Stolkin, R., and McDonald-Maier, K. (2018). “Weather Classification: A New Multi-Class Dataset, Data Augmentation Approach and Comprehensive Evaluations of Convolutional Neural Networks”. In: *2018 NASA/ESA Conference on Adaptive Hardware and Systems (AHS)*. 2018 NASA/ESA Conference on Adaptive Hardware and Systems (AHS). Edinburgh: IEEE, pp. 305–310. DOI: 10.1109/AHS.2018.8541482.
- Vitry, M. Moy de, Dicht, S., and Leitão, J. P. (2017). “floodX: Urban Flash Flood Experiments Monitored with Conventional and Alternative Sensors”. In: *Earth System Science Data* 9.2, pp. 657–666. DOI: 10.5194/essd-9-657-2017.
- Wada, K., Takei, N., Sato, T., and Tsuno, H. (2015). “Sources of Organic Matter in First Flush Runoff from Urban Roadways”. In: *Water Science and Technology* 72.7, pp. 1234–1242. DOI: 10.2166/wst.2015.307.
- Wainwright, J., Turnbull, L., Ibrahim, T. G., Lexartza-Artza, I., Thornton, S. F., and Brazier, R. E. (2011). “Linking Environmental Régimes, Space and Time: Interpretations of Structural and Functional Connectivity”. In: *Geomorphology* 126.3-4, pp. 387–404. DOI: 10.1016/j.geomorph.2010.07.027.
- Wang, L. and Liu, H. (2006). “An Efficient Method for Identifying and Filling Surface Depressions in Digital Elevation Models for Hydrologic Analysis and Modelling”. In: *International Journal of Geographical Information Science* 20.2, pp. 193–213. DOI: 10.1080/13658810500433453.
- Wang, Y., Montas, H. J., Brubaker, K. L., Leisnham, P. T., Shirmohammadi, A., Chanse, V., and Rockler, A. K. (2017). “A Diagnostic Decision Support System for BMP Selection in Small Urban Watershed”. In: *Water Resources Management* 31.5, pp. 1649–1664. DOI: 10.1007/s11269-017-1605-x.
- Wasko, C., Fowler, H. J., and Blenkinsop, S. (2021). *How Hourly Rainfall Extremes Are Changing in a Warming Climate*. Carbon Brief. URL: <https://www.carbonbrief.org/guest-post-how-hourly-rainfall-extremes-are-changing-in-a-warming-climate>.

- Wasko, C., Sharma, A., and Westra, S. (2016). “Reduced Spatial Extent of Extreme Storms at Higher Temperatures: Reduced Spatial Extent of Extreme Storms”. In: *Geophysical Research Letters* 43.8, pp. 4026–4032. DOI: 10.1002/2016GL068509.
- Weng, Q. (2020). *Remote Sensing of Impervious Surfaces*. 1st ed. Boca Raton, FL: CRC Press, Taylor & Friends Group. 494 pp.
- Wenger, S. J., Roy, A. H., Jackson, C. R., Bernhardt, E. S., Carter, T. L., Filoso, S., Gibson, C. A., Hession, W. C., Kaushal, S. S., Martí, E., Meyer, J. L., Palmer, M. A., Paul, M. J., Purcell, A. H., Ramírez, A., Rosemond, A. D., Schofield, K. A., Sudduth, E. B., and Walsh, C. J. (2009). “Twenty-Six Key Research Questions in Urban Stream Ecology: An Assessment of the State of the Science”. In: *Journal of the North American Benthological Society* 28.4, pp. 1080–1098. DOI: 10.1899/08-186.1.
- Wenzel, H. G. and Voorhees, M. L. (1981). *Evaluation of the Urban Design Storm Concept*. Illinois: University of Illinois at Urbana-Champaign. Water Resources Center. URL: <https://www.ideals.illinois.edu/handle/2142/90287> (visited on 05/27/2021).
- Werner, P. and Gerstengarbe, F.-W. (2010). *KATALOG DER GROSSWETTERLAGEN EUROPAS (1881-2009)*. 119. Potsdam: Potsdam Institute for Climate Impact Research, p. 146.
- Wessolek, G., Kluge, B., Toland, A., Nehls, T., Klingelmann, E., Rim, Y. N., Mekiffer, B., and Trinks, S. (2011). “Urban Soils in the Vadose Zone”. In: *Perspectives in Urban Ecology*. Ed. by W. Endlicher. Berlin, Heidelberg: Springer Berlin Heidelberg, pp. 89–133. DOI: 10.1007/978-3-642-17731-6_4.
- Wessolek, G., Kluge, B., Trinks, S., Facklam, M., and Zeuschner, O. (2016). “From a Stinking Wastewater Disposal Field toward a Recreation Area—the Story of an Unconventional Soil Remediation in Berlin, Germany”. In: *Journal of Soils and Sediments* 18.2, pp. 481–493. DOI: 10.1007/s11368-016-1609-9.
- Westra, S., Fowler, H. J., Evans, J. P., Alexander, L. V., Berg, P., Johnson, F., Kendon, E. J., Lenderink, G., and Roberts, N. M. (2014). “Future Changes to the Intensity and Frequency of Short-Duration Extreme Rainfall”. In: *Reviews of Geophysics* 52.3, pp. 522–555. DOI: 10.1002/2014RG000464.
- Westra, S., Alexander, L. V., and Zwiers, F. W. (2013). “Global Increasing Trends in Annual Maximum Daily Precipitation”. In: *Journal of Climate* 26.11, pp. 3904–3918. DOI: 10.1175/JCLI-D-12-00502.1.
- Wicke, D., Cochrane, T., and O’Sullivan, A. (2012). “Build-up Dynamics of Heavy Metals Deposited on Impermeable Urban Surfaces”. In: *Journal of Environmental Management* 113, pp. 347–354. DOI: 10.1016/j.jenvman.2012.09.005.
- Wicke, D., Tatis-Muvdi, R., Rouault, P., Baar, P., Zerball-van, Dünnbier, U., Rohr, M., and Burkhardt, M. (2022). “Emissions from Building Materials—A Threat to the Environment?” In: *Water* 14.3, p. 303. DOI: 10.3390/w14030303.
- World Meteorological Organization (2018). *Guide to Climatological Practices*. 100. Geneva, Switzerland: World Meteorological Organization.

- Wu, X., Zhang, L., and Zang, S. (2019). “Examining Seasonal Effect of Urban Heat Island in a Coastal City”. In: *PLOS ONE* 14.6, e0217850. DOI: 10.1371/journal.pone.0217850.
- Wu, Y., Liu, J., Zhai, J., Cong, L., Wang, Y., Ma, W., Zhang, Z., and Li, C. (2018). “Comparison of Dry and Wet Deposition of Particulate Matter in Near-Surface Waters during Summer”. In: *PLOS ONE* 13.6. Ed. by F. Li, e0199241. DOI: 10.1371/journal.pone.0199241.
- Xiao, M., Zhang, Q., and Singh, V. P. (2017). “Spatiotemporal Variations of Extreme Precipitation Regimes during 1961–2010 and Possible Teleconnections with Climate Indices across China”. In: *International Journal of Climatology* 37.1, pp. 468–479. DOI: 10.1002/joc.4719.
- Xing, Y., Liang, Q., Wang, G., Ming, X., and Xia, X. (2019). “City-Scale Hydrodynamic Modelling of Urban Flash Floods: The Issues of Scale and Resolution”. In: *Natural Hazards* 96.1, pp. 473–496. DOI: 10.1007/s11069-018-3553-z.
- Xu, Z., Fan, K., and Wang, H. (2015). “Decadal Variation of Summer Precipitation over China and Associated Atmospheric Circulation after the Late 1990s”. In: *Journal of Climate* 28.10, pp. 4086–4106. DOI: 10.1175/JCLI-D-14-00464.1.
- Yaqub, A., Seibert, P., and Formayer, H. (2011). “Diurnal Precipitation Cycle in Austria”. In: *Theoretical and Applied Climatology* 103.1-2, pp. 109–118. DOI: 10.1007/s00704-010-0281-z.
- Yoo, C. and Park, C. (2012). “Comparison of Annual Maximum Rainfall Series and Annual Maximum Independent Rainfall Event Series”. In: *Journal of Korea Water Resources Association* 45.5, pp. 431–444. DOI: 10.3741/JKWRA.2012.45.5.431.
- Yuan, X., Zheng, N., Ye, F., and Fu, W. (2019). “Critical Runoff Depth Estimation for Incipient Motion of Non-Cohesive Sediment on Loose Soil Slope under Heavy Rainfall”. In: *Geomatics, Natural Hazards and Risk* 10.1, pp. 2330–2345. DOI: 10.1080/19475705.2019.1697760.
- Zanardo, S., Nicotina, L., Hilberts, A. G. J., and Jewson, S. P. (2019). “Modulation of Economic Losses From European Floods by the North Atlantic Oscillation”. In: *Geophysical Research Letters* 46, pp. 2563–2572. DOI: 10.1029/2019GL081956.
- Zeder, J. and Fischer, E. M. (2020). “Observed Extreme Precipitation Trends and Scaling in Central Europe”. In: *Weather and Climate Extremes* 29, p. 100266. DOI: 10.1016/j.wace.2020.100266.
- Z+F LaserControl (2017). *Laserscanning Software*. Version 9.0. Wangen im Allgäu: Z+F LaserControl. URL: <https://www.zofre.de/en/laser-scanners/laserscanning-software/z-f-lasercontrolr>.
- Zhai, P., Zhang, X., Wan, H., and Pan, X. (2005). “Trends in Total Precipitation and Frequency of Daily Precipitation Extremes over China”. In: *Journal of Climate* 18.7, pp. 1096–1108. DOI: 10.1175/JCLI-3318.1.

- Zhang, H. and Zhai, P. (2011). “Temporal and Spatial Characteristics of Extreme Hourly Precipitation over Eastern China in the Warm Season”. In: *Advances in Atmospheric Sciences* 28.5, p. 1177. DOI: 10.1007/s00376-011-0020-0.
- Zhang, X., Alexander, L., Hegerl, G. C., Jones, P., Tank, A. K., Peterson, T. C., Trewin, B., and Zwiers, F. W. (2011). “Indices for Monitoring Changes in Extremes Based on Daily Temperature and Precipitation Data”. In: *WIREs Climate Change* 2.6, pp. 851–870. DOI: 10.1002/wcc.147.
- Zhao, A. D., Stevenson, D. S., and Bollasina, M. A. (2019). “The Role of Anthropogenic Aerosols in Future Precipitation Extremes over the Asian Monsoon Region”. In: *Climate Dynamics* 52.9, pp. 6257–6278. DOI: 10.1007/s00382-018-4514-7.
- Zhao, H., Zou, C., Zhao, J., and Li, X. (2018). “Role of Low-Impact Development in Generation and Control of Urban Diffuse Pollution in a Pilot Sponge City: A Paired-Catchment Study”. In: *Water* 10.7, p. 852. DOI: 10.3390/w10070852.
- Zhu, Z., Arp, P. A., Mazumder, A., Meng, F., Bourque, C. P.-A., and Foster, N. W. (2005). “Modeling Stream Water Nutrient Concentrations and Loadings in Response to Weather Condition and Forest Harvesting”. In: *Ecological Modelling* 185.2-4, pp. 231–243. DOI: 10.1016/j.ecolmodel.2004.12.006.
- Zolina, O., Simmer, C., Kapala, A., Bachner, S., Gulev, S., and Maechel, H. (2008). “Seasonally Dependent Changes of Precipitation Extremes over Germany since 1950 from a Very Dense Observational Network”. In: *J. Geophys. Res* 113. DOI: 10.1029/2007JD008393.